

Deep Network Approximation: Achieving Arbitrary Accuracy with Fixed Number of Neurons

Zuowei Shen

*Department of Mathematics
National University of Singapore*

MATZUOWS@NUS.EDU.SG

Haizhao Yang

*Department of Mathematics
Purdue University*

HAIZHAO@PURDUE.EDU

Shijun Zhang*

*Department of Mathematics
National University of Singapore*

ZHANGSHIJUN@U.NUS.EDU

Abstract

This paper develops simple feed-forward neural networks that achieve the universal approximation property for all continuous functions with a fixed finite number of neurons. These neural networks are simple because they are designed with a simple and computable continuous activation function σ leveraging a triangular-wave function and the softsign function. We prove that σ -activated networks with width $36d(2d+1)$ and depth 11 can approximate any continuous function on a d -dimensional hypercube within an arbitrarily small error. Hence, for supervised learning and its related regression problems, the hypothesis space generated by these networks with a size not smaller than $36d(2d+1) \times 11$ is dense in the continuous function space $C([a, b]^d)$ and therefore dense in the Lebesgue spaces $L^p([a, b]^d)$ for $p \in [1, \infty)$. Furthermore, classification functions arising from image and signal classification are in the hypothesis space generated by σ -activated networks with width $36d(2d+1)$ and depth 12, when there exist pairwise disjoint bounded closed subsets of \mathbb{R}^d such that the samples of the same class are located in the same subset. Finally, we use numerical experimentation to show that replacing the ReLU activation function by ours would improve the experiment results.

Keywords: Universal Approximation Theorem; Fixed-Size Neural Network; Classification Function; Nonlinear Approximation; Periodic Function; Continuous Function.

1. Introduction

Deep neural networks have been widely used in data science and artificial intelligence. Their tremendous successes in various applications have motivated extensive research to establish the theoretical foundation of deep learning. Understanding the approximation capacity of deep neural networks is one of the keys to revealing the power of deep learning. The most basic layers of deep neural networks are nonlinear functions as the composition of an affine linear transform and a nonlinear activation function. The composition of these simple

*. Corresponding author.

nonlinear functions can generate a complicated deep neural network with powerful approximation capacity, which is the key difference to classic approximation tools. In this paper, we show that the hypothesis space of deep neural networks generated from the composition of 11 such simple nonlinear functions is dense in the continuous function space $C([a, b]^d)$, when the affine linear transforms are parameterized with $\mathcal{O}(d^2)$ non-zero parameters in total and the nonlinear activation function is constructed from a simple triangular-wave function and the softsign function.

1.1 Main results

One of the key elements of a neural network is its activation functions. Searching for simple activation functions enabling powerful approximation capacity of neural networks is an important mathematical problem that probably originated in the Kolmogorov superposition theorem (KST) (Kolmogorov, 1957) for Hilbert’s 13-th problem, where a two-hidden-layer neural network with $\mathcal{O}(d)$ neurons and complicated activation functions depending on the target functions are constructed to represent an arbitrary function in $C([0, 1]^d)$. Since then, whether simple and computable activation functions independent of the target function exist to make the space of neural networks with $\mathcal{O}(d)$ neurons dense in $C([0, 1]^d)$ or even equal to $C([0, 1]^d)$ has been an open problem. A function $\varrho: \mathbb{R} \rightarrow \mathbb{R}$ is said to be a universal activation function (UAF) if the function space generated by ϱ -activated networks with $C_{\varrho, d}$ neurons is dense in $C([0, 1]^d)$, where $C_{\varrho, d}$ is a constant determined by ϱ and d . That is, if ϱ is a UAF, then ϱ -activated networks with $C_{\varrho, d}$ neurons can approximate any continuous function within an arbitrary error on $[0, 1]^d$ by only adjusting the parameters.

In this paper, we first construct a simple and computable example of UAFs. As a typical and simple UAF, this activation function is called the elementary universal activation function (EUAF), and the corresponding networks are called EUAF networks. Then, we prove that the function space generated by EUAF networks with $\mathcal{O}(d^2)$ neurons is dense in $C([a, b]^d)$. Furthermore, it is shown that EUAF networks with $\mathcal{O}(d^2)$ neurons can exactly represent d -dimensional classification functions.

While a good activation function should be simple and numerically implementable, the neural network activated by it should be able to approximate continuous functions well with a manageable size. Considering these requirements and motivated by previous works (Yarotsky and Zhevnerchuk, 2020; Shen et al., 2021a,b), the activation function to be chosen should have appropriate nonlinearity, periodicity, and the capacity to reproduce step functions. It is challenging to find a single activation function with all these properties. Here, we propose an activation function with all required properties by using two simple functions σ_1 and σ_2 defined below.

Let σ_1 be the continuous triangular-wave function with period 2, i.e.,

$$\sigma_1(x) := |x| \quad \text{for any } x \in [-1, 1] \quad (1)$$

and $\sigma_1(x + 2) = \sigma_1(x)$ for any $x \in \mathbb{R}$. Alternatively, σ_1 can also be written as:

$$\sigma_1(x) = \left| x - 2 \left\lfloor \frac{x+1}{2} \right\rfloor \right| \quad \text{for any } x \in \mathbb{R}, \quad \text{where } \lfloor \cdot \rfloor \text{ is the floor function.}$$

Clearly, σ_1 is periodic and $x - \sigma_1(x)$ is a continuous variant of the floor function as desired.

To introduce high nonlinearity, let σ_2 be the softsign activation function commonly used in machine learning (Turian et al., 2009; Le and Zuidema, 2015):

$$\sigma_2(x) := \frac{x}{|x| + 1} \quad \text{for any } x \in \mathbb{R}. \quad (2)$$

Then the activation function σ is defined as:

$$\sigma(x) := \begin{cases} \sigma_1(x) & \text{for } x \in [0, \infty), \\ \sigma_2(x) & \text{for } x \in (-\infty, 0). \end{cases} \quad (3)$$

See an illustration of σ in Figure 1. This activation function σ is the EUAF used to construct powerful neural networks in this paper.

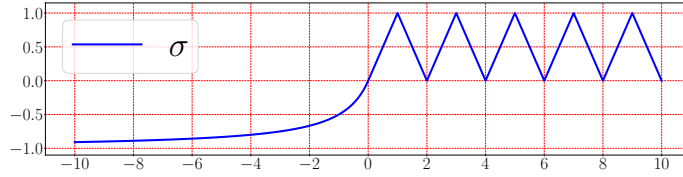


Figure 1: An illustration of σ on $[-10, 10]$.

As we shall see later, the periodicity of the triangular-wave function σ_1 and the (high) nonlinearity of the softsign function σ_2 play crucial roles in the proofs of our main results. One may find more details Section 2.2, which provides the ideas of proving our main results. Observe that σ_1 is an even function and σ_2 is an odd function, i.e., $\sigma(x) = \sigma_1(x) = \sigma_1(-x)$ for any $x \geq 0$ and $-\sigma(-x) = -\sigma_2(-x) = \sigma_2(x)$ for any $x \geq 0$. This implies that $\sigma(x)$ and $-\sigma(-x)$ with $x \geq 0$ have both required periodicity and nonlinearity features and play the same roles as $\sigma_1(x)$ and $\sigma_2(x)$, respectively. These requirements lead to our choice of σ as the activation function. If allowed to be more complicated, one can design many other UAFs satisfying stronger requirements for various applications. For example, the idea of designing a C^s UAF is given in Section 4.1 and a sigmoidal UAF (see Figure 8) is constructed in Section 4.2.

With the activation function σ in hand, let us introduce the network (architecture) using σ as the activation function, called σ -activated network (architecture). To be precise, a σ -activated network with a (vector) input $\mathbf{x} \in \mathbb{R}^d$, an output $\Phi(\mathbf{x}, \boldsymbol{\theta}) \in \mathbb{R}$, and $L \in \mathbb{N}^+$ hidden layers can be briefly described as follows:

$$\mathbf{x} = \tilde{\mathbf{h}}_0 \xrightarrow[\mathcal{L}_0]{\mathbf{A}_0, \mathbf{b}_0} \mathbf{h}_1 \xrightarrow{\sigma} \tilde{\mathbf{h}}_1 \quad \dots \quad \xrightarrow[\mathcal{L}_{L-1}]{\mathbf{A}_{L-1}, \mathbf{b}_{L-1}} \mathbf{h}_L \xrightarrow{\sigma} \tilde{\mathbf{h}}_L \xrightarrow[\mathcal{L}_L]{\mathbf{A}_L, \mathbf{b}_L} \mathbf{h}_{L+1} = \Phi(\mathbf{x}, \boldsymbol{\theta}), \quad (4)$$

where $N_0 = d \in \mathbb{N}^+$, $N_1, N_2, \dots, N_L \in \mathbb{N}^+$, $N_{L+1} = 1$, $\mathbf{A}_i \in \mathbb{R}^{N_{i+1} \times N_i}$ and $\mathbf{b}_i \in \mathbb{R}^{N_{i+1}}$ are the weight matrix and the bias vector in the i -th affine linear transform \mathcal{L}_i , respectively, i.e.,

$$\mathbf{h}_{i+1} = \mathbf{A}_i \cdot \tilde{\mathbf{h}}_i + \mathbf{b}_i =: \mathcal{L}_i(\tilde{\mathbf{h}}_i) \quad \text{for } i = 0, 1, \dots, L$$

and

$$\tilde{\mathbf{h}}_{i,j} = \sigma(h_{i,j}) \quad \text{for } j = 1, 2, \dots, N_i \text{ and } i = 1, 2, \dots, L.$$

93 Here, $\tilde{h}_{i,j}$ and $h_{i,j}$ are the j -th entry of $\tilde{\mathbf{h}}_i$ and \mathbf{h}_i , respectively, for $j = 1, 2, \dots, N_i$ and
 94 $i = 1, 2, \dots, L$. $\boldsymbol{\theta}$ is a flattened vector consisting of all parameters in $\mathbf{A}_0, \mathbf{b}_0, \dots, \mathbf{A}_L, \mathbf{b}_L$.

95 If σ is applied to a vector entry wisely, i.e., given any $k \in \mathbb{N}^+$,

$$96 \quad \sigma(\mathbf{y}) = [\sigma(y_1), \dots, \sigma(y_k)]^T \quad \text{for any } \mathbf{y} = [y_1, \dots, y_k]^T \in \mathbb{R}^k,$$

97 then Φ can be represented in a form of function compositions as follows:

$$98 \quad \Phi(\mathbf{x}, \boldsymbol{\theta}) = \mathcal{L}_L \circ \sigma \circ \mathcal{L}_{L-1} \circ \sigma \circ \dots \circ \sigma \circ \mathcal{L}_1 \circ \sigma \circ \mathcal{L}_0(\mathbf{x}) \quad \text{for any } \mathbf{x} \in \mathbb{R}^d.$$

99 Given $N, L \in \mathbb{N}^+$, let $\Phi_{N,L}(\mathbf{x}, \boldsymbol{\theta})$ denote the σ -activated network architecture $\Phi(\mathbf{x}, \boldsymbol{\theta})$
 100 in Equation (4) with $N_1 = N_2 = \dots = N_L = N$. Let

$$101 \quad W = W_{d,N,L} = d \times N + N + (N \times N + N) \times (L - 1) + 1 \times N + 1 = \mathcal{O}(dN + N^2L)$$

102 be the total number of parameters in $\Phi_{N,L}(\mathbf{x}, \boldsymbol{\theta})$, i.e., $\boldsymbol{\theta} \in \mathbb{R}^W$.

103 Define the hypothesis space $\mathcal{H}_d(N, L)$ as the function space generated by EUAF net-
 104 works with width N and depth L , i.e.,

$$105 \quad \mathcal{H}_d(N, L) := \left\{ \phi : \phi(\mathbf{x}) = \Phi_{N,L}(\mathbf{x}, \boldsymbol{\theta}) \text{ for any } \mathbf{x} \in \mathbb{R}^d, \quad \boldsymbol{\theta} \in \mathbb{R}^W \right\}. \quad (5)$$

106 Let $C([a, b]^d)$ be the space of all continuous functions $f : [a, b]^d \rightarrow \mathbb{R}$ with the max-
 107 imum norm. Our first main result, Theorem 1.1 below, shows that σ -activated networks
 108 with a fixed size $\mathcal{O}(d^2)$ enjoy the universal approximation property by only adjusting their
 109 parameters.

110 **Theorem 1.1.** *Let $f \in C([a, b]^d)$ be a continuous function and $\mathcal{H}_d(N, L)$ be the hypothesis*
 111 *space defined in (5) with $N = 36d(2d + 1)$ and $L = 11$. Then, for an arbitrary $\varepsilon > 0$, there*
 112 *exists $\phi \in \mathcal{H}_d(N, L)$ such that*

$$113 \quad |\phi(\mathbf{x}) - f(\mathbf{x})| < \varepsilon \quad \text{for any } \mathbf{x} \in [a, b]^d.$$

114 To prove Theorem 1.1, we first summarize key proof ideas in Section 2.2 and then
 115 present the detailed proof later in Section 5.1.

116 *Remark.* The network realizing ϕ in Theorem 1.1 has

$$117 \quad d \times N + N + (N \times N + N) \times (L - 1) + N \times 1 + 1 \sim d^4$$

118 parameters, where $N = 36d(2d + 1)$ and $L = 11$. However, as shown in our constructive proof
 119 of Theorem 1.1, it is enough to adjust $5437(d + 1)(2d + 1) = \mathcal{O}(d^2) \ll d^4$ parameters and set
 120 all the others to 0.

121 Since for an arbitrary $M > 0$, $2M\sigma(\frac{x+M}{2M}) - M = x$ for all $x \in [-M, M]$, we can manually
 122 add hidden layers to EUAF networks without changing the output. This leads to the
 123 following immediate corollary of Theorem 1.1.

124 **Corollary 1.2.** *Assume $N \geq 36d(2d + 1)$ and $L \geq 11$, then the hypothesis space $\mathcal{H}_d(N, L)$*
 125 *defined in (5) is dense in $C([a, b]^d)$.*

The stable and accurate approximation of discontinuities has many real-world applications and has been widely studied (Bernholdt et al., 2019; Beck et al., 2020; Gupta et al., 2020; Gedeon et al., 2021; Hu et al., 2021). Most of common discontinuous functions are in Lebesgue spaces. Let us consider the denseness of our hypothesis space in Lebesgue spaces. Since $C([a, b]^d)$ is dense in $L^p([a, b]^d)$ for $p \in [1, \infty)$ (e.g., see Theorem 2.4 of (Stein and Shakarchi, 2005)), the hypothesis space in Corollary 1.2 is also dense in $L^p([a, b]^d)$ as shown in the following corollary.

Corollary 1.3. *Assume $N \geq 36d(2d + 1)$, $L \geq 11$, and $p \in [1, \infty)$, then the hypothesis space $\mathcal{H}_d(N, L)$ defined in (5) is dense in $L^p([a, b]^d)$.*

This corollary implies that, for $f \in L^p([a, b]^d)$ and an arbitrary $\varepsilon > 0$, there exists $\phi \in \mathcal{H}_d(N, L)$ such that $\|\phi - f\|_{L^p([a, b]^d)} \leq \varepsilon$.

One can ask whether the arbitrary error $\varepsilon > 0$ in Theorem 1.1 can be further reduced to 0. This is not true in general, but it is true for a class of interesting functions widely used in image classifications. Given any pairwise disjoint bounded closed subsets $E_1, E_2, \dots, E_J \subseteq \mathbb{R}^d$, define “the classification function space” of these subsets as

$$\mathcal{C}_d(E_1, E_2, \dots, E_J) := \left\{ f : f = \sum_{j=1}^J r_j \cdot \mathbf{1}_{E_j} \text{ for any } r_1, r_2, \dots, r_J \in \mathbb{Q} \right\},$$

where $\mathbf{1}_{E_n}$ is the indicator function of E_j for each j . Our second main result, Theorem 1.4 below, shows that each element of $\mathcal{C}_d(E_1, E_2, \dots, E_J)$ can be exactly represented by a σ -activated network with $\mathcal{O}(d^2)$ neurons in $\bigcup_{j=1}^J E_j$.

Theorem 1.4. *Let $E_1, E_2, \dots, E_J \subseteq \mathbb{R}^d$ be pairwise disjoint bounded closed subsets and $\mathcal{H}_d(N, L)$ be the hypothesis space defined in (5) with $N = 36d(2d + 1)$ and $L = 12$. Then, for $f \in \mathcal{C}_d(E_1, E_2, \dots, E_J)$, there exists $\phi \in \mathcal{H}_d(N, L)$ such that*

$$\phi(\mathbf{x}) = f(\mathbf{x}) \quad \text{for any } \mathbf{x} \in \bigcup_{j=1}^J E_j.$$

Remark. The network realizing ϕ in Theorem 1.4 has

$$d \times N + N + (N \times N + N) \times (L - 1) + N \times 1 + 1 \sim d^4$$

parameters, where $N = 36d(2d + 1)$ and $L = 12$. However, as shown in our constructive proof of Theorem 1.4 in Section 5.2, it is enough to adjust $5509(d + 1)(2d + 1) = \mathcal{O}(d^2) \ll d^4$ parameters and set all the others to 0.

For a general function space \mathcal{F} , define $\mathcal{F}|_E := \{f|_E : f \in \mathcal{F}\}$, where $f|_E$ is the function achieved via limiting f on E . Then, we have a corollary of Theorem 1.4 as follows.

Corollary 1.5. *Let $E_1, E_2, \dots, E_J \subseteq \mathbb{R}^d$ be pairwise disjoint bounded closed subsets and $\mathcal{H}_d(N, L)$ be the hypothesis space defined in (5). Assume $N \geq 36d(2d + 1)$ and $L \geq 12$, then*

$$\mathcal{C}_d(E_1, E_2, \dots, E_J)|_E \subseteq \mathcal{H}_d(N, L)|_E,$$

where $E = \bigcup_{j=1}^J E_j$.

One of the most successful applications of deep learning is the image and signal classifications. In supervised classification problems, given a few samples and their labels (usually integers), the goal of the task is to learn how to assign a label to a new sample. For example, in binary classification via deep learning, a neural network is trained based on given samples (and labels) to approximate a classification function mapping one class of samples to 0 and the other class of samples to 1. Theorem 1.4 (or Corollary 1.5) implies that the classification function can be exactly realized by an EUAF network with a size depending only on the dimension of the problem domain via adjusting its parameters. This means that the best approximation error of EUAF networks to classification functions in the classification problem is 0.

We remark that, in the worst scenario, there might exist complicated high-dimensional functions such that, the parameters of the EUAF network in Theorem 1.1 (or 1.4) require high computer precision for storage, and the precision might be exponentially large in the problem dimension. We refer to this as the curse of memory, which may make Theorem 1.1 and 1.4 less interesting in real-world applications, though the number of parameters can be very small. The key question to be addressed is how rare the curse of memory would happen in real-world applications. If the target functions in real-world applications typically have no curse of memory with a high probability, then EUAF networks would be very useful in real-world applications. In future work, we will explore the statistical characterization of high-dimensional functions for the curse of memory of EUAF networks. Another approach to reducing the memory requirement is to increase the network size. Our main result has provided a network size $\mathcal{O}(d^2)$ to achieve an arbitrary error. If a larger network size is used, the curse of memory can be lessened as we shall discuss in Section 1.4.

1.2 Related work

In recent years, there has been an increasing amount of literature on the approximation power of neural networks as a special case of nonlinear approximation (DeVore, 1998; Cohen et al., 2020; Daubechies et al., 2021). In the early works of approximation theory for neural networks, the universal approximation theorem (Cybenko, 1989; Hornik, 1991; Hornik et al., 1989) without approximation errors showed that there exists a sufficiently large neural network approximating a target function in a certain function space within any given error $\varepsilon > 0$. There are also other versions of the universal approximation theorem. For example, it was shown in (Lin and Jegelka, 2018) that the ReLU-activated residual neural networks with one neuron per hidden layer and a sufficiently large depth are a universal approximator. The universal approximation property for general residual neural networks was proved in (Li et al., to appear) via a dynamical system approach. In all papers discussed above, the network size goes to infinity when the target approximation error approaches 0. However, our result in Theorem 1.1 implies that EUAF networks with a fixed size ($\mathcal{O}(d^2)$ neurons in total) can achieve an arbitrary small error for approximating $f \in C([a, b]^d)$.

The approximation errors in terms of the total number of parameters of ReLU networks are well studied for basic function spaces with (nearly) optimal approximation errors, e.g., (nearly) optimal asymptotic errors for continuous functions (Yarotsky, 2018), C^s functions (Yarotsky and Zhevnerchuk, 2020), piecewise smooth functions (Petersen and Voigtlaender, 2018), solutions of special PDEs (Elbrächter et al., 2021; Beck et al., 2020), functions that

can be optimally approximated by affine systems (Bölcskei et al., 2019), and Sobolev spaces (Yang et al., 2022; Hon and Yang, 2021). Approximation errors in terms of width and depth would be more useful than those in terms of the total number of nonzero parameters in practice, because width and depth are two essential hyper-parameters in every numerical algorithm instead of the number of nonzero parameters. This motivated the works on the (nearly) optimal non-asymptotic errors in terms of width and depth with explicit pre-factors for approximating continuous functions in (Shen et al., 2020, 2022; Zhang, 2020) and for C^s functions in (Lu et al., 2021; Zhang, 2020). As the errors are optimal, there are two possible directions to improve the approximation error in order to reduce the effect of the curse of dimensionality. The first one is to consider smaller target function spaces, e.g., analytic functions (E and Wang, 2018; Bonito et al., 2021), Barron spaces (Barron, 1993; E et al., 2019b; E and Wojtowytsch, 2022; Siegel and Xu, 2021), and band-limited functions (Chen and Wu, 2019; Montanelli et al., 2021).

Another direction is to design advanced activation functions, where one can use multiple activation functions, to enhance the power of neural networks, especially to conquer the curse of dimensionality in network approximation. There have been several papers designing activation functions to achieve good approximation errors. The results in (Yarotsky and Zhevnerchuk, 2020) imply that (sin, ReLU)-activated neural networks (i.e., the activation function of a neuron can be chosen from either sin or ReLU) with W parameters can approximate Lipschitz continuous functions with an asymptotic approximation error $\mathcal{O}(e^{-c_d\sqrt{W}})$, where c_d is a constant depending on d and might cause the curse of dimensionality, though the approximation error is root-exponentially small in W . In (Shen et al., 2021a), it was shown that (Floor, ReLU)-activated neural networks with width $\mathcal{O}(N)$ and depth $\mathcal{O}(L)$ admit an quantitative approximation error $\mathcal{O}(\sqrt{d}N^{-\sqrt{L}})$ for Lipschitz continuous functions, conquering the curse of dimensionality in approximation with a root-exponentially small error in depth L .¹ In (Shen et al., 2021b), it was shown that, even if the depth is as small as 3, neural networks with width N and $\mathcal{O}(d+N)$ nonzero parameters can approximate Lipschitz continuous functions with an exponentially small error $\mathcal{O}(\sqrt{d}2^{-N})$, if the floor function $\lfloor x \rfloor$, the exponential function 2^x , and the step function $\mathbb{1}_{\{x \geq 0\}}$ are used as activation functions. Recently in (Jiao et al., 2021), the results in (Yarotsky and Zhevnerchuk, 2020; Shen et al., 2021b) were combined to avoid the curse of dimensionality using ReLU, sin, and 2^x activation functions. Corollary 1.2 implies that the hypothesis space of EUAF networks activated by a single activation function with $\mathcal{O}(d^2)$ neurons is dense in $C([a, b]^d)$. Particularly, all continuous functions can be arbitrarily approximated by fixed-size EUAF networks with width N and depth L on a d -dimensional hypercube, whenever $N \geq 36d(2d+1)$ and $L \geq 11$.

There is another research line for the approximation error of neural networks: apply KST (Kolmogorov, 1957) or its variants to explore new activation functions for a fixed-size network to achieve an arbitrary error. The original KST shows that any multivariate function $f \in C([0, 1]^d)$ can be represented as $f(\mathbf{x}) = \sum_{i=0}^{2d} g_i(\sum_{j=1}^d h_{i,j}(x_j))$ for any $\mathbf{x} = [x_1, \dots, x_d]^T \in [0, 1]^d$, where g_i and $h_{i,j}$ are univariate continuous functions. In fact, the composition architecture of KST can be regarded as a special neural network with

1. Although there is no curse of dimensionality in network approximation, the construction requires exponentially many data samples of the target function and computer memory. Hence, there would be a curse of dimensionality in inferring a target function from its finite samples when standard learning techniques are applied on a computer.

(complicated) activation functions depending on the target function, which results in the failure of KST in practice. To alleviate this issue, a single activation function independent of the target function is designed in (Maierov and Pinkus, 1999) to construct networks with a fixed size ($\mathcal{O}(d)$ neurons) to achieve an arbitrary error for approximating functions in $C([-1, 1]^d)$. However, the activation function in (Maierov and Pinkus, 1999) has no closed form and is hardly computable. See Section 2.2 for a detailed discussion of (Maierov and Pinkus, 1999). The computability issue of activation functions was addressed recently in (Yarotsky, 2021). It was shown in (Yarotsky, 2021) that, for an arbitrary $\varepsilon > 0$ and any function f in $C([0, 1]^d)$, there exists a network of size only depending on d constructed with multiple activation functions either (\sin & \arcsin) or ($[\cdot]$ & a non-polynomial analytic function) to approximate f within an error ε . To the best of our knowledge, there is no explicit characterization of the size dependence on d in (Yarotsky, 2021). For example, a very important question is whether the dependence can be mild, e.g., only a polynomial of d , or has to be severe, e.g., exponentially in d . The results of current paper provide positive answers to all the issues discussed above: we show that EUAF networks with a single simple and computable activation function, width $36d(2d + 1)$, and depth 11 can approximate functions in $C([a, b]^d)$ within an arbitrary pre-specified error $\varepsilon > 0$.

In summary, the aim of this paper is to design a simple and computable activation function σ to construct fixed-size neural networks with the universal approximation property. The network sizes of the width and depth have an explicit characterization that only depends on the dimension d . The fixed-size neural network is designed to approximate any continuous functions on a hypercube within an arbitrary error by only adjusting $\mathcal{O}(d^2)$ network parameters. Moreover, we prove that an arbitrary classification function can be exactly represented by such a fixed-size network architecture via only adjusting $\mathcal{O}(d^2)$ network parameters. The main contribution of this paper is to develop a rigorous mathematical analysis for the universal approximation property of fixed-size neural networks. The mathematical analysis developed here may be applied to understand other neural networks. The approximation results discussed here can be applied to the full error analysis of deep learning in the next subsection.

1.3 Error analysis

We will briefly discuss the full error analysis of deep neural networks. Let $\Phi(\mathbf{x}, \boldsymbol{\theta})$ denote a function of $\mathbf{x} \in \mathcal{X}$ generated by a network architecture parameterized with $\boldsymbol{\theta} \in \mathbb{R}^W$. Given a target function f defined on \mathcal{X} , the final goal is to find the expected risk minimizer

$$\boldsymbol{\theta}_{\mathcal{D}} \in \arg \min_{\boldsymbol{\theta} \in \mathbb{R}^W} R_{\mathcal{D}}(\boldsymbol{\theta}), \quad \text{where } R_{\mathcal{D}}(\boldsymbol{\theta}) := \mathbb{E}_{\mathbf{x} \sim U(\mathcal{X})} [\ell(\Phi(\mathbf{x}, \boldsymbol{\theta}), f(\mathbf{x}))]$$

with an unknown data distribution $U(\mathcal{X})$ over \mathcal{X} and a loss function $\ell(\cdot, \cdot)$ typically taken as $\ell(y_1, y_2) = \frac{1}{2}|y_1 - y_2|^2$. Note that $\boldsymbol{\theta}_{\mathcal{D}}$ may not be always achievable. For any pre-specified $\eta > 0$, one can always identify $\boldsymbol{\theta}_{\mathcal{D}, \eta} \in \mathbb{R}^W$ instead of $\boldsymbol{\theta}_{\mathcal{D}}$ such that

$$R_{\mathcal{D}}(\boldsymbol{\theta}_{\mathcal{D}, \eta}) \leq \inf_{\boldsymbol{\theta} \in \mathbb{R}^W} R_{\mathcal{D}}(\boldsymbol{\theta}) + \eta/2. \quad (6)$$

Since the expected risk $R_{\mathcal{D}}(\boldsymbol{\theta})$ is not available in practice, we use the empirical risk $R_{\mathcal{S}}(\boldsymbol{\theta})$ to approximate $R_{\mathcal{D}}(\boldsymbol{\theta})$ for given samples $\{(\mathbf{x}_i, f(\mathbf{x}_i))\}_{i=1}^n$ and our goal is to identify the

284 empirical risk minimizer

$$285 \quad \boldsymbol{\theta}_S \in \arg \min_{\boldsymbol{\theta} \in \mathbb{R}^W} R_S(\boldsymbol{\theta}), \quad \text{where } R_S(\boldsymbol{\theta}) := \frac{1}{n} \sum_{i=1}^n \ell(\Phi(\mathbf{x}_i, \boldsymbol{\theta}), f(\mathbf{x}_i)).$$

286 Similarly, $\boldsymbol{\theta}_S$ is not always achievable. For any pre-specified $\eta > 0$, one can always identify
 287 $\boldsymbol{\theta}_{S,\eta} \in \mathbb{R}^W$ instead of $\boldsymbol{\theta}_S$ such that

$$288 \quad R_S(\boldsymbol{\theta}_{S,\eta}) \leq \inf_{\boldsymbol{\theta} \in \mathbb{R}^W} R_S(\boldsymbol{\theta}) + \eta/2. \quad (7)$$

289 In practical implementation, only a numerical minimizer $\boldsymbol{\theta}_N$ of $R_S(\boldsymbol{\theta})$ can be achieved
 290 via a numerical optimization method. The discrepancy between the learned function $\Phi(\mathbf{x}, \boldsymbol{\theta}_N)$
 291 and the target function f is measured by $R_D(\boldsymbol{\theta}_N)$, which is bounded by

$$\begin{aligned} 292 \quad R_D(\boldsymbol{\theta}_N) &= \underbrace{[R_D(\boldsymbol{\theta}_N) - R_S(\boldsymbol{\theta}_N)]}_{\text{GE}} + \underbrace{[R_S(\boldsymbol{\theta}_N) - R_S(\boldsymbol{\theta}_{S,\eta})]}_{\text{OE}} + \underbrace{[R_S(\boldsymbol{\theta}_{S,\eta}) - R_S(\boldsymbol{\theta}_{D,\eta})]}_{\leq \eta/2 \text{ by (7)}} + \underbrace{[R_S(\boldsymbol{\theta}_{D,\eta}) - R_D(\boldsymbol{\theta}_{D,\eta})]}_{\text{GE}} + \underbrace{R_D(\boldsymbol{\theta}_{D,\eta})}_{\leq \inf_{\boldsymbol{\theta} \in \mathbb{R}^W} R_D(\boldsymbol{\theta}) + \eta/2 \text{ by (6)}} \\ &\leq \underbrace{\eta}_{\text{Perturbation}} + \underbrace{\inf_{\boldsymbol{\theta} \in \mathbb{R}^W} R_D(\boldsymbol{\theta})}_{\text{Approximation error}} + \underbrace{[R_S(\boldsymbol{\theta}_N) - \inf_{\boldsymbol{\theta} \in \mathbb{R}^W} R_S(\boldsymbol{\theta})]}_{\text{Optimization error (OE)}} + \underbrace{[R_D(\boldsymbol{\theta}_N) - R_S(\boldsymbol{\theta}_N)] + [R_S(\boldsymbol{\theta}_{D,\eta}) - R_D(\boldsymbol{\theta}_{D,\eta})]}_{\text{Generalization error (GE)}}. \end{aligned}$$

293 If $\Phi(\mathbf{x}, \boldsymbol{\theta})$ is realized by EUAF networks, then Theorem 1.1 implies

$$294 \quad \inf_{\boldsymbol{\theta} \in \mathbb{R}^W} \|\Phi(\cdot, \boldsymbol{\theta}) - f(\cdot)\|_{L^\infty(\mathcal{X})} = 0 \quad \text{for all } f \in C(\mathcal{X}) \text{ with } \mathcal{X} = [a, b]^d.$$

295 It follows that

$$296 \quad \inf_{\boldsymbol{\theta} \in \mathbb{R}^W} R_D(\boldsymbol{\theta}) = \inf_{\boldsymbol{\theta} \in \mathbb{R}^W} \mathbb{E}_{\mathbf{x} \sim U(\mathcal{X})} [\ell(\Phi(\mathbf{x}, \boldsymbol{\theta}), f(\mathbf{x}))] = 0.$$

297 Since the pre-specified hyper-parameter η can be arbitrarily small, the full error analysis
 298 can be reduced to the analysis of the optimization and generalization errors, which de-
 299 pends on data samples, optimization algorithms, etc. One could refer to (Neyshabur et al.,
 300 2019; E et al., 2019b,a; E and Wojtowytsch, 2020; Kawaguchi, 2016; Nguyen and Hein,
 301 2017; Kawaguchi and Bengio, 2019; He et al., 2020; Li et al., 2019) for the analysis of the
 302 generalization and optimization errors.

303 1.4 Computability

304 The EUAF network is simple and computable in the sense that the output and subgra-
 305 dient of EUAF networks can be efficiently evaluated. The computability of EUAF implies
 306 that we can numerically implement the optimization algorithm to find a minimizer of the
 307 empirical risk. Therefore, EUAF can be directly applied to existing deep learning software
 308 in the same way as other popular activation functions (such as ReLU or Sigmoid). For fur-
 309 ther discussion on the computability of EUAF, one may refer to Section 3, which provides
 310 experiments to explore the numerical properties of EUAF. As opposed to the computability
 311 of our EUAF, the powerful activation function proposed in (Maierov and Pinkus, 1999) is
 312 not computable in the sense that there is no numerical algorithm to evaluate the output
 313 and subgradient of the corresponding network.

314 As we shall see later in the proof of Theorem 1.1, our EUAF network may require
 315 sufficiently large parameters to achieve an arbitrarily small error. Theorem 1.1 has provided

316 an example of width $\mathcal{O}(d^2)$ and depth $\mathcal{O}(1)$ to achieve an arbitrarily small error. The
 317 magnitude of parameters can be dramatically reduced by increasing the network size. In
 318 particular, if we replace each elemental block like Figure 2(a) by a block like Figure 2(b),
 319 then the magnitude of parameters can be roughly reduced to its square root. By repeatedly
 320 applying this idea, it is easy to prove that the magnitude of parameters can be exponentially
 321 reduced as the network size increases linearly. If we fix the size of these larger networks
 322 and only tune their parameters, they can still approximate high-dimensional continuous
 323 functions within an arbitrarily small error. How to fix a network size to balance between
 324 the number of parameters and their memory depends on both the computer hardware and
 325 software. The goal of this paper is to demonstrate the existence of a simple network with a
 326 small and fixed size achieving an arbitrary error in spite of the magnitude of parameters and
 327 we have shown that the network size can be as small as $\mathcal{O}(d^2)$. It is interesting to investigate
 328 the balance between the network size and the memory requirement in the future.

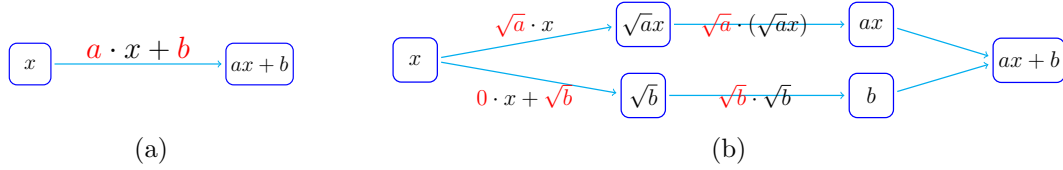


Figure 2: Illustrations of the magnitude reduction of parameters for a sub-network. The parameters are marked in red. Without loss of generality, $a \gg 1$ and $b \gg 1$. (a) Return $ax + b$ via two large parameters a and b . (b) Return $ax + b$ via several small parameters bounded by $\max\{\sqrt{a}, \sqrt{b}\}$.

329 In real-world applications, the parameters of the EUAF network are learned from the
 330 samples of the target function, which involves sophisticated numerical optimization. We
 331 refer to the learnability of network parameters as the existence of a numerical optimization
 332 algorithm that can identify network parameters to achieve a target approximation error.
 333 The computability of the EUAF networks does not imply learnability, which involves ap-
 334 proximation, optimization, and generalization error analysis. The result in this paper shows
 335 that there exist computable EUAF networks achieving an arbitrarily small approximation
 336 error. This means the learnability of the best approximation is reduced to achieving small
 337 generalization and optimization errors, which depends on the given data, the empirical risk
 338 model, and the optimization algorithm. Therefore, whether or not EUAF networks would
 339 be useful in real-world applications also depends on optimization and generalization, which
 340 is out of the scope of this paper. The optimization and generalization error analysis of
 341 practical deep neural networks including EUAF networks is a challenging problem. To the
 342 best of our knowledge, there is no complete error analysis to address the learnability of
 343 neural networks with nonlinear activation functions.

344 The rest of this paper is organized as follows. In Section 2, we first summarize notation
 345 used in this paper and then discuss the ideas of proving Theorem 1.1. Section 3 focuses
 346 on numerical experimentation of EUAF, which acts as a proof of concept to explore the
 347 numerical properties of EUAF. Next, several UAFs with better properties are proposed in
 348 Section 4. After that, we use several sections to present the complete proofs of Theorems 1.1
 349 and 1.4. In Section 5, by assuming Theorem 2.1 is true, we give the detailed proofs of

350 Theorems 1.1 and 1.4. Theorem 2.1 is proved in Section 6 based on Proposition 2.2, the
 351 proof of which can be found in Section 7. Finally, Section 8 concludes this paper with a
 352 short discussion.

353 2. Notation and proof ideas

354 In this section, we first summarize notation used in this paper and then discuss the
 355 ideas of proving Theorem 1.1.

356 2.1 Notation

357 Let us summarize all basic notation used in this paper as follows.

- 358 • Let \mathbb{R} , \mathbb{Q} , and \mathbb{Z} denote the set of real numbers, rational numbers, and integers,
 359 respectively.
- 360 • Let \mathbb{N} and \mathbb{N}^+ denote the set of natural numbers and positive natural numbers, re-
 361 spectively. That is, $\mathbb{N}^+ = \{1, 2, 3, \dots\}$ and $\mathbb{N} = \mathbb{N}^+ \cup \{0\}$.
- 362 • For any $x \in \mathbb{R}$, let $\lfloor x \rfloor := \max\{n : n \leq x, n \in \mathbb{Z}\}$ and $\lceil x \rceil := \min\{n : n \geq x, n \in \mathbb{Z}\}$.
- 363 • Let $\mathbb{1}_S$ be the indicator (characteristic) function of a set S , i.e., $\mathbb{1}_S$ is equal to 1 on S
 364 and 0 outside S .
- 365 • The set difference of two sets A and B is denoted by $A \setminus B := \{x : x \in A, x \notin B\}$.
- 366 • Matrices are denoted by bold uppercase letters. For instance, $\mathbf{A} \in \mathbb{R}^{m \times n}$ is a real
 367 matrix of size $m \times n$, and \mathbf{A}^T denotes the transpose of \mathbf{A} . Vectors are denoted as bold
 368 lowercase letters. For example, $\mathbf{v} = \begin{bmatrix} v_1 \\ \vdots \\ v_d \end{bmatrix} \in \mathbb{R}^d$ is a column vector. Besides, “[” and “]”
 369 are used to partition matrices (vectors) into blocks, e.g., $\mathbf{A} = \begin{bmatrix} \mathbf{A}_{11} & \mathbf{A}_{12} \\ \mathbf{A}_{21} & \mathbf{A}_{22} \end{bmatrix}$.
- 370 • For any $p \in [1, \infty)$, the p -norm (or ℓ^p -norm) of a vector $\mathbf{x} = [x_1, x_2, \dots, x_d]^T \in \mathbb{R}^d$ is
 371 defined by

$$372 \quad \|\mathbf{x}\|_p = \|\mathbf{x}\|_{\ell^p} := \left(|x_1|^p + |x_2|^p + \dots + |x_d|^p\right)^{1/p}.$$

373 In the case $p = \infty$,

$$374 \quad \|\mathbf{x}\|_\infty = \|\mathbf{x}\|_{\ell^\infty} := \max\{|x_i| : i = 1, 2, \dots, d\}.$$

- 375 • For any $a_1, a_2, \dots, a_J \in \mathbb{R}$, we say a_1, a_2, \dots, a_J are **rationally independent** if they are
 376 linearly independent over the rational numbers \mathbb{Q} . That is, if there exist $\lambda_1, \lambda_2, \dots, \lambda_J \in$
 377 \mathbb{Q} such that $\sum_{j=1}^J \lambda_j \cdot a_j = 0$, then $\lambda_1 = \lambda_2 = \dots = \lambda_J = 0$. For a simple example, 1, $\sqrt{2}$,
 378 and $\sqrt{3}$ are rationally independent.
- 379 • An **algebraic** number is any complex number (including real numbers) that is a root
 380 of a polynomial equation with rational coefficients, i.e., α is an algebraic number if
 381 and only if there exist $\lambda_0, \lambda_1, \dots, \lambda_J \in \mathbb{Q}$ with $\sum_{j=0}^J \lambda_j \alpha^j = 0$.² Denote the set of all

2. For simplicity, we denote $1 = x^0$ for any $x \in \mathbb{R}$, including the case 0^0 .

algebraic numbers by \mathbb{A} . A complex number is called **transcendental** if it is not in \mathbb{A} . The set \mathbb{A} is countable, and, therefore, almost all numbers are transcendental. The best known transcendental numbers are π (the ratio of a circle’s circumference to its diameter) and e (the natural logarithmic base).

- The expression “a network (architecture) with width N and depth L ” means
 - The number of neurons in each **hidden** layer of this network (architecture) is no more than N .
 - The number of **hidden** layers of this network (architecture) is no more than L .

2.2 Key ideas of proving Theorem 1.1

The proof of Theorem 1.1 has two main steps: 1) prove the one-dimensional case; 2) reduce the d -dimensional approximation to the one-dimensional case via KST (Kolmogorov, 1957). In fact, in the case of $d = 1$, the size of the network in Theorem 1.1 can be further reduced as shown in Theorem 2.1 below. Theorem 2.1 is actually an enhanced version of Theorem 1.1, and, therefore, implies Theorem 1.1 in the case $d = 1$.

Theorem 2.1. *Let $f \in C([a, b])$ be a continuous function. Then, for an arbitrary $\varepsilon > 0$, there exists a function ϕ generated by an EUAF network with width 36 and depth 5 such that*

$$|\phi(x) - f(x)| < \varepsilon \quad \text{for any } x \in [a, b] \subseteq \mathbb{R}.$$

The detailed proof of Theorem 2.1 can be found in Section 6. The main ideas of proving Theorem 2.1 are developed from some ideas of our early works (Shen et al., 2021a,b). Roughly speaking, we eventually convert a function approximation problem to a point-fitting problem via the composition architecture of neural networks in the following three steps.³

- Divide $[0, 1)$ into small intervals $\mathcal{I}_k = [\frac{k-1}{K}, \frac{k}{K})$ with a left endpoint x_k for $k \in \{1, 2, \dots, K\}$, where K is an integer determined by the given error and the target function f .
- Construct a sub-network to generate a function ϕ_1 mapping the whole interval \mathcal{I}_k to k for each k . The floor function $\lfloor \cdot \rfloor$ is a good choice to implement this step. Precisely, we can define $\phi_1(x) = \lfloor Kx \rfloor$. The floor function is not continuous and has zero-derivative almost everywhere. As we shall see later, σ_1 (or σ) can be a continuous alternative to implement this step, but the construction is more complicated.
- The final step is to design another sub-network to generate a function ϕ_2 mapping k approximately to $f(x_k)$ for each k . Then $\phi_2 \circ \phi_1(x) = \phi_2(k) \approx f(x_k) \approx f(x)$ for any $x \in \mathcal{I}_k$ and $k \in \{1, 2, \dots, K\}$, which implies $\phi_2 \circ \phi_1 \approx f$ on $[0, 1)$. After the above two steps, we simplify the approximation problem to a point-fitting problem, where k is approximately mapped to $f(k)$. This step is the bottleneck of the construction in our

3. The goal of a point-fitting problem is to identify a function $\phi : \mathbb{R}^d \rightarrow \mathbb{R}$ in a given hypothesis space (e.g., the space of functions realized by neural networks) such that $|\phi(\mathbf{x}_i) - y_i| \leq \varepsilon$ for $i = 1, 2, \dots, n$ and a pre-specified error $\varepsilon > 0$, where $\{(\mathbf{x}_i, y_i)\}_{i=1}^n \subseteq \mathbb{R}^{d+1}$ are given samples.

previous papers (Shen et al., 2021a,b). Roughly speaking, the final approximation error is essentially determined by how many points we can fit using a neural network.

For the second step, the capacity to generate step functions with sufficiently many “steps” via a sub-network with a limited number of neurons plays an important role. The reproduced step functions can be considered as a continuous version of the floor function ($\lfloor \cdot \rfloor$) in (Shen et al., 2021a,b), which is a perfect step function with infinite “steps” that improves the approximation power of networks as shown in (Shen et al., 2021a,b). The key ingredient in the third step of the proof of Theorem 2.1 is essentially a point-fitting problem with arbitrarily many points. This requires the following proposition motivated by the well-known fact that an irrational winding on the torus is dense. See Figure 3 for illustrations of such a fact. Here, we propose a new point-fitting technique that can fit arbitrarily many points within an arbitrary error using neural networks.

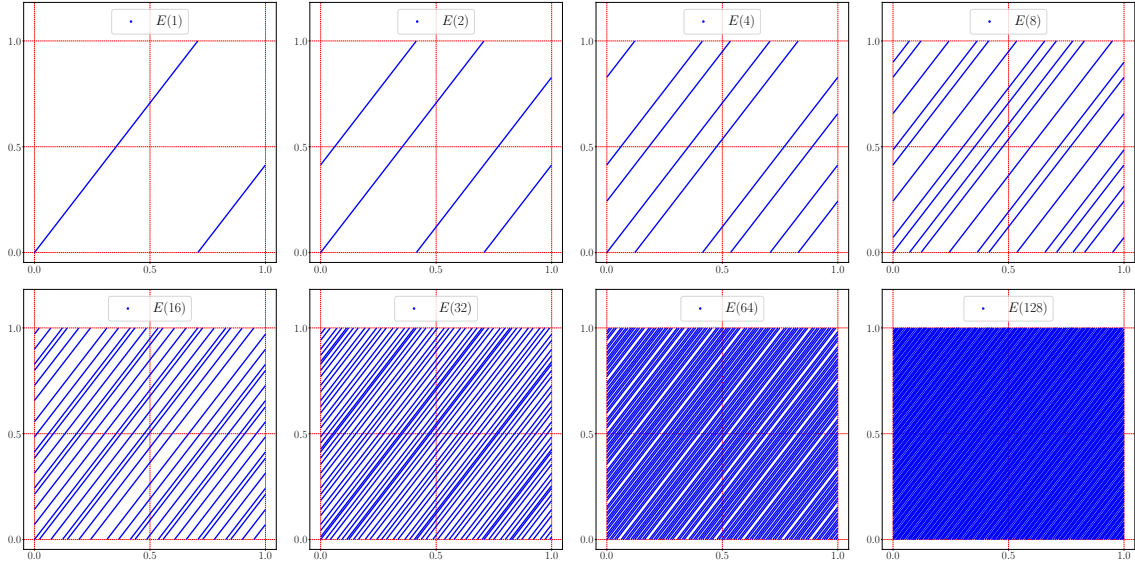


Figure 3: Illustrations of the denseness of $E(\infty)$ in $[0,1]^2$, where $E(r)$ is a winding of an “irrational” direction $[1, \sqrt{2}]^T$ on $[0, r)$, i.e., $E(r) = \{[\tau(t), \tau(\sqrt{2}t)]^T : t \in [0, r)\}$ with $\tau(t) = t - \lfloor t \rfloor$.

Proposition 2.2. *For any $K \in \mathbb{N}^+$, the following point set*

$$\left\{ \left[\sigma_1\left(\frac{w}{\pi+1}\right), \sigma_1\left(\frac{w}{\pi+2}\right), \dots, \sigma_1\left(\frac{w}{\pi+K}\right) \right]^T : w \in \mathbb{R} \right\} \subseteq [0,1]^K$$

is dense in $[0,1]^K$, where π is the ratio of the circumference of a circle to its diameter.

The proof of Proposition 2.2 can be found in Section 7. To prove the denseness in Proposition 2.2, we borrow some ideas from transcendental number theory and Diophantine approximations in number theory. The number π used in Proposition 2.2 is transcendental. It can be replaced by any other transcendental number.

Proposition 2.2 implies that for any given sample points $(k, y_k) \in \mathbb{R}^2$ with $y_k \in [0, 1]$ for $k = 1, 2, \dots, K$ and any $K \in \mathbb{N}^+$, there exists $w_0 \in \mathbb{R}$ such that the function $x \mapsto \sigma_1\left(\frac{w_0}{\pi+x}\right)$ can

fit the points $(k, y_k) \in \mathbb{R}^2$ for $k = 1, 2, \dots, K$ within an arbitrary pre-specified error $\varepsilon > 0$. To put it another way, for any $\varepsilon > 0$, there exists $w_0 \in \mathbb{R}$ such that $|\sigma_1(\frac{w_0}{\pi+k}) - y_k| < \varepsilon$ for all k .

As we shall see later in the proof of Proposition 2.2, the key point is the periodicity of the outer function σ_1 . Of course, the inner function $x \mapsto \frac{w_0}{\pi+x}$ is also necessary since it helps to adjust sample points for $x = 1, 2, \dots, K$. In fact, the inner function $x \mapsto \frac{w_0}{\pi+x}$ can be regarded as a variant of σ_2 via scaling and shifting. The periodicity has been explored to improve neural network approximation in the literature, e.g. the sine function in (Yarotsky and Zhevnerchuk, 2020) is periodic and the floor function $(\lfloor \cdot \rfloor)$ in (Shen et al., 2021a,b) is implicitly periodic because $x - \lfloor x \rfloor$ is periodic. We remark that a similar result holds if we replace σ_1 by a non-trivial periodic function and replace the sample locations $x = 1, 2, \dots, K$ by distinct rational numbers $r_1, r_2, \dots, r_K \in \mathbb{Q}$. See Section 7 for a further discussion.

Theorem 2.1 essentially proves Theorem 1.1 for the univariate case. To prove the general case, we need KST (Kolmogorov, 1957) given below to reduce a multivariate problem to a one-dimensional case.

Theorem 2.3 (Kolmogorov superposition theorem (KST) (Kolmogorov, 1957)). *There exist continuous functions $h_{i,j} \in C([0, 1])$ for $i = 0, 1, \dots, 2d$ and $j = 1, 2, \dots, d$ such that any continuous function $f \in C([0, 1]^d)$ can be represented as*

$$f(\mathbf{x}) = \sum_{i=0}^{2d} g_i \left(\sum_{j=1}^d h_{i,j}(x_j) \right) \quad \text{for any } \mathbf{x} = [x_1, x_2, \dots, x_d]^T \in [0, 1]^d,$$

where $g_i : \mathbb{R} \rightarrow \mathbb{R}$ is a continuous function for each $i \in \{0, 1, \dots, 2d\}$.

KST (Kolmogorov, 1957) is often used to reduce a multidimensional problem to a one-dimensional one. In fact, the compositional representation in KST can be regarded as a special neural network with (complicated) activation functions depending on the target function, which makes KST useless in practical computation. To avoid this dependency, an activation function was designed in (Maiorov and Pinkus, 1999) to construct neural network representations with $\mathcal{O}(d)$ neurons that can approximate functions in $C([-1, 1]^d)$ within an arbitrary error. Let us briefly summarize the main ideas in (Maiorov and Pinkus, 1999): 1) Identify a dense and countable subset $\{u_k\}_{k=1}^\infty$ of $C([-1, 1])$, e.g., polynomials with rational coefficients. 2) Construct an activation function ϱ to encode all $u_k(x)$ for $x \in [-1, 1]$. In fact, for each k , $u_k|_{[-1, 1]}$ is “stored” in ϱ on $[4k, 4k+2]$, and the values of ϱ on $[4k+2, 4k+4]$ are properly assigned to make ϱ a smooth and monotonically increasing function. That is, let $\varrho(x + 4k + 1) = a_k + b_k x + c_k u_k(x)$ for any $x \in [-1, 1]$ with carefully chosen constants a_k , b_k , and $c_k \neq 0$ such that $\varrho(x)$ can be a sigmoidal function. 3) For any $g \in C([-1, 1])$, there exists a one-hidden-layer ϱ -activated network with width 3 approximating g within an arbitrary error δ , i.e., there exists k such that $g \stackrel{\delta}{\approx} u_k =: \frac{\varrho(x+4k+1)-a_k-b_k x}{c_k}$. 4) Replace the inner and outer functions in KST with these one-hidden-layer networks to achieve a two-hidden-layer ϱ -activated network with width $\mathcal{O}(d)$ to approximate $f \in C([0, 1]^d)$ within an arbitrary error ε . As we can see, the key point of the construction in (Maiorov and Pinkus, 1999) is to encode a dense and countable subset of the target function space in an activation function.

Note that both (Maiorov and Pinkus, 1999) and this paper use KST to reduce dimension. However, the activation function of (Maiorov and Pinkus, 1999) is complicated without

any close form and there is no efficient numerical algorithm to evaluate it. After encoding a dense subset of continuous function into a single but complicated activation function, one only needs to construct affine linear transformations to select appropriate functions of this dense subset from this complicated activation function to construct approximation. Hence, such a complicated activation function simplifies the proof of the denseness, since the denseness is encoded in the activation function. As a contrast, we design a simple activation function with efficient numerical implementation (see Figure 1 for an illustration) achieving the universal approximation property with fixed-size networks, because simple and implementable activation functions are a basic requirement for a neural network to be used in applications. However, the proof of the denseness of a neural network generated by such a simple activation function becomes difficult. A sophisticated analysis will be developed in the rest of this paper to overcome the difficulties.

3. Experimentation

In this section, we will conduct two simple experiments as a proof of concept to explore the numerical performances of the EUAF activation function. Let us first discuss the numerical implementation of EUAF in PyTorch. To enable the automatic differentiation feature for EUAF, we need to implement EUAF based on PyTorch built-in functions. With the following four built-in functions $\text{abs}(x) = |x|$, $\text{floor}(x) = \lfloor x \rfloor$,

$$\text{softsign}(x) = \frac{x}{|x| + 1}, \quad \text{and} \quad \text{sign}(x) = \begin{cases} 1 & \text{if } x > 0, \\ 0 & \text{if } x = 0, \\ -1 & \text{if } x < 0, \end{cases}$$

we can represent EUAF as

$$\begin{aligned} \text{EUAF}(x) &= \begin{cases} \text{softsign}(x) & \text{if } x < 0, \\ \left\lfloor x - 2 \left\lfloor \frac{x+1}{2} \right\rfloor \right\rfloor & \text{if } x \geq 0 \end{cases} = \text{softsign}(x) \cdot \frac{1 - \text{sign}(x)}{2} + \left\lfloor x - 2 \left\lfloor \frac{x+1}{2} \right\rfloor \right\rfloor \cdot \frac{1 + \text{sign}(x)}{2}, \\ &= \text{softsign}(x) \cdot \frac{1 - \text{sign}(x)}{2} + \text{abs}\left(x - 2 \cdot \text{floor}\left(\frac{x+1}{2}\right)\right) \cdot \frac{1 + \text{sign}(x)}{2}. \end{aligned}$$

Thus, it is numerically cheap to compute EUAF and its subgradient. We believe the EUAF activation function can achieve good results in some real-world applications if proper optimization algorithms are developed for EUAF. Since our numerical experimentation just acts as a proof of concept, we choose two simple experiments: a function approximation experiment in Section 3.1 and a classification experiment in Section 3.2.

Next, let us briefly discuss when our EUAF activation function would outperform the practically used ones (e.g., ReLU, Sigmoid, and Softsign), which is based on full error analysis in Section 1.3. In our discussion, we take ReLU as an example and suppose the optimization error is well-controlled. Clearly, replacing the ReLU activation function by EUAF can reduce the approximation error, but would result in a large generalization error. Thus, we would expect that EUAF achieves better results than ReLU if the approximation error is larger than the generalization error. That means, the EUAF activation function would outperform ReLU in the following two cases.

514 • The approximation error is pretty large (e.g., the target function is sufficiently complicated).
515

516 • The generalization error is well-controlled (e.g., there are sufficiently many samples).

517 If a given problem does not belong to these two cases, one may consider replacing only
518 a small number of ReLUs by EUAFs. In the function approximation experiment in Section 3.1,
519 we first choose a complicated target function and then generate sufficiently many
520 samples to reduce the generalization error. In the classification experiment in Section 3.2,
521 we control the generalization error via three common methods: keeping network parameters
522 small via L2 regularization, dropout (Hinton et al., 2012; Srivastava et al., 2014), and batch
523 normalization (Ioffe and Szegedy, 2015).

524 3.1 Function approximation

525 We will design fully connected neural network (FCNN) architectures activated by ReLU
526 or EUAF to solve a function approximation problem. To better compare the approximation
527 power of ReLU and EUAF activation functions, we choose a complicated (oscillatory)
528 function f as the target function, where f is defined as

$$529 \quad f(x_1, x_2) = 0.6 \sin(8x_1) + 0.4 \sin(16x_2) \quad \text{for any } (x_1, x_2) \in [0, 1]^2.$$

530 To compare the numerical performances of ReLU and EUAF activation functions, we
531 design two FCNN architectures with different activation functions. Both of them have 4
532 hidden layers and each hidden layer has 80 neurons. For simplicity, we denote them as
533 FCNN1 and FCNN2. See illustrations of them in Figure 4. FCNN1 is a standard fully
534 connected ReLU network and FCNN2 can be regarded as a variant of FCNN1 by replacing
535 ReLU by EUAF.

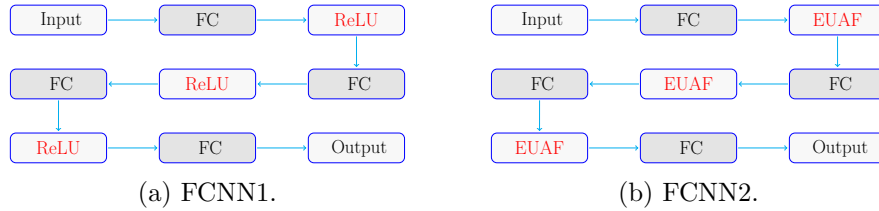


Figure 4: Illustrations of FCNN1 and FCNN2. FC represents a fully connected layer.

536 Before presenting the numerical results, let us present the hyper-parameters for training
537 FCNN1 and FCNN2. We randomly choose 10^6 training samples and 10^5 test samples in
538 $[0, 1]^2$. The number of epochs and the batch size are set to 500 and 256, respectively.
539 We adopt RAdam (Liu et al., 2020) as the optimization method and the learning rate is
540 $0.002 \times 0.9^{i-1}$ in epochs $5(i-1) + 1$ to $5i$ for $i = 1, 2, \dots, 100$. Several loss functions are used
541 to estimate the training and test losses, including the mean squared error (MSE), the mean
542 absolute error (MAE), and the maximum (MAX) loss functions. To explain MSE, MAE
543 and MAX losses, we denote ϕ as the network-generated function and $\mathbf{x}_1, \dots, \mathbf{x}_m$ as the test
544 samples ($m = 10^5$ in our setting). Then, the MSE loss is given by $\frac{1}{m} \sum_{i=1}^m (\phi(\mathbf{x}_i) - f(\mathbf{x}_i))^2$,
545 the MAE loss is given by $\frac{1}{m} \sum_{i=1}^m |\phi(\mathbf{x}_i) - f(\mathbf{x}_i)|$, and the MAX loss is given by $\max \{|\phi(\mathbf{x}_i) -$

546 $f(x_i) : i = 1, 2, \dots, m\}$. The MSE loss is used in our training process. In the settings above,
 547 we repeat the experiment 12 times and discard 2 top-performing and 2 bottom-performing
 548 trials by using the average of test losses (MSE) in the last 100 epochs as the performance
 549 criterion. For each epoch, we adopt the average of training (test) losses in the rest 8 trials
 550 as the target training (test) loss.

551 Next, let us present the experiment results to compare the numerical performances
 552 of ReLU and EUAF activation functions. Training and test losses (MSE) over epochs for
 553 FCNN1 and FCNN2 are summarized in Figure 5. In Table 1, we present a comparison of
 554 FCNN1 and FCNN2 for the average of the test losses in the last 100 epochs measured in
 555 several loss functions. As we can see from Figure 5 and Table 1, FCNN2 performs better
 556 than FCNN1. That means replacing ReLU by EUAF would improve experiment results.

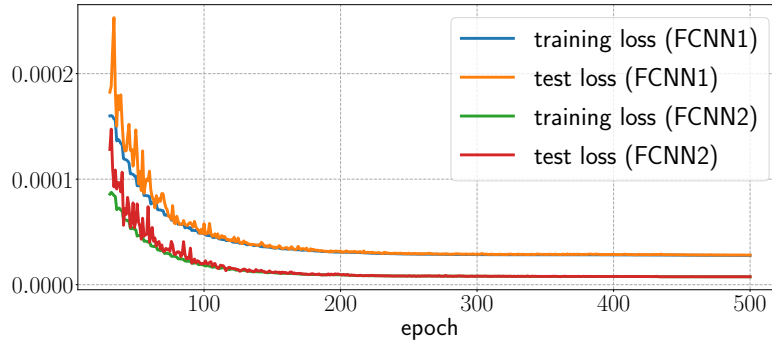


Figure 5: Training and test losses (MSE) in epochs 25-500 for FCNN1 and FCNN2.

Table 1: Test loss comparison.

activation function		Test loss		
		MSE	MAE	MAX
FCNN1	ReLU	2.34×10^{-5}	3.04×10^{-3}	2.49×10^{-2}
FCNN2	EUAF	5.00×10^{-6}	1.42×10^{-3}	9.68×10^{-3}

557 3.2 Classification

558 The goal of a classification problem with $J \in \mathbb{N}^+$ classes is to identify a classification
 559 function f defined by

$$560 \quad f(\mathbf{x}) = j \quad \text{for any } \mathbf{x} \in E_j \text{ and } j = 0, 1, \dots, J-1,$$

561 where E_0, E_1, \dots, E_{J-1} are pairwise disjoint bounded closed subsets of \mathbb{R}^d and all samples
 562 with a label j are contained in E_j for each j . Such a classification function f can be
 563 continuously extended to \mathbb{R}^d , which means a classification problem can also be regarded as
 564 a continuous function approximation problem. We take the case $J = 2$ as an example to
 565 illustrate the extension. The multiclass case is similar. By defining

$$566 \quad \text{dist}(\mathbf{x}, E_i) := \inf_{\mathbf{y} \in E_i} \|\mathbf{x} - \mathbf{y}\|_2 \quad \text{for any } \mathbf{x} \in \mathbb{R}^d \text{ and } i = 0, 1,$$

we have $\text{dist}(\mathbf{x}, E_0) + \text{dist}(\mathbf{x}, E_1) > 0$ for any $\mathbf{x} \in \mathbb{R}^d$. Thus, we can define

$$\tilde{f}(\mathbf{x}) := \frac{\text{dist}(\mathbf{x}, E_0)}{\text{dist}(\mathbf{x}, E_0) + \text{dist}(\mathbf{x}, E_1)} \quad \text{for any } \mathbf{x} \in \mathbb{R}^d.$$

It is easy to verify that \tilde{f} is continuous on \mathbb{R}^d and

$$\tilde{f}(\mathbf{x}) = \begin{cases} 0 & \text{if } \mathbf{x} \in E_0, \\ 1 & \text{if } \mathbf{x} \in E_1 \end{cases} = f(\mathbf{x}) \quad \text{for any } \mathbf{x} \in E_0 \cup E_1.$$

That means \tilde{f} is a continuous extension of f . That means we can apply our theory to classification problems.

We will design convolutional neural network (CNN) architectures activated by ReLU or EUAF to solve a classification problem corresponding to a standard benchmark dataset Fashion-MNIST (Xiao et al., 2017). This dataset consists of a training set of 60000 samples and a test set of 10000 samples. Each sample is a 28×28 grayscale image, associated with a label from 10 classes. To compare the numerical performances of ReLU and EUAF activation functions, we design two small CNN architectures with different activation functions. Both of them have two convolutional layers and two fully connected layers. For simplicity, we denote them as CNN1 and CNN2. See illustrations of them in Figure 6. We present more details of CNN1 and CNN2 in Table 2. CNN1 is activated by ReLU, while CNN2 is activated by ReLU and EUAF. In CNN2, only one channel (neuron) of a convolutional (fully connected) hidden layer is activated by EUAF. CNN2 can be regarded as a variant of CNN1 by replacing a small number of ReLUs by EUAFs. This follows a natural question: Why do we not make all (or most) neurons (channels) of CNN2 activated by EUAF? We use only a few EUAFs in CNN2 for two reasons listed below.

- Since the number of available training samples is limited, using too many EUAF activation functions would lead to a large generalization error.
- The key difference of EUAF to the practical used activation functions (e.g., ReLU, Sigmoid, and Softsign) is the periodic part on $[0, \infty)$. As we shall see later in the proof of our main theorem, only a small number of neurons in the constructed network require the periodic property. Thus, we would expect that neural networks activated by the practical used activation functions and a few EUAFs are super expressive.

Next, let us discuss why we choose relatively small network architectures. Since the Fashion-MNIST classification problem is simple, the expressive power of a relatively large ReLU CNN architecture is enough. That means there is no need to introduce EUAF if the network architecture is relatively large. Acting as a proof of concept, our experimentation only considers a simple classification problem that classifies images in the Fashion-MNIST dataset. We believe EUAF would be useful for complicated classification problems.

We remark that we use CNNs to approximate an equivalent variant \hat{f} of the original classification function f mentioned previously, where \hat{f} is given by

$$\hat{f}(\mathbf{x}) = \mathbf{e}_j \quad \text{for any } \mathbf{x} \in E_j \text{ and } j = 0, 1, \dots, J-1,$$

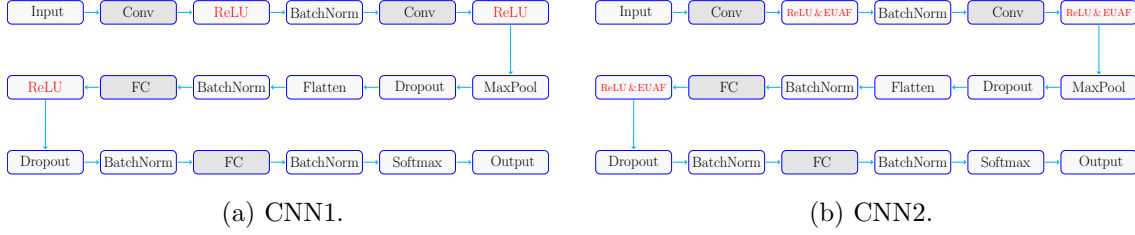


Figure 6: Illustrations of CNN1 and CNN2. Conv and FC represent convolutional and fully connected layers, respectively.

Table 2: Details of CNN1 and CNN2.

layers	activation function		output size of each layer	dropout	batch normalization
	CNN1	CNN2			
input $\in \mathbb{R}^{28 \times 28}$			28×28		
Conv-1: $1 \times (3 \times 3)$, 24	ReLU	EUAF, $1 \times (26 \times 26)$ ReLU, $23 \times (26 \times 26)$	$24 \times (26 \times 26)$		yes
Conv-2: $24 \times (3 \times 3)$, 24	ReLU	EUAF, $1 \times (24 \times 24)$ ReLU, $23 \times (24 \times 24)$	3456 (MaxPool & Flatten)	0.25	yes
FC-1: 3456, 48	ReLU	EUAF, 1 ReLU, 47	48	0.5	yes
FC-2: 48, 10			10 (Softmax)		yes
output $\in \mathbb{R}^{10}$					

where $\{\mathbf{e}_1, \mathbf{e}_2, \dots, \mathbf{e}_J\}$ is the standard basis of \mathbb{R}^J , i.e., $\mathbf{e}_j \in \mathbb{R}^J$ denotes the vector with a 1 in the j -th coordinate and 0's elsewhere.

Before presenting the numerical results, let us present the hyper-parameters for training two CNN architectures above. We use the cross-entropy loss function to evaluate the loss. The number of epochs and the batch size are set to 500 and 128, respectively. We adopt RAdam (Liu et al., 2020) as the optimization method. The weight decay of the optimizer is 0.0001 and the learning rate is $0.002 \times 0.9^{i-1}$ in epochs $5(i-1)+1$ to $5i$ for $i = 1, 2, \dots, 100$. All training (test) samples in the Fashion-MNIST dataset are standardized in our experiment, i.e., we rescale all training (test) samples to have a mean of 0 and a standard deviation of 1. In the settings above, we repeat the experiment 48 times and discard 8 top-performing and 8 bottom-performing trials by using the average of test accuracy in the last 100 epochs as the performance criterion. For each epoch, we adopt the average of test accuracies in the rest 32 trials as the target test accuracy.

Let us present the experiment results to compare the numerical performances of CNN1 and CNN2. The test accuracy comparison of CNN1 and CNN2 is summarized in Table 3. For each of CNN1 and CNN2, we present the largest test accuracy, the average of largest 100 test accuracies over epochs, and the average of test accuracies in the last 100 epochs. For an intuitive comparison, we also provide illustrations of the test accuracy over epochs for CNN1 and CNN2 in Figure 7. As we can see from Table 3 and Figure 7, CNN2 performs better than CNN1. That means replacing a small number of ReLUs by EUAFs would improve the experiment results.

Table 3: Test accuracy comparison.

	activation function	largest accuracy	average of largest 100 accuracies	average accuracy in last 100 epochs
CNN1	ReLU	0.933066	0.932852	0.932698
CNN2	ReLU and EUAF	0.933922	0.933685	0.933508

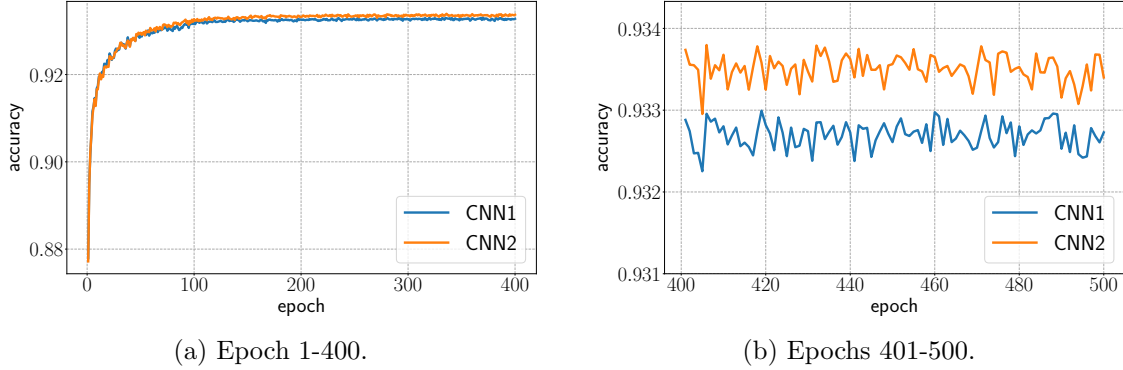


Figure 7: Test accuracy over epochs.

4. Other examples of UAFs

This section aims at designing new UAFs with additional properties such as smooth or sigmoidal functions. As discussed in the introduction and shown in the proof of our main theorem, the construction of UAFs mainly relies on three properties: high nonlinearity, periodicity, and the capacity to reproduce step functions. The EUAF σ defined in Equation (3) is a simple and typical example of UAFs satisfying these three properties. Indeed, having these properties plays an important role in our proof and is a necessary but not sufficient condition for designing a UAF. In other words, these properties are important, but cannot guarantee the successful construction of UAFs.

Here, we present another idea to design new UAFs, which mainly relies on the following observation: If a UAF ϱ can be approximated by a fixed-size network activated by a new function $\tilde{\varrho}$ within an arbitrary error on any bounded interval, then $\tilde{\varrho}$ is also a UAF. Such an observation is a direct result of the lemma below.

Lemma 4.1. *Let $\varrho, \tilde{\varrho} : \mathbb{R} \rightarrow \mathbb{R}$ be two functions with $\varrho \in C(\mathbb{R})$. For an arbitrary given function $f \in [a, b]^d \rightarrow \mathbb{R}$ and $\varepsilon > 0$, suppose that the following two conditions hold:*

- *There exists a function ϕ_ϱ realized by a ϱ -activated network with width N and depth L such that*

$$|\phi_\varrho(\mathbf{x}) - f(\mathbf{x})| < \varepsilon/2 \quad \text{for any } \mathbf{x} \in [a, b]^d.$$

- *For any $M > 0$ and each $\delta \in (0, 1)$, there exists a function ϱ_δ realized by a $\tilde{\varrho}$ -activated network with width \tilde{N} and depth \tilde{L} such that*

$$\varrho_\delta(t) \rightrightarrows \varrho(t) \quad \text{as } \delta \rightarrow 0^+ \quad \text{for any } t \in [-M, M],$$

where \rightrightarrows denotes the uniform convergence.

Then, there exists a function $\phi = \phi_{\tilde{\varrho}}$ generated by a $\tilde{\varrho}$ -activated network with width $N \cdot \tilde{N}$ and depth $L \cdot \tilde{L}$ such that

$$|\phi(\mathbf{x}) - f(\mathbf{x})| < \varepsilon \quad \text{for any } \mathbf{x} \in [a, b]^d.$$

The proof of Lemma 4.1 is placed in Section 4.3. Based on Lemma 4.1, we will propose two UAFs with better mathematical properties. That is, the idea of designing a C^s UAF is given in Section 4.1 and a sigmoidal UAF is constructed in detail in Section 4.2.

4.1 Smooth UAF

The smoothness of a function is one of the most desired properties in mathematical modeling and computation. The EUAF σ is continuous but not smooth. So we will show how to construct a C^s UAF based on an existing one. The key point is the fact that the integral of a continuous function is continuously differentiable.

Suppose ϱ is a continuous UAF. Define

$$\tilde{\varrho}(x) := \int_0^x \varrho(t) dt \quad \text{for any } x \in \mathbb{R}.$$

For any $M > 0$, it holds that

$$\frac{\tilde{\varrho}(x + \delta) - \tilde{\varrho}(x)}{\delta} = \frac{1}{\delta} \int_x^{x+\delta} \varrho(t) dt \rightrightarrows \varrho(x) \quad \text{as } \delta \rightarrow 0^+ \quad \text{for any } x \in [-M, M].$$

This means ϱ can be approximated by a one-hidden-layer $\tilde{\varrho}$ -activated network with width 2 arbitrarily well on any bounded interval. It follows that $\tilde{\varrho}$ is also a UAF. By repeated applications of the above idea, one could easily construct a C^s UAF.

In particular, set $\varrho_0 = \sigma$ and define $\varrho_1, \varrho_2, \dots, \varrho_s$ by induction as follows.

$$\varrho_{i+1}(x) := \int_0^x \varrho_i(t) dt \quad \text{for any } x \in \mathbb{R} \text{ and } i \in \{0, 1, \dots, s-1\}. \quad (8)$$

Then, ϱ_s is a C^s UAF as shown in the following theorem.

Theorem 4.2. *Let $\varrho_s \in C^s(\mathbb{R})$ be the function defined in Equation (8) for any $s \in \mathbb{N}^+$. Then, for any $f \in C([a, b]^d)$ and $\varepsilon > 0$, there exists a function ϕ generated by a ϱ_s -activated network with width $72sd(2d+1)$ and depth 11 such that*

$$|\phi(\mathbf{x}) - f(\mathbf{x})| < \varepsilon \quad \text{for any } \mathbf{x} \in [a, b]^d.$$

Proof. For any $i \in \{0, 1, \dots, s-1\}$ and any $M > 0$, it is easy to verify that

$$\frac{\varrho_{i+1}(x + \delta) - \varrho_{i+1}(x)}{\delta} = \frac{1}{\delta} \int_x^{x+\delta} \varrho_i(t) dt \rightrightarrows \varrho_i(x) \quad \text{as } \delta \rightarrow 0^+ \quad \text{for any } x \in [-M, M].$$

This means ϱ_i can be approximated by a one-hidden-layer ϱ_{i+1} -activated network with width 2 arbitrarily well on any bounded interval. By induction, one could easily prove that $\varrho_0 = \sigma$ can be approximated by a one-hidden-layer ϱ_s -activated network with width $2s$ arbitrarily well on any bounded interval. That is, for each $\delta \in (0, 1)$, there exists a function $\sigma_{s,\delta}$ realized by a ϱ_s -activated network with width $2s$ and depth 1 such that

$$\sigma_{s,\delta}(t) \rightrightarrows \sigma(t) \quad \text{as } \delta \rightarrow 0^+ \quad \text{for any } t \in [-M, M].$$

By Theorem 1.1, there exists a function ϕ_σ generated by a σ -activated network with width $36d(2d+1)$ and depth 11 such that

$$|\phi_\sigma(\mathbf{x}) - f(\mathbf{x})| < \varepsilon/2 \quad \text{for any } \mathbf{x} \in [a, b]^d.$$

Then, by Lemma 4.1, there exists another function $\phi = \phi_{\varrho_s}$ realized by a ϱ_s -activated network with width $2s \times 36d(2d+1) = 72sd(2d+1)$ and depth $1 \times 11 = 11$ such that

$$|\phi(\mathbf{x}) - f(\mathbf{x})| < \varepsilon \quad \text{for any } \mathbf{x} \in [a, b]^d.$$

So we finish the proof. \square

4.2 Sigmoidal UAF

Many activation functions used in real-world applications are sigmoidal functions. Generally, we say a function $g : \mathbb{R} \rightarrow \mathbb{R}$ is sigmoidal (or sigmoid, e.g., see (Han and Moraga, 1995)) if it satisfies the following conditions.

- Bounded: $\lim_{x \rightarrow \infty} g(x) = 1$ and $\lim_{x \rightarrow -\infty} g(x) = -1$ (or 0).
- Differentiable: $g'(x)$ exists and continuous for all $x \in \mathbb{R}$.
- Increasing: $g'(x)$ is non-negative for all $x \in \mathbb{R}$.

Our goal is to construct a sigmoidal UAF. To this end, we need to design a new function $\tilde{\sigma}$ based on σ such that σ can be reproduced/approximated by a $\tilde{\sigma}$ -activated network with a fixed size. Making $\tilde{\sigma}$ bounded and increasing is not difficult. The key is to make $\tilde{\sigma}$ continuously differentiable, which can be true by the fact that the integral of a continuous function is continuously differentiable. To be exact, we can define $\tilde{\sigma}$ as follows.

- For $x \in (-\infty, 0]$, define $\tilde{\sigma}(x) := \sigma(x) = \frac{x}{-x+1}$.
- For $x \in (0, \infty)$, define

$$\tilde{\sigma}(x) := \int_0^x \frac{c\sigma(t) + 1}{(2t+1)^2} dt, \quad \text{where } c = \frac{1}{2 \int_0^\infty \frac{\sigma(t)}{(2t+1)^2} dt} \approx 2.554.$$

We remark that there are many possible choices for the integrand in the above definition of $\sigma(x)$ for $x \in (0, \infty)$. Here, we just give a simple example. See an illustration of $\tilde{\sigma}$ in Figure 8.

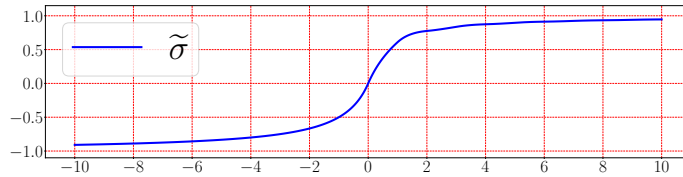


Figure 8: An illustration of $\tilde{\sigma}$ on $[-10, 10]$.

Then, $\tilde{\sigma}$ is a sigmoidal function as verified below.

705 • Clearly, $\lim_{x \rightarrow -\infty} \tilde{\sigma}(x) = \lim_{x \rightarrow -\infty} \frac{x}{-x+1} = -1$. Moreover,

$$706 \quad \lim_{x \rightarrow \infty} \tilde{\sigma}(x) = \int_0^\infty \frac{c\sigma(t) + 1}{(2t+1)^2} dt = \frac{1}{2} + \int_0^\infty \frac{1}{(2t+1)^2} dt = 1.$$

707 • Obviously, $\tilde{\sigma}$ is continuously differentiable on $(-\infty, 0)$ and $(0, \infty)$. Meanwhile, we have
708 $\tilde{\sigma}'(0) = 1$ and $\lim_{x \rightarrow 0} \tilde{\sigma}'(x) = 1$. Therefore, we have $\tilde{\sigma} \in C^1(\mathbb{R})$ as desired.

709 • For $x \in (-\infty, 0)$, $\tilde{\sigma}'(x) = \frac{1}{(-x+1)^2} > 0$. For $x = 0$, $\tilde{\sigma}'(x) = 1 > 0$. For $x \in (0, \infty)$,
710 $\tilde{\sigma}'(x) = \frac{c\sigma(x)+1}{(2x+1)^2} > 0$. That is, $\tilde{\sigma}'(x) > 0$ for all $x \in \mathbb{R}$.

711 Based on Theorem 1.1 corresponding to σ , we establish a similar theorem for $\tilde{\sigma}$, Theo-
712 rem 4.3 below, showing that fixed-size $\tilde{\sigma}$ -activated networks can also approximate continuous
713 functions within an arbitrary error on a hypercube.

714 **Theorem 4.3.** *For any $f \in C([a, b]^d)$ and $\varepsilon > 0$, there exists a function ϕ generated by a*
715 *$\tilde{\sigma}$ -activated network with width $1044d(2d+1)$ and depth 66 such that*

$$716 \quad |\phi(\mathbf{x}) - f(\mathbf{x})| < \varepsilon \quad \text{for any } \mathbf{x} \in [a, b]^d.$$

717 To prove this theorem based on Theorem 1.1, we only need to show σ can be approx-
718 imated by a fixed-size $\tilde{\sigma}$ -activated network within an arbitrary error on any pre-specified
719 interval as presented in the following lemma.

720 **Lemma 4.4.** *For any $\varepsilon > 0$ and any $M > 0$, there exists a function ϕ realized by a $\tilde{\sigma}$ -activated*
721 *network with width 29 and depth 6 such that*

$$722 \quad |\phi(x) - \sigma(x)| < \varepsilon \quad \text{for any } x \in [-M, M].$$

723 The proof of Lemma 4.4 can be found later. By assuming Lemma 4.4 is true, we can
724 give the proof of Theorem 4.3.

725 *Proof of Theorem 4.3.* By Theorem 1.1, there exists a function ϕ_σ generated by a σ -activated
726 network with width $36d(2d+1)$ and depth 11 such that

$$727 \quad |\phi_\sigma(\mathbf{x}) - f(\mathbf{x})| < \varepsilon/2 \quad \text{for any } \mathbf{x} \in [a, b]^d.$$

728 By Lemma 4.4, for any $M > 0$ and each $\delta \in (0, 1)$, there exists a function σ_δ realized by a
729 $\tilde{\sigma}$ -activated network with width 29 and depth 6 such that

$$730 \quad \sigma_\delta(t) \rightrightarrows \sigma(t) \quad \text{as } \delta \rightarrow 0^+ \quad \text{for any } t \in [-M, M].$$

731 Then, by Lemma 4.1, there exists another function $\phi = \phi_{\tilde{\sigma}}$ realized by a $\tilde{\sigma}$ -activated network
732 with width $29 \times 36d(2d+1) = 1044d(2d+1)$ and depth $6 \times 11 = 66$ such that

$$733 \quad |\phi(\mathbf{x}) - f(\mathbf{x})| < \varepsilon \quad \text{for any } \mathbf{x} \in [a, b]^d.$$

734 So we finish the proof. □

735 Finally, let us present the detailed proof of Lemma 4.4.

736 *Proof of Lemma 4.4.* Since $1 = \tilde{\sigma}'(0) = \lim_{x \rightarrow 0} \frac{\tilde{\sigma}(x)}{x}$, it is easy to show: For any $\mathcal{E} > 0$ and
 737 any $R > 0$, there exists a sufficiently small $w > 0$ such that

$$738 \quad \|\tilde{\sigma}(wx)/w - x\|_{L^\infty([-R, R])} < \mathcal{E}.$$

739 Thus, we may assume the identity map is allowed to be the activation function in $\tilde{\sigma}$ -activated
 740 networks. Without loss of generality, we may assume $M \geq 2$ because $\widetilde{M} = \max\{2, M\}$ implies
 741 $[-M, M] \subseteq [-\widetilde{M}, \widetilde{M}]$.

742 For simplicity, we denote $\mathcal{H}_{\tilde{\sigma}}(N, L)$ as the (hypothesis) space of functions generated
 743 by $\tilde{\sigma}$ -activated networks with width N and depth L . Then the proof can be roughly divided
 744 into three steps as follows.

- 745 (1) Design $\Gamma \in \mathcal{H}_{\tilde{\sigma}}(9, 2)$ to reproduce xy on $[-4\widetilde{M}, 4\widetilde{M}]^2$, where $\widetilde{M} = (M + 1)^2$.
- 746 (2) Design $\psi_\delta \in \mathcal{H}_{\tilde{\sigma}}(20, 4)$ based on the first step to approximate σ well on $[0, M]$.
- 747 (3) Design $\phi \in \mathcal{H}_{\tilde{\sigma}}(29, 6)$ based on the previous two steps to approximate σ well on $[-M, M]$.

748 The details of the three steps can be found below.

749 **Step 1:** Design $\Gamma \in \mathcal{H}_{\tilde{\sigma}}(9, 2)$ to reproduce xy on $[-4\widetilde{M}, 4\widetilde{M}]^2$.

750 Observe that

$$751 \quad \tilde{\sigma}(y) + 1 = \frac{y}{|y| + 1} + 1 = \frac{y}{-y + 1} + 1 = \frac{1}{-y + 1} \quad \text{for any } y \leq 0.$$

752 For any $x \in [-4, 4]$, we have $-x - 4 \leq 0$ and $-x - 5 \leq 0$, implying

$$\begin{aligned} 753 \quad & \tilde{\sigma}(-x - 4) - \tilde{\sigma}(-x - 5) = \left(\tilde{\sigma}(-x - 4) + 1 \right) - \left(\tilde{\sigma}(-x - 5) + 1 \right) \\ & = \frac{1}{-(-x - 4) + 1} - \frac{1}{-(-x - 5) + 1} = \frac{1}{x + 5} - \frac{1}{x + 6} = \frac{1}{(x + 5)(x + 6)}. \end{aligned}$$

754 It follows from $1 - \frac{90}{(x+5)(x+6)} \leq 0$ for any $x \in [-4, 4]$ that

$$755 \quad \tilde{\sigma}\left(1 - \frac{90}{(x+5)(x+6)}\right) + 1 = \frac{1}{-\left(1 - \frac{90}{(x+5)(x+6)}\right) + 1} = \frac{x^2 + 11x + 30}{90},$$

756 implying

$$\begin{aligned} & x^2 = 90\tilde{\sigma}\left(1 - \frac{90}{(x+5)(x+6)}\right) + 90 - (11x + 30) \\ 757 \quad & = 90\tilde{\sigma}\left(1 - 90(\tilde{\sigma}(-x - 4) - \tilde{\sigma}(-x - 5))\right) - 11x + 60 \\ & = 90\tilde{\sigma}\left(1 - 90\tilde{\sigma}(-x - 4) + 90\tilde{\sigma}(-x - 5)\right) - 11x + 60. \end{aligned} \tag{9}$$

758 Thus, x^2 can be realized by a $\tilde{\sigma}$ -activated network with width 3 and depth 2 on $[-4, 4]$. Set
 759 $\widetilde{M} = (M + 1)^2$. Then, for any $x, y \in [-4\widetilde{M}, 4\widetilde{M}]$, we have $\frac{x}{2\widetilde{M}}, \frac{y}{2\widetilde{M}}, \frac{x+y}{2\widetilde{M}} \in [-4, 4]$. Recall the
 760 fact

$$761 \quad xy = 2\widetilde{M}^2 \left(\left(\frac{x+y}{2\widetilde{M}} \right)^2 - \left(\frac{x}{2\widetilde{M}} \right)^2 - \left(\frac{y}{2\widetilde{M}} \right)^2 \right).$$

Thus, xy can be realized by a $\tilde{\sigma}$ -activated network with width 9 and depth 2 for any $x, y \in [-4\widetilde{M}, 4\widetilde{M}]$. That is, there exists $\Gamma \in \mathcal{H}_{\tilde{\sigma}}(9, 2)$ such that $\Gamma(x, y) = xy$ on $[-4\widetilde{M}, 4\widetilde{M}]^2$.

Step 2: Design $\psi_\delta \in \mathcal{H}_{\tilde{\sigma}}(9, 4)$ to approximate σ well on $[0, M]$.

Recall that x^2 can be realized by a $\tilde{\sigma}$ -activated network with width 3 and depth 2 on $[-4, 4]$. There exists $\psi_1 \in \mathcal{H}_{\tilde{\sigma}}(3, 2)$ such that

$$\psi_1(x) = \frac{(2x+1)^2}{(2M+1)^2} \quad \text{for any } x \in [-M, M].$$

Define

$$\psi_{2,\delta}(x) := \frac{\tilde{\sigma}(x+\delta) - \tilde{\sigma}(x)}{\delta} \quad \text{for any } x \in \mathbb{R}.$$

Then, we have $\psi_{2,\delta} \in \mathcal{H}_{\tilde{\sigma}}(2, 1)$ and

$$\psi_{2,\delta}(x) := \frac{\tilde{\sigma}(x+\delta) - \tilde{\sigma}(x)}{\delta} \Rightarrow \frac{d}{dx} \tilde{\sigma}(x) = \frac{c\sigma(x)+1}{(2x+1)^2} \quad \text{as } \delta \rightarrow 0^+,$$

for any $x \in [0, M]$ and

$$c = \frac{1}{2 \int_0^\infty \frac{\sigma(t)}{(2t+1)^2} dt} \approx 2.554.$$

Define

$$\psi_\delta(x) := \frac{(2M+1)^2}{c} \Gamma(\psi_1(x), \psi_{2,\delta}(x)) - \frac{1}{c} \quad \text{for any } x \in \mathbb{R}.$$

Since $\Gamma \in \mathcal{H}_{\tilde{\sigma}}(9, 2)$, $\psi_1 \in \mathcal{H}_{\tilde{\sigma}}(3, 2)$, and $\psi_{2,\delta} \in \mathcal{H}_{\tilde{\sigma}}(2, 1)$, we have $\psi_\delta \in \mathcal{H}_{\tilde{\sigma}}(9, 4)$.

Clearly, for any $x \in [0, M]$, we have $\psi_1(x) = \frac{(x+1)^2}{(2M+1)^2} \in [0, 1]$ and $\psi_{2,\delta}(x) \approx \frac{c\sigma(x)+1}{(2x+1)^2} \in [0, 3.6]$, implying $\psi_1(x), \psi_{2,\delta}(x) \in [-4, 4] \subseteq [-4\widetilde{M}, 4\widetilde{M}]^2$ for any small $\delta > 0$. Thus, for any $x \in [0, M]$, as δ goes to 0^+ , we get

$$\begin{aligned} \psi_\delta(x) &= \frac{(2M+1)^2}{c} \Gamma(\psi_1(x), \psi_{2,\delta}(x)) - \frac{1}{c} = \frac{(2M+1)^2}{c} \cdot \psi_1(x) \cdot \psi_{2,\delta}(x) - \frac{1}{c} \\ &\Rightarrow \frac{(2M+1)^2}{c} \cdot \frac{(2x+1)^2}{(2M+1)^2} \cdot \frac{c\sigma(x)+1}{(2x+1)^2} - \frac{1}{c} = \sigma(x). \end{aligned}$$

That is, for any $x \in [0, M]$,

$$\psi_\delta(x) \Rightarrow \sigma(x) \quad \text{as } \delta \rightarrow 0^+.$$

Step 3: Design $\phi \in \mathcal{H}_{\tilde{\sigma}}(29, 6)$ to approximate σ well on $[-M, M]$.

Note that $\tilde{\sigma}(x) = \sigma(x)$ for all $x \in [-M, 0)$ and $\psi_\delta(x)$ approximates $\sigma(x)$ well for all $x \in [0, M]$. Then, $\tilde{\sigma}(x) \cdot \mathbb{1}_{\{x \in [-M, 0)\}} + \psi_\delta(x) \cdot \mathbb{1}_{\{x \in [0, M]\}}$ approximates $\sigma(x)$ well for all $x \in [-M, M]$. To design ϕ approximating σ well on $[-M, M]$, we need to design a $\tilde{\sigma}$ -activated network to approximate an indicator function $\mathbb{1}_{\{x \in [0, M]\}}$ well.

It is impossible to approximate $\mathbb{1}_{\{x \in [0, M]\}}$ well by a $\tilde{\sigma}$ -activated network due to the continuity of $\tilde{\sigma}$. However, we define a continuous function g to replace $\mathbb{1}_{\{x \in [0, M]\}}$. By the continuity of $\tilde{\sigma}$ and σ , there exists $\eta_0 \in (0, 1)$ such that

$$|\tilde{\sigma}(x)| < \varepsilon/6 \quad \text{and} \quad |\sigma(x)| < \varepsilon/6 \quad \text{for any } x \in [0, \eta_0]. \quad (10)$$

792 Then we define

$$793 \quad g(x) := \frac{\text{ReLU}(x) - \text{ReLU}(x - \eta_0)}{\eta_0}, \quad \text{where } \text{ReLU}(x) = \max\{0, x\} \quad \text{for any } x \in \mathbb{R}.$$

794 See Figure 9 for an illustration of g .

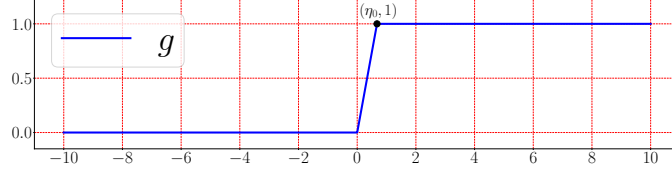


Figure 9: An illustration of g on $[-10, 10]$.

795 We will construct a $\tilde{\sigma}$ -activated network to approximate g well. To this end, we first
 796 design a $\tilde{\sigma}$ -activated network to approximate the ReLU function well. For $x \in [-M-1, M+1]$,
 797 we have $\frac{x}{M+1} + 1 \in [0, 2] \subseteq [0, M]$, implying

$$798 \quad 1 - \psi_\delta\left(\frac{x}{M+1} + 1\right) \rightrightarrows 1 - \sigma\left(\frac{x}{M+1} + 1\right) = \left|\frac{x}{M+1}\right| \quad \text{as } \delta \rightarrow 0^+,$$

799 where the last equality comes from $1 - \sigma(y) = |y - 1|$ for any $y \in [0, 2]$. Note that $\text{ReLU}(x) =$
 800 $\frac{x}{2} + \frac{|x|}{2} = \frac{x}{2} + \frac{M+1}{2} \cdot \left|\frac{x}{M+1}\right|$ for any $x \in [-M-1, M+1]$. Define

$$801 \quad \tilde{g}_\delta(x) := \frac{x}{2} + \frac{M+1}{2} \left(1 - \psi_\delta\left(\frac{x}{M+1} + 1\right)\right) \quad \text{for any } x \in \mathbb{R}.$$

802 Then, $\psi_\delta \in \mathcal{H}_{\tilde{\sigma}}(9, 4)$ implies $\tilde{g}_\delta \in \mathcal{H}_{\tilde{\sigma}}(10, 4)$. Moreover, for any $x \in [-M-1, M+1]$,

$$803 \quad \tilde{g}_\delta(x) \rightrightarrows \frac{x}{2} + \frac{M+1}{2} \cdot \left|\frac{x}{M+1}\right| = \text{ReLU}(x) \quad \text{as } \delta \rightarrow 0^+.$$

804 Define

$$805 \quad g_\delta(x) := \frac{\tilde{g}_\delta(x) - \tilde{g}_\delta(x - \eta_0)}{\eta_0} \quad \text{for any } x \in \mathbb{R}.$$

806 Clearly, $\tilde{g}_\delta \in \mathcal{H}_{\tilde{\sigma}}(10, 4)$ implies $g_\delta \in \mathcal{H}_{\tilde{\sigma}}(20, 4)$. For any $x \in [-M, M]$, we have $x, x - \eta_0 \in$
 807 $[-M-1, M+1]$, implying

$$808 \quad g_\delta(x) = \frac{\tilde{g}_\delta(x) - \tilde{g}_\delta(x - \eta_0)}{\eta_0} \rightrightarrows \frac{\text{ReLU}(x) - \text{ReLU}(x - \eta_0)}{\eta_0} = g(x) \quad \text{as } \delta \rightarrow 0^+.$$

809 Next, define

$$810 \quad \phi_\delta(x) := \Gamma\left(\psi_\delta(x), g_\delta(x)\right) + \Gamma\left(\tilde{\sigma}(x), 1 - g_\delta(x)\right) \quad \text{for any } x \in \mathbb{R}.$$

811 Since $\Gamma \in \mathcal{H}_{\tilde{\sigma}}(9, 2)$, $\psi_\delta \in \mathcal{H}_{\tilde{\sigma}}(9, 4)$, and $g_\delta \in \mathcal{H}_{\tilde{\sigma}}(20, 4)$, we have $\phi_\delta \in \mathcal{H}_{\tilde{\sigma}}(29, 6)$.

812 Clearly, $\tilde{\sigma}(x)$, $g_\delta(x)$, and $1 - g_\delta(x)$ are all in $[-4\widetilde{M}, 4\widetilde{M}]$ for any small $\delta > 0$ and all
 813 $x \in [-M, M]$. We will show $\psi_\delta(x) \in [-4\widetilde{M}, 4\widetilde{M}]$ for any small $\delta > 0$ and all $x \in [-M, M]$ via
 814 two cases as follows.

- 815 • For $x \in [0, M]$, $\psi_\delta(x) \rightrightarrows \sigma(x)$ implies $\psi_\delta(x) \in [-4\widetilde{M}, 4\widetilde{M}]$ for any small $\delta > 0$.

816 • For $x \in [-M, 0)$, we have $\psi_1(x) = \frac{(x+1)^2}{(2M+1)^2} \in [0, 1]$ and

$$817 \quad \psi_{2,\delta}(x) = \frac{\tilde{\sigma}(x+\delta) - \tilde{\sigma}(x)}{\delta} \Rightarrow \frac{d}{dx} \tilde{\sigma}(x) = \frac{1}{(-x+1)^2} \quad \text{as } \delta \rightarrow 0^+.$$

818 Thus, for any $x \in [-M, 0)$, as δ goes to 0^+ , we get

$$819 \quad \begin{aligned} \psi_\delta(x) &= \frac{(2M+1)^2}{c} \Gamma\left(\psi_1(x), \psi_{2,\delta}(x)\right) - \frac{1}{c} = \frac{(2M+1)^2}{c} \cdot \psi_1(x) \cdot \psi_{2,\delta}(x) - \frac{1}{c} \\ &\Rightarrow \frac{(2M+1)^2}{c} \cdot \frac{(2x+1)^2}{(2M+1)^2} \cdot \frac{1}{(-x+1)^2} - \frac{1}{c} = \frac{(2x+1)^2 - 1}{c(-x+1)^2}. \end{aligned}$$

820 Since $\widetilde{M} = (M+1)^2$, we have $\frac{(2x+1)^2 - 1}{c(-x+1)^2} \in [0, 4\widetilde{M} - 1]$ for all $x \in [-M, 0)$, implying
821 $\psi_\delta(x) \in [-4\widetilde{M}, 4\widetilde{M}]$ for any small $\delta > 0$.

822 Thus, for any $x \in [\eta_0, M]$, we have $1 - g(x) = 0$, implying

$$823 \quad \phi_\delta(x) = \psi_\delta(x) \cdot g_\delta(x) + \tilde{\sigma}(x) \cdot (1 - g_\delta(x)) \Rightarrow \sigma(x) \cdot g(x) + 0 = \sigma(x) \quad \text{as } \delta \rightarrow 0^+.$$

824 Similarly, for any $x \in [-M, 0]$, we have $g(x) = 0$, implying

$$825 \quad \phi_\delta(x) = \psi_\delta(x) \cdot g_\delta(x) + \tilde{\sigma}(x) \cdot (1 - g_\delta(x)) \Rightarrow 0 + \tilde{\sigma}(x) \cdot (1 - g(x)) = \sigma(x) \quad \text{as } \delta \rightarrow 0^+.$$

826 Therefore, there exists a small $\delta_0 > 0$ such that

$$827 \quad |\phi_{\delta_0}(x) - \sigma(x)| < \varepsilon \quad \text{for any } x \in [-M, 0] \cup [\eta_0, M],$$

$$828 \quad \|g_{\delta_0}\|_{L^\infty([0, \eta_0])} \leq 2, \quad \|1 - g_{\delta_0}\|_{L^\infty([0, \eta_0])} \leq 2, \quad \text{and}$$

$$829 \quad \|\psi_{\delta_0}\|_{L^\infty([0, \eta_0])} \leq \|\sigma\|_{L^\infty([0, \eta_0])} + \varepsilon/12,$$

830 where the above inequality comes from $\psi_\delta(x)$ uniformly converges to $\sigma(x)$ for any $x \in$
831 $[0, \eta_0] \subseteq [0, M]$.

832 Clearly, for $x \in [0, \eta_0]$, by Equation (10), we have

$$\begin{aligned} |\phi_{\delta_0}(x) - \sigma(x)| &\leq |\phi_{\delta_0}(x)| + |\sigma(x)| < \left| \psi_{\delta_0}(x) \cdot g_{\delta_0}(x) + \tilde{\sigma}(x) \cdot (1 - g_{\delta_0}(x)) \right| + \varepsilon/6 \\ &\leq |\psi_{\delta_0}(x)| \cdot |g_{\delta_0}(x)| + |\tilde{\sigma}(x)| \cdot |1 - g_{\delta_0}(x)| + \varepsilon/6 \\ 833 \quad &\leq \left(\|\sigma\|_{L^\infty([0, \eta_0])} + \frac{\varepsilon}{12} \right) \cdot 2 + \frac{\varepsilon}{6} \cdot 2 + \frac{\varepsilon}{6} \\ &\leq \left(\frac{\varepsilon}{6} + \frac{\varepsilon}{12} \right) \cdot 2 + \frac{\varepsilon}{6} \cdot 2 + \frac{\varepsilon}{6} = \varepsilon. \end{aligned}$$

834 By setting $\phi = \phi_{\delta_0}$, we have $\phi = \phi_{\delta_0} \in \mathcal{H}_\sigma(29, 6)$ and

$$835 \quad |\phi(x) - \sigma(x)| = |\phi_{\delta_0}(x) - \sigma(x)| < \varepsilon \quad \text{for any } x \in [-M, M].$$

836 So we finish the proof. □

837 4.3 Proof of Lemma 4.1

838 Let the activation function be applied to a vector elementwisely. Then, ϕ_ϱ can be
839 represented in a form of function compositions as follows:

$$840 \quad \phi_\varrho(\mathbf{x}) = \mathcal{L}_L \circ \varrho \circ \mathcal{L}_{L-1} \circ \varrho \circ \cdots \circ \varrho \circ \mathcal{L}_1 \circ \varrho \circ \mathcal{L}_0(\mathbf{x}) \quad \text{for any } \mathbf{x} \in \mathbb{R}^d,$$

841 where $N_0 = d$, $N_1, N_2, \dots, N_L \in \mathbb{N}^+$, $N_{L+1} = 1$, $\mathbf{A}_\ell \in \mathbb{R}^{N_{\ell+1} \times N_\ell}$ and $\mathbf{b}_\ell \in \mathbb{R}^{N_{\ell+1}}$ are the weight
842 matrix and the bias vector in the ℓ -th affine linear transform $\mathcal{L}_\ell : \mathbf{y} \mapsto \mathbf{A}_\ell \mathbf{y} + \mathbf{b}_\ell$ for each
843 $\ell \in \{0, 1, \dots, L\}$. Define

$$844 \quad \phi_{\varrho_\delta}(\mathbf{x}) := \mathcal{L}_L \circ \varrho_\delta \circ \mathcal{L}_{L-1} \circ \varrho_\delta \circ \cdots \circ \varrho_\delta \circ \mathcal{L}_1 \circ \varrho_\delta \circ \mathcal{L}_0(\mathbf{x}) \quad \text{for any } \mathbf{x} \in \mathbb{R}^d.$$

845 Recall that ϱ_δ can be realized by a $\tilde{\varrho}$ -activated network with width \tilde{N} and depth \tilde{L} . Thus,
846 ϕ_{ϱ_δ} can be realized by a $\tilde{\varrho}$ -activated network with width $N \cdot \tilde{N}$ and depth $L \cdot \tilde{L}$.

847 We will prove

$$848 \quad \phi_{\varrho_\delta}(\mathbf{x}) \rightrightarrows \phi_\varrho(\mathbf{x}) \quad \text{as } \delta \rightarrow 0^+ \quad \text{for any } \mathbf{x} \in [a, b]^d.$$

849 For any $\mathbf{x} \in \mathbb{R}^d$ and each $\ell \in \{1, 2, \dots, L+1\}$, define

$$850 \quad \mathbf{h}_\ell(\mathbf{x}) := \mathcal{L}_{\ell-1} \circ \varrho \circ \mathcal{L}_{\ell-2} \circ \varrho \circ \cdots \circ \varrho \circ \mathcal{L}_1 \circ \varrho \circ \mathcal{L}_0(\mathbf{x})$$

851 and

$$852 \quad \mathbf{h}_{\ell,\delta}(\mathbf{x}) := \mathcal{L}_{\ell-1} \circ \varrho_\delta \circ \mathcal{L}_{\ell-2} \circ \varrho_\delta \circ \cdots \circ \varrho_\delta \circ \mathcal{L}_1 \circ \varrho_\delta \circ \mathcal{L}_0(\mathbf{x}).$$

853 Note that \mathbf{h}_ℓ and $\mathbf{h}_{\ell,\delta}$ are two maps from \mathbb{R}^d to \mathbb{R}^{N_ℓ} for each ℓ .

854 We will prove by induction that

$$855 \quad \mathbf{h}_{\ell,\delta}(\mathbf{x}) \rightrightarrows \mathbf{h}_\ell(\mathbf{x}) \quad \text{as } \delta \rightarrow 0^+ \tag{11}$$

856 for any $\mathbf{x} \in [a, b]^d$ and each $\ell \in \{1, 2, \dots, L+1\}$.

857 First, we consider the case $\ell = 1$. Clearly,

$$858 \quad \mathbf{h}_{1,\delta}(\mathbf{x}) = \mathcal{L}_0(\mathbf{x}) = \mathbf{h}_1(\mathbf{x}) \quad \text{as } \delta \rightarrow 0^+ \quad \text{for any } \mathbf{x} \in [a, b]^d.$$

859 This means Equation (11) holds for $\ell = 1$.

860 Next, suppose Equation (11) holds for $\ell = i \in \{1, 2, \dots, L\}$. Our goal is to prove that it
861 also holds for $\ell = i + 1$. Define

$$862 \quad M := \sup \left\{ \|\mathbf{h}_j(\mathbf{x})\|_{\ell^\infty} + 1 : \mathbf{x} \in [a, b]^d, \quad j = 1, 2, \dots, L+1 \right\},$$

863 where the continuity of ϱ guarantees the above supremum is finite. By the induction hy-
864 pothesis, we have

$$865 \quad \mathbf{h}_{i,\delta}(\mathbf{x}) \rightrightarrows \mathbf{h}_i(\mathbf{x}) \quad \text{as } \delta \rightarrow 0^+ \quad \text{for any } \mathbf{x} \in [a, b]^d.$$

866 Clearly, for any $\mathbf{x} \in [a, b]^d$, we have $\|\mathbf{h}_i(\mathbf{x})\|_{\ell^\infty} \leq M$ and $\|\mathbf{h}_{i,\delta}(\mathbf{x})\|_{\ell^\infty} \leq \|\mathbf{h}_i(\mathbf{x})\|_{\ell^\infty} + 1 \leq M$
867 for any small $\delta > 0$.

868 Recall the fact $\varrho_\delta(t) \rightrightarrows \varrho(t)$ as $\delta \rightarrow 0^+$ for any $t \in [-M, M]$. Then

$$869 \quad \varrho_\delta \circ \mathbf{h}_{i,\delta}(\mathbf{x}) - \varrho \circ \mathbf{h}_{i,\delta}(\mathbf{x}) \rightrightarrows \mathbf{0} \quad \text{as } \delta \rightarrow 0^+.$$

870 The continuity of ϱ implies the uniform continuity of ϱ on $[-M, M]$, deducing

$$871 \quad \varrho \circ \mathbf{h}_{i,\delta}(\mathbf{x}) - \varrho \circ \mathbf{h}_i(\mathbf{x}) \rightrightarrows \mathbf{0} \quad \text{as } \delta \rightarrow 0^+ \quad \text{for any } \mathbf{x} \in [a, b]^d.$$

872 Therefore, for any $\mathbf{x} \in [a, b]^d$, as $\delta \rightarrow 0^+$, we have

$$873 \quad \varrho_\delta \circ \mathbf{h}_{i,\delta}(\mathbf{x}) - \varrho \circ \mathbf{h}_i(\mathbf{x}) = \underbrace{\varrho_\delta \circ \mathbf{h}_{i,\delta}(\mathbf{x}) - \varrho \circ \mathbf{h}_{i,\delta}(\mathbf{x})}_{\rightrightarrows \mathbf{0}} + \underbrace{\varrho \circ \mathbf{h}_{i,\delta}(\mathbf{x}) - \varrho \circ \mathbf{h}_i(\mathbf{x})}_{\rightrightarrows \mathbf{0}} \rightrightarrows \mathbf{0},$$

874 implying

$$875 \quad \mathbf{h}_{i+1,\delta}(\mathbf{x}) = \mathcal{L}_i \circ \varrho_\delta \circ \mathbf{h}_{i,\delta}(\mathbf{x}) \rightrightarrows \mathcal{L}_i \circ \varrho \circ \mathbf{h}_i(\mathbf{x}) = \mathbf{h}_{i+1}(\mathbf{x}).$$

876 This means Equation (11) holds for $\ell = i + 1$. So we complete the inductive step.

877 By the principle of induction, we have

$$878 \quad \phi_{\varrho_\delta}(\mathbf{x}) = \mathbf{h}_{L+1,\delta}(\mathbf{x}) \rightrightarrows \mathbf{h}_{L+1}(\mathbf{x}) = \phi_{\varrho}(\mathbf{x}) \quad \text{as } \delta \rightarrow 0^+ \quad \text{for any } \mathbf{x} \in [a, b]^d.$$

879 There exists a small $\delta_0 > 0$ such that

$$880 \quad |\phi_{\varrho_{\delta_0}}(\mathbf{x}) - \phi_{\varrho}(\mathbf{x})| < \varepsilon/2 \quad \text{for any } \mathbf{x} \in [a, b]^d.$$

881 By setting $\phi = \phi_{\varrho_{\delta_0}}$, we have

$$882 \quad |\phi(\mathbf{x}) - f(\mathbf{x})| \leq |\phi_{\varrho_{\delta_0}}(\mathbf{x}) - \phi_{\varrho}(\mathbf{x})| + |\phi_{\varrho}(\mathbf{x}) - f(\mathbf{x})| < \varepsilon/2 + \varepsilon/2 = \varepsilon$$

883 for any $\mathbf{x} \in [a, b]^d$. Moreover, $\phi = \phi_{\varrho_{\delta_0}}$ can be generated by a $\tilde{\varrho}$ -activated network with
884 width $N \cdot \tilde{N}$ and depth $L \cdot \tilde{L}$. So we finish the proof.

885 5. Detailed proofs of Theorems 1.1 and 1.4

886 In this section, we will give the detailed proofs of Theorems 1.1 and 1.4. First, we
887 prove Theorem 1.1 based on Theorem 2.1, which will be proved in Section 6. Next, we
888 apply Theorem 1.1 to prove Theorem 1.4.

889 5.1 Proof of Theorem 1.1

890 The detailed proof of Theorem 1.1 converts the above ideas mentioned in Section 2.2 to
891 implementations using neural networks with fixed sizes. The whole construction procedure
892 can be divided into three steps.

893 (1) Apply KST to reduce dimension, i.e., represent $f \in C([a, b]^d)$ by the compositions and
894 combinations of univariate continuous functions.

895 (2) Apply Theorem 2.1 to design sub-networks to approximate the univariate continuous
896 functions in the previous step within the desired error.

897 (3) Integrate the sub-networks to form the final network and estimate its size.

898 **Step 1:** Apply KST to reduce dimension.

899 To apply KST, we define a linear function $\mathcal{L}_1(t) = (b-a)t - a$ for any $t \in [0, 1]$. Clearly,
900 \mathcal{L}_1 is a bijection from $[0, 1]$ to $[a, b]$. Define

$$901 \quad \tilde{f}(\mathbf{y}) := f(\mathcal{L}_1(y_1), \mathcal{L}_1(y_2), \dots, \mathcal{L}_1(y_d)) \quad \text{for any } \mathbf{y} = [y_1, y_2, \dots, y_d]^T \in [0, 1]^d.$$

902 Then $\tilde{f} : [0, 1]^d \rightarrow \mathbb{R}$ is a continuous function since $f \in C([a, b]^d)$. By Theorem 2.3, there
903 exists $\tilde{h}_{i,j} \in C([0, 1])$ and $\tilde{g}_i \in C(\mathbb{R})$ for $i = 0, 1, \dots, 2d$ and $j = 1, 2, \dots, d$ such that

$$904 \quad \tilde{f}(\mathbf{y}) = \sum_{i=0}^{2d} \tilde{g}_i \left(\sum_{j=1}^d \tilde{h}_{i,j}(y_j) \right) \quad \text{for any } \mathbf{y} = [y_1, y_2, \dots, y_d]^T \in [0, 1]^d.$$

905 Let $\tilde{\mathcal{L}}_1$ be the inverse of \mathcal{L}_1 , i.e., define $\tilde{\mathcal{L}}_1(t) = (t-a)/(b-a)$ for any $t \in [a, b]$. Then, for
906 any $x_j \in [a, b]$, there exists a unique $y_j \in [0, 1]$ such that $\mathcal{L}_1(y_j) = x_j$ and $y_j = \tilde{\mathcal{L}}_1(x_j)$ for
907 any $j = 1, 2, \dots, d$, which implies

$$\begin{aligned} f(\mathbf{x}) &= f(x_1, x_2, \dots, x_d) = f(\mathcal{L}_1(y_1), \mathcal{L}_1(y_2), \dots, \mathcal{L}_1(y_d)) = \tilde{f}(\mathbf{y}) \\ 908 \quad &= \sum_{i=0}^{2d} \tilde{g}_i \left(\sum_{j=1}^d \tilde{h}_{i,j}(y_j) \right) = \sum_{i=0}^{2d} \tilde{g}_i \left(\sum_{j=1}^d \tilde{h}_{i,j}(\tilde{\mathcal{L}}_1(x_j)) \right) = \sum_{i=0}^{2d} \tilde{g}_i \left(\sum_{j=1}^d \tilde{h}_{i,j} \circ \tilde{\mathcal{L}}_1(x_j) \right). \end{aligned}$$

909 It follows that

$$910 \quad f(\mathbf{x}) = \sum_{i=0}^{2d} \tilde{g}_i \left(\sum_{j=1}^d \tilde{h}_{i,j} \circ \tilde{\mathcal{L}}_1(x_j) \right) = \sum_{i=0}^{2d} \tilde{g}_i \circ \widehat{h}_i(\mathbf{x}) \quad \text{for any } \mathbf{x} \in [a, b]^d,$$

911 where

$$912 \quad \widehat{h}_i(\mathbf{x}) = \sum_{j=1}^d \tilde{h}_{i,j} \circ \tilde{\mathcal{L}}_1(x_j) \quad \text{for any } \mathbf{x} = [x_1, x_2, \dots, x_d]^T \in [a, b]^d. \quad (12)$$

913 Denote

$$914 \quad M = \max_{i \in \{0, 1, \dots, 2d\}} \|\tilde{h}_i\|_{L^\infty([a, b]^d)} + 1 > 0.$$

915 Define $\mathcal{L}_2(t) = (t+2M)/4M$ and $\tilde{\mathcal{L}}_2(t) = 4Mt - 2M$ for any $t \in \mathbb{R}$. Then \mathcal{L}_2 is a bijection from
916 $[-M, M]$ to $[\frac{1}{4}, \frac{3}{4}]$ and $\tilde{\mathcal{L}}_2$ is the inverse of \mathcal{L}_2 . Clearly, $\tilde{\mathcal{L}}_2 \circ \mathcal{L}_2(t) = t$ for any $t \in [-M, M]$,
917 which implies $\widehat{h}_i(\mathbf{x}) = \tilde{\mathcal{L}}_2 \circ \mathcal{L}_2 \circ \widehat{h}_i(\mathbf{x})$ for any $\mathbf{x} \in [a, b]^d$. Therefore, for any $\mathbf{x} \in [a, b]^d$, we
918 have

$$919 \quad f(\mathbf{x}) = \sum_{i=0}^{2d} \tilde{g}_i \circ \widehat{h}_i(\mathbf{x}) = \sum_{i=0}^{2d} \tilde{g}_i \circ \tilde{\mathcal{L}}_2 \circ \mathcal{L}_2 \circ \widehat{h}_i(\mathbf{x}) = \sum_{i=0}^{2d} g_i \circ h_i(\mathbf{x}),$$

920 where

$$921 \quad g_i = \tilde{g}_i \circ \tilde{\mathcal{L}}_2 \quad \text{and} \quad h_i = \mathcal{L}_2 \circ \widehat{h}_i \quad \text{for } i = 0, 1, \dots, 2d. \quad (13)$$

922 Clearly, $\mathcal{L}_2(t) \in [\frac{1}{4}, \frac{3}{4}]$ for any $t \in [-M, M]$, which implies

$$923 \quad h_i(\mathbf{x}) = \mathcal{L}_2 \circ \widehat{h}_i(\mathbf{x}) \in [\frac{1}{4}, \frac{3}{4}] \quad \text{for any } \mathbf{x} \in [a, b] \text{ and } i = 0, 1, \dots, 2d.$$

924 **Step 2:** Design sub-networks to approximate g_i and h_i .

925 Next, we represent g_i and h_i by sub-networks. Obviously, $g_i = \tilde{g}_i \circ \tilde{\mathcal{L}}_2$ is continuous on
 926 \mathbb{R} , and, therefore, uniformly continuous on $[0, 1]$ for each i . Thus, for $i = 0, 1, \dots, 2d$, there
 927 exists $\delta_i > 0$ such that

$$928 \quad |g_i(z_1) - g_i(z_2)| < \varepsilon / (4d + 2) \quad \text{for any } z_1, z_2 \in [0, 1] \text{ with } |z_1 - z_2| < \delta_i.$$

929 Set $\delta = \min(\{\delta_i : i = 0, 1, \dots, 2d\} \cup \{\frac{1}{4}\})$. Then, for $i = 0, 1, \dots, 2d$, we have

$$930 \quad |g_i(z_1) - g_i(z_2)| < \varepsilon / (4d + 2) \quad \text{for any } z_1, z_2 \in [0, 1] \text{ with } |z_1 - z_2| < \delta. \quad (14)$$

931 For each $i \in \{0, 1, \dots, 2d\}$, by Theorem 2.1, there exists a function ϕ_i generated by an
 932 EUAF network with width 36 and depth 5 such that

$$933 \quad |g_i(z) - \phi_i(z)| < \varepsilon / (4d + 2) \quad \text{for any } z \in [0, 1]. \quad (15)$$

934 Fix $i \in \{0, 1, \dots, 2d\}$, we will design an EUAF network to generate a function $\psi_i :$
 935 $[a, b]^d \rightarrow \mathbb{R}$ satisfying

$$936 \quad |h_i(\mathbf{x}) - \psi_i(\mathbf{x})| < \delta \quad \text{for any } \mathbf{x} \in [a, b]^d.$$

937 For any $\mathbf{x} = [x_1, x_2, \dots, x_d]^T \in [a, b]^d$, by Equations (12) and (13), we have

$$\begin{aligned} 938 \quad h_i(\mathbf{x}) &= \mathcal{L}_2 \circ \tilde{h}_i(\mathbf{x}) = \mathcal{L}_2 \left(\sum_{j=1}^d \tilde{h}_{i,j} \circ \tilde{\mathcal{L}}_1(x_j) \right) = \frac{\left(\sum_{j=1}^d \tilde{h}_{i,j} \circ \tilde{\mathcal{L}}_1(x_j) \right) + 2M}{4M} \\ &= \sum_{j=1}^d \left(\frac{\tilde{h}_{i,j} \circ \tilde{\mathcal{L}}_1(x_j)}{4M} + \frac{1}{2d} \right) =: \sum_{j=1}^d h_{i,j}(x_j), \end{aligned}$$

939 where

$$940 \quad h_{i,j}(t) := \frac{\tilde{h}_{i,j} \circ \tilde{\mathcal{L}}_1(t)}{4M} + \frac{1}{2d} \quad \text{for any } t \in [a, b] \text{ and } j = 1, 2, \dots, d.$$

941 For each $j \in \{1, 2, \dots, d\}$, by Theorem 2.1, there exists a function $\psi_{i,j}$ generated by an
 942 EUAF network with width 36 and depth 5 such that

$$943 \quad |h_{i,j}(t) - \psi_{i,j}(t)| < \delta / d \quad \text{for any } t \in [a, b].$$

944 Define $\psi_i(\mathbf{x}) := \sum_{j=1}^d \psi_{i,j}(x_j)$ for any $\mathbf{x} = [x_1, x_2, \dots, x_d]^T \in [a, b]^d$. Then, for any $\mathbf{x} =$
 945 $[x_1, x_2, \dots, x_d]^T \in [a, b]^d$, we have

$$946 \quad |h_i(\mathbf{x}) - \psi_i(\mathbf{x})| = \left| \sum_{j=1}^d h_{i,j}(x_j) - \sum_{j=1}^d \psi_{i,j}(x_j) \right| = \sum_{j=1}^d |h_{i,j}(x_j) - \psi_{i,j}(x_j)| < \sum_{j=1}^d \delta / d = \delta.$$

947 **Step 3:** Integrate sub-networks.

948 Finally, we build an integrated network with the desired size to approximate the target
 949 function f . The desired function ϕ can be defined as

$$950 \quad \phi(\mathbf{x}) := \sum_{i=0}^{2d} \phi_i \circ \psi_i(\mathbf{x}) = \sum_{i=0}^{2d} \phi_i \left(\sum_{j=1}^d \psi_{i,j}(x_j) \right) \quad \text{for any } \mathbf{x} = [x_1, x_2, \dots, x_d]^T \in [a, b]^d.$$

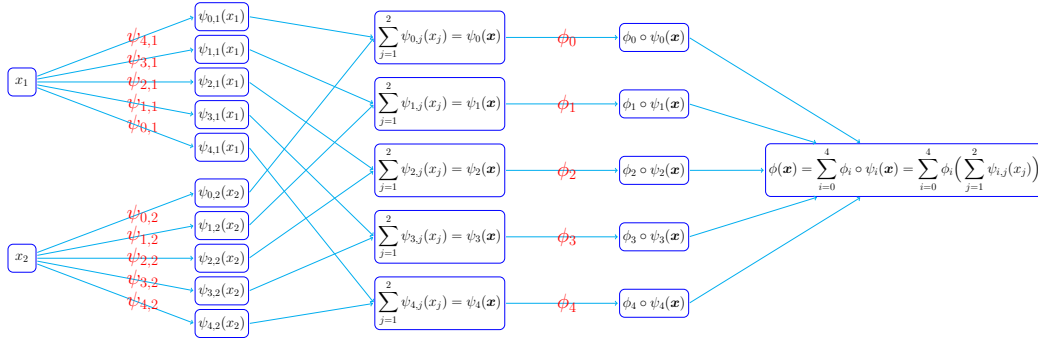


Figure 10: An illustration of the target network realizing ϕ for any $\mathbf{x} \in [a, b]^d$ in the case of $d = 2$. This network contains $(2d + 1)d + (2d + 1) = (d + 1)(2d + 1)$ sub-networks that realize $\psi_{i,j}$ and ϕ_i for $i = 0, 1, \dots, 2d$ and $j = 1, 2, \dots, d$.

Let us first estimate the approximation error and then determine the size of the target network realizing ϕ . See Figure 10 for an illustration of the target network realizing ϕ for the case $d = 2$.

Fix $\mathbf{x} \in [a, b]^d$ and $i \in \{0, 1, \dots, 2d\}$. Recall that $h_i(\mathbf{x}) \in [\frac{1}{4}, \frac{3}{4}]$ and $|h_i(\mathbf{x}) - \psi_i(\mathbf{x})| < \delta \leq \frac{1}{4}$, which implies $\psi_i(\mathbf{x}) \in [0, 1]$. Then by Equation (14) (set $z_1 = h_i(\mathbf{x})$ and $z_2 = \psi_i(\mathbf{x})$ therein), we have

$$|g_i \circ h_i(\mathbf{x}) - g_i \circ \psi_i(\mathbf{x})| = |g_i(h_i(\mathbf{x})) - g_i(\psi_i(\mathbf{x}))| < \varepsilon / (4d + 2).$$

By Equation (15) (set $z = \psi_i(\mathbf{x}) \in [0, 1]$ therein), we have

$$|g_i \circ \psi_i(\mathbf{x}) - \phi_i \circ \psi_i(\mathbf{x})| = |g_i(\psi_i(\mathbf{x})) - \phi_i(\psi_i(\mathbf{x}))| < \varepsilon / (4d + 2).$$

Therefore, for any $\mathbf{x} \in [a, b]^d$, we have

$$\begin{aligned} |f(\mathbf{x}) - \phi(\mathbf{x})| &= \left| \sum_{i=0}^{2d} g_i \circ h_i(\mathbf{x}) - \sum_{i=0}^{2d} \phi_i \circ \psi_i(\mathbf{x}) \right| = \sum_{i=0}^{2d} |g_i \circ h_i(\mathbf{x}) - \phi_i \circ \psi_i(\mathbf{x})| \\ &\leq \sum_{i=0}^{2d} \left(|g_i \circ h_i(\mathbf{x}) - g_i \circ \psi_i(\mathbf{x})| + |g_i \circ \psi_i(\mathbf{x}) - \phi_i \circ \psi_i(\mathbf{x})| \right) \\ &< \sum_{i=0}^{2d} \left(\varepsilon / (4d + 2) + \varepsilon / (4d + 2) \right) = \varepsilon. \end{aligned}$$

It remains to show ϕ can be generated by an EUAF network with the desired size. Recall that, for each $i \in \{0, 1, \dots, 2d\}$ and each $j \in \{1, 2, \dots, d\}$, $\psi_{i,j}$ can be generated by an EUAF network with width 36, depth 5, and, therefore, at most

$$(36 + 36) + (36 \times 36 + 36) \times 4 + (36 + 1) = 5437$$

nonzero parameters. Hence, for each $i \in \{0, 1, \dots, 2d\}$, ψ_i , given by $\psi_i(\mathbf{x}) = \sum_{j=1}^d \psi_{i,j}(x_j)$, can be generated by an EUAF network with width $36d$, depth 5, and at most $5437d$ nonzero parameters.

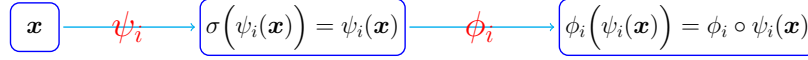


Figure 11: An illustration of the target EUAF network generating $\phi_i \circ \psi_i(\mathbf{x})$ for any $\mathbf{x} \in [a, b]^d$ and $i = 0, 1, \dots, 2d$.

969 Since $\psi_i(\mathbf{x}) \in [0, 1]$ for any $\mathbf{x} \in [a, b]^d$ and $i = 0, 1, \dots, 2d$, we have $\sigma(\psi_i(\mathbf{x})) = \psi_i(\mathbf{x})$
 970 for any $\mathbf{x} \in [a, b]^d$. Hence, $\phi_i \circ \psi_i$ can be generated by an EUAF network as visualized in
 971 Figure 11.

972 Recall that ϕ_i can be generated by an EUAF network with width 36 and depth 5.
 973 Hence, the network generating ϕ_i has at most 5437 nonzero parameters. As we can see
 974 from Figure 11, $\phi_i \circ \psi_i$ can be generated by an EUAF network with width $36d$, depth
 975 $5 + 1 + 5 = 11$, and at most $5437d + 5437 = 5437(d + 1)$ nonzero parameters. This means
 976 $\phi = \sum_{i=0}^{2d} \phi_i \circ \psi_i$ can be generated by an EUAF network with width $36d(2d + 1)$, depth 11,
 977 and, therefore, at most $5437(d + 1)(2d + 1)$ nonzero parameters as desired. So we finish the
 978 proof.

979 5.2 Proof of Theorem 1.4

980 The proof of Theorem 1.4 relies on a basic result of real analysis given in the following
 981 lemma.

982 **Lemma 5.1.** *Suppose $A, B \subseteq \mathbb{R}^d$ are two disjoint bounded closed sets. Then there exists*
 983 *a continuous function $f \in C(\mathbb{R}^d)$ such that $f(\mathbf{x}) = 1$ for any $\mathbf{x} \in A$ and $f(\mathbf{y}) = 0$ for any*
 984 *$\mathbf{y} \in B$.*

985 *Proof.* Define $\text{dist}(\mathbf{x}, A) = \inf\{\|\mathbf{x} - \mathbf{y}\|_2 : \mathbf{y} \in A\}$ and $\text{dist}(\mathbf{x}, B) = \inf\{\|\mathbf{x} - \mathbf{y}\|_2 : \mathbf{y} \in B\}$ for
 986 any $\mathbf{x} \in \mathbb{R}^d$. It is easy to verify that $\text{dist}(\mathbf{x}, A)$ and $\text{dist}(\mathbf{x}, B)$ are continuous in $\mathbf{x} \in \mathbb{R}^d$.
 987 Since $A, B \subseteq \mathbb{R}^d$ are two disjoint bounded closed subsets, we have $\text{dist}(\mathbf{x}, A) + \text{dist}(\mathbf{x}, B) > 0$
 988 for any $\mathbf{x} \in \mathbb{R}^d$. Finally, define

$$989 \quad f(\mathbf{x}) := \frac{\text{dist}(\mathbf{x}, B)}{\text{dist}(\mathbf{x}, A) + \text{dist}(\mathbf{x}, B)} \quad \text{for any } \mathbf{x} \in \mathbb{R}^d.$$

990 Then f meets the requirements. So we finish the proof. \square

991 With Lemma 5.1, we can prove Theorem 1.4.

992 *Proof of Theorem 1.4.* For any $f = \sum_{j=1}^J r_j \cdot \mathbf{1}_{E_j} \in \mathcal{C}_d(E_1, E_2, \dots, E_J)$, our goal is to construct
 993 a function ϕ generated by a σ -activated network such that $\phi(\mathbf{x}) = f(\mathbf{x})$ for any $\mathbf{x} \in \bigcup_{j=1}^J E_j$,
 994 where E_1, E_2, \dots, E_J are pairwise disjoint bounded closed subsets of \mathbb{R}^d . Set $E := \bigcup_{j=1}^J E_j$
 995 and choose $a, b \in \mathbb{R}$ properly such that $E \subseteq [a, b]^d$.

996 For each $j \in \{1, 2, \dots, J\}$, E_j and $\tilde{E}_j := E \setminus E_j$ are two disjoint bounded closed subsets.
 997 Then, for each j , by Lemma 5.1, there exists $g_j \in C(\mathbb{R}^d)$ such that $g_j(\mathbf{x}) = 1$ for any
 998 $\mathbf{x} \in E_j$ and $g_j(\mathbf{y}) = 0$ for any $\mathbf{y} \in \tilde{E}_j$. By defining $g := \sum_{j=1}^J r_j \cdot g_j \in C(\mathbb{R}^d)$, we have
 999 $g(\mathbf{x}) = \sum_{j=1}^J r_j \cdot \mathbf{1}_{E_j}(\mathbf{x}) = f(\mathbf{x})$ for any $\mathbf{x} \in E = \bigcup_{j=1}^J E_j$.

1000 Since r_1, r_2, \dots, r_J are rational numbers and $g : [a, b]^d \rightarrow \mathbb{R}$ is continuous, there exist
 1001 $n_1, n_2 \in \mathbb{Z}$ such that

- $n_1 \cdot r_j + n_2 \in \mathbb{N}^+$ for $j = 1, 2, \dots, J$;
- $n_1 \cdot g(\mathbf{x}) + n_2 \geq 0$ for any $\mathbf{x} \in [a, b]^d$.

By applying Theorem 1.1 to $2(n_1 \cdot g + n_2) + 1$, there exists a function ϕ_1 generated by an EUAF network with width $36d(2d + 1)$, depth 11, and at most $5437(d + 1)(2d + 1)$ nonzero parameters such that

$$\left| 2(n_1 \cdot g(\mathbf{x}) + n_2) + 1 - \phi_1(\mathbf{x}) \right| \leq 1/2 \quad \text{for any } \mathbf{x} \in [a, b]^d. \quad (16)$$

It follows that

$$\left| 2\left(n_1 \cdot \sum_{j=1}^J r_j \cdot \mathbb{1}_{E_j}(\mathbf{x}) + n_2\right) + 1 - \phi_1(\mathbf{x}) \right| \leq 1/2 \quad \text{for any } \mathbf{x} \in E = \bigcup_{j=1}^J E_j.$$

Since E_1, E_2, \dots, E_J are pairwise disjoint, we have

$$\left| 2(n_1 \cdot r_j + n_2) + 1 - \phi_1(\mathbf{x}) \right| \leq 1/2 \quad \text{for any } \mathbf{x} \in E_j \text{ and each } j \in \{1, 2, \dots, J\}. \quad (17)$$

Define $\phi_2(x) = x + 1/2 - \sigma(x + 3/2)$ for any $x \in \mathbb{R}$. See Figure 12 for an illustration. It is

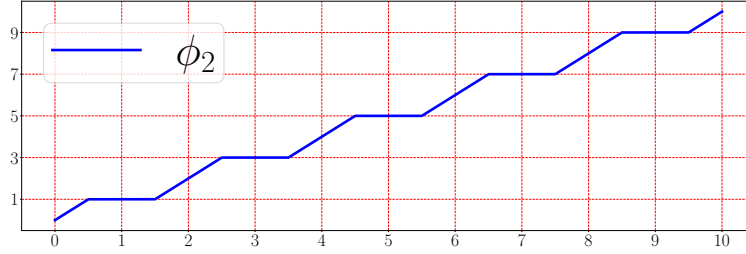


Figure 12: An illustration of ϕ_2 on $[0, 10]$.

easy to verify that

$$\phi_2(y) = 2k + 1 \quad \text{for any } y \text{ and } k \in \mathbb{N}^+ \text{ with } |2k + 1 - y| \leq 1/2. \quad (18)$$

Therefore, by Equations (17) and (18) (set $y = \phi_1(\mathbf{x})$ and $k = n_1 \cdot r_j + n_2$ therein), we have $\phi_2 \circ \phi_1(\mathbf{x}) = 2(n_1 \cdot r_j + n_2) + 1$ for any $\mathbf{x} \in E_j$ and any $j \in \{1, 2, \dots, J\}$, which implies

$$\frac{\phi_2 \circ \phi_1(\mathbf{x}) - 2n_2 - 1}{2n_1} = r_j \quad \text{for any } \mathbf{x} \in E_j \text{ and any } j \in \{1, 2, \dots, J\}.$$

Define

$$\phi(\mathbf{x}) := \frac{\phi_2 \circ \phi_1(\mathbf{x}) - 2n_2 - 1}{2n_1} \quad \text{for any } \mathbf{x} \in [a, b]^d.$$

Clearly, we have $\phi(\mathbf{x}) = r_j$ for any $\mathbf{x} \in E_j$ and each $j \in \{1, 2, \dots, J\}$, which implies $\phi(\mathbf{x}) = \sum_{j=1}^J r_j \cdot \mathbb{1}_{E_j}(\mathbf{x}) = f(\mathbf{x})$ for any $\mathbf{x} \in E = \bigcup_{j=1}^J E_j$ as desired.

Set $M = 2\|n_1 g + n_2\|_{L^\infty([a, b]^d)} + 3/2 > 0$. By Equation (16) and the fact $n_1 \cdot g(\mathbf{x}) + n_2 \geq 0$ for any $\mathbf{x} \in [a, b]^d$, we have

$$\phi_1(\mathbf{x}) \in [1/2, 2\|n_1 g + n_2\|_{L^\infty([a, b]^d)} + 1 + 1/2] \subseteq [0, M] \quad \text{for any } \mathbf{x} \in [a, b]^d.$$

1025 Then, for any $\mathbf{x} \in [a, b]^d$, we have

$$1026 \quad \phi_2 \circ \phi_1(\mathbf{x}) = \phi_1(\mathbf{x}) + 1/2 - \sigma(\phi_1(\mathbf{x}) + 3/2) = M\sigma(\phi_1(\mathbf{x})/M) + 1/2 - \sigma(\phi_1(\mathbf{x}) + 3/2).$$

1027 It follows that

$$1028 \quad \phi(\mathbf{x}) = \frac{\phi_2 \circ \phi_1(\mathbf{x}) - 2n_2 - 1}{2n_1} = \frac{M\sigma(\phi_1(\mathbf{x})/M) - \sigma(\phi_1(\mathbf{x}) + 3/2) - 2n_2 - 1/2}{2n_1},$$

1029 for any $\mathbf{x} \in [a, b]^d$. The network realizing ϕ has just one more hidden layer with 2 neurons,
 1030 compared to the network realizing ϕ_1 . Recall that ϕ_1 can be generated by an EUAF network
 1031 with width $36d(2d + 1)$, depth 11, and at most $5437(d + 1)(2d + 1)$ nonzero parameters.
 1032 Therefore, ϕ , limited on $[a, b]^d$, can be generated by an EUAF network with width $36d(2d +$
 1033 $1)$, depth 12, and at most

$$1034 \quad 5437(d + 1)(2d + 1) + \underbrace{36d(2d + 1) \times 2 + 2 + 2 + 1}_{\text{all possible new parameters}} \leq 5509(d + 1)(2d + 1)$$

1035 nonzero parameters. So we finish the proof. \square

1036 6. Proof of Theorem 2.1

1037 To prove Theorem 2.1, we need to introduce two auxiliary theorems, Theorems 6.1 and
 1038 6.2, which serve as two important intermediate steps.

1039 **Theorem 6.1.** *Let $f \in C([0, 1])$ be a continuous function. Given any $\varepsilon > 0$, if K is a*
 1040 *positive integer satisfying*

$$1041 \quad |f(x_1) - f(x_2)| < \varepsilon/2 \quad \text{for any } x_1, x_2 \in [0, 1] \text{ with } |x_1 - x_2| < 1/K, \quad (19)$$

1042 *then there exists a function ϕ generated by an EUAF network with width 2 and depth 3 such*
 1043 *that $\|\phi\|_{L^\infty([0, 1])} \leq \|f\|_{L^\infty([0, 1])} + 1$ and*

$$1044 \quad |\phi(x) - f(x)| < \varepsilon \quad \text{for any } x \in \bigcup_{k=0}^{K-1} \left[\frac{2k}{2K}, \frac{2k+1}{2K} \right].$$

1045 **Theorem 6.2.** *Let $f \in C([0, 1])$ be a continuous function. Then, for an arbitrary $\varepsilon > 0$,*
 1046 *there exists a function ϕ generated by an EUAF network with width 36 and depth 5 such*
 1047 *that⁴*

$$1048 \quad |\phi(x) - f(x)| < \varepsilon \quad \text{for any } x \in [0, \frac{9}{10}].$$

1049 To prove Theorem 6.1, we only need to care about the approximation on “half” of
 1050 $[0, 1]$. It is not necessary to care about the approximation on the other “half” of $[0, 1]$.
 1051 Such an idea is similar to the “trifling region” in (Lu et al., 2021; Zhang, 2020). As we shall

4. Theorem 6.2 still holds via replacing $\frac{9}{10}$ by any number in $[0, 1)$. In fact, it is true for $[0, \frac{1}{K}]$, and K can be arbitrarily large.

see later, the proof of Theorem 6.1 can eventually be converted to a point-fitting problem, which can be solved by applying Proposition 2.2.

The key idea to prove Theorem 6.2 is to apply Theorem 6.1 to several horizontally shifted variants of the target function. Then a good approximation can be constructed via the combinations and multiplications of these variants, similar to the idea of (Lu et al., 2021; Zhang, 2020) to obtain an error estimation with the L^∞ -norm from a result with the L^p -norm for $p \in [1, \infty)$.

The proofs of Theorems 6.1 and 6.2 will be presented in Sections 6.1 and 6.2, respectively. Let us first prove Theorem 2.1 by assuming Theorem 6.2 is true.

Proof of Theorem 2.1. Define a linear function \mathcal{L} by $\mathcal{L}(x) = a + \frac{10(b-a)}{9}x$ for any $x \in [0, \frac{9}{10}]$. Then \mathcal{L} is a bijection from $[0, \frac{9}{10}]$ to $[a, b]$. It follows that $f \circ \mathcal{L}$ is a continuous function on $[0, \frac{9}{10}]$. By Theorem 6.2, there exists a function $\tilde{\phi}$ generated by an EUAF network with width 36 and depth 5 such that

$$|f \circ \mathcal{L}(x) - \tilde{\phi}(x)| < \varepsilon \quad \text{for any } x \in [0, \frac{9}{10}].$$

Define $\tilde{\mathcal{L}}(y) = \frac{9(y-a)}{10(b-a)}$ for any $y \in [a, b]$. Clearly, it is the inverse of \mathcal{L} , i.e., $\mathcal{L} \circ \tilde{\mathcal{L}}(y) = y$ for any $y \in [a, b]$. Therefore, for any $y \in [a, b]$, we have $x = \tilde{\mathcal{L}}(y) \in [0, \frac{9}{10}]$, which implies

$$\begin{aligned} |f(y) - \tilde{\phi} \circ \tilde{\mathcal{L}}(y)| &= |f \circ \mathcal{L} \circ \tilde{\mathcal{L}}(y) - \tilde{\phi} \circ \tilde{\mathcal{L}}(y)| \\ &= |f \circ \mathcal{L}(\tilde{\mathcal{L}}(y)) - \tilde{\phi}(\tilde{\mathcal{L}}(y))| \leq |f \circ \mathcal{L}(x) - \tilde{\phi}(x)| < \varepsilon. \end{aligned}$$

By defining $\phi := \tilde{\phi} \circ \tilde{\mathcal{L}}$, we have $|f(y) - \phi(y)| < \varepsilon$ for any $y \in [a, b]$ as desired. Note that $\tilde{\phi}$ can be realized by an EUAF network with width 36 and depth 5. We can compose $\tilde{\mathcal{L}}$ and the affine linear map of the network $\tilde{\phi}$ that connects the input layer and the first hidden layer. Therefore, $\phi = \tilde{\phi} \circ \tilde{\mathcal{L}}$ can also be realized by an EUAF network with width 36 and depth 5. So we finish the proof. \square

6.1 Proof of Theorem 6.1

Partition $[0, 1]$ into $2K$ small intervals \mathcal{I}_k and $\tilde{\mathcal{I}}_k$ for $k = 1, 2, \dots, K$, i.e.,

$$\mathcal{I}_k = \left[\frac{2k-2}{2K}, \frac{2k-1}{2K} \right] \quad \text{and} \quad \tilde{\mathcal{I}}_k = \left[\frac{2k-1}{2K}, \frac{2k}{2K} \right].$$

Clearly, $[0, 1] = \bigcup_{k=1}^K (\mathcal{I}_k \cup \tilde{\mathcal{I}}_k)$. Let x_k be the right endpoint of \mathcal{I}_k , i.e., $x_k = \frac{2k-1}{2K}$ for $k = 1, 2, \dots, K$. See an illustration of \mathcal{I}_k , $\tilde{\mathcal{I}}_k$, and x_k in Figure 13 for the case $K = 5$.

Our goal is to construct a function ϕ generated by an EUAF network with the desired size to approximate f well on \mathcal{I}_k for $k = 1, 2, \dots, K$. It is not necessary to care about the values of ϕ on $\tilde{\mathcal{I}}_k$ for all k . In other words, we only need to care about the approximation on a “half” of $[0, 1]$, which is the key for our proof.

Define $\psi(x) = x - \sigma(x)$ for any $x \in \mathbb{R}$, where σ is defined in Equation (3). See Figure 14 for an illustration of ψ .

It is easy to verify that

$$\psi(y) = 2k - 2 \quad \text{for any } y \in [2k - 2, 2k - 1] \text{ and each } k \in \{1, 2, \dots, K\}.$$

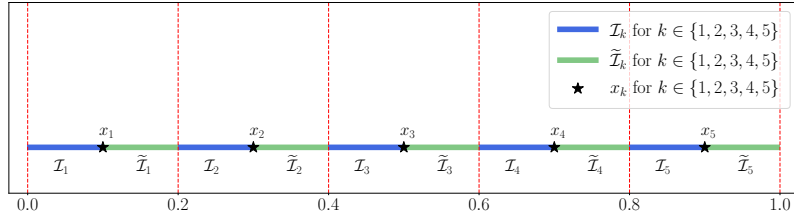


Figure 13: An illustration of \mathcal{I}_k and $\tilde{\mathcal{I}}_k$ for $k \in \{1, 2, \dots, K\}$ with $K = 5$.

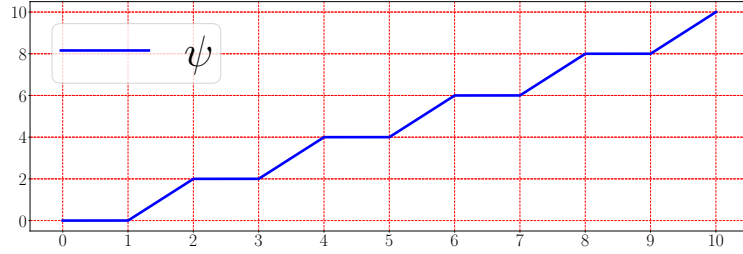


Figure 14: An illustration of ψ on $[0, 10]$.

1087 It follows that

1088
$$\psi(2Kx)/2 + 1 = k \quad \text{for any } x \in [\frac{2k-2}{2K}, \frac{2k-1}{2K}] = \mathcal{I}_k \text{ and each } k \in \{1, 2, \dots, K\}.$$

1089 Recall that x_k is the right endpoint of \mathcal{I}_k for $k = 1, 2, \dots, K$. Set $M = \|f\|_{L^\infty([0,1])} + 1$
 1090 and define

1091
$$\xi_k := \frac{f(x_k) + M}{2M} \in [0, 1] \quad \text{for } k = 1, 2, \dots, K.$$

1092 Then $[\xi_1, \xi_2, \dots, \xi_K]^T$ is in $[0, 1]^K$. By Proposition 2.2, there exists $w_0 \in \mathbb{R}$ such that

1093
$$\left| \sigma_1\left(\frac{w_0}{\pi+k}\right) - \xi_k \right| < \varepsilon/(4M) \quad \text{for } k = 1, 2, \dots, K.$$

1094 Let m_0 be an integer larger than $|w_0|$, e.g., set $m_0 = \lfloor |w_0| \rfloor + 1$. It is easy to verify that

1095
$$\frac{w_0}{\pi+k} + 2m_0 \geq 0 \quad \text{for any } x \in [0, 1].$$

1096 Since $\sigma(x) = \sigma_1(x)$ for $x \geq 0$ and σ_1 is periodic with period 2, we have

1097
$$\left| \sigma\left(\frac{w_0}{\pi+k} + 2m_0\right) - \xi_k \right| = \left| \sigma_1\left(\frac{w_0}{\pi+k} + 2m_0\right) - \xi_k \right| = \left| \sigma_1\left(\frac{w_0}{\pi+k}\right) - \xi_k \right| < \varepsilon/(4M),$$

1098 for $k = 1, 2, \dots, K$. It follows that

1099
$$\begin{aligned} \left| 2M\sigma\left(\frac{w_0}{\pi+k} + 2m_0\right) - M - f(x_k) \right| &= \left| 2M\sigma\left(\frac{w_0}{\pi+k} + 2m_0\right) - M - (2M\xi_k - M) \right| \\ &= 2M \left| \sigma\left(\frac{w_0}{\pi+k} + 2m_0\right) - \xi_k \right| < 2M \frac{\varepsilon}{4M} = \varepsilon/2, \end{aligned} \quad (20)$$

1100 for $k = 1, 2, \dots, K$.

The desired ϕ is defined as

$$\phi(x) := 2M\sigma\left(\frac{w_0}{\pi+\psi(2Kx)/2+1} + 2m_0\right) - M \quad \text{for any } x \in [0, 1].$$

Recall that $m_0 \geq |w_0|$ and $\psi(x) \geq 0$ for any $x \geq 0$, which implies $\frac{w_0}{\pi+\psi(2Kx)/2+1} + 2m_0 \geq 0$ for any $x \in [0, 1]$. Thus, $\|\phi\|_{L^\infty([0,1])} \leq M = \|f\|_{L^\infty([0,1])} + 1$ since $0 \leq \sigma(y) \leq 1$ for any $y \geq 0$.

For any $x \in \mathcal{I}_k$ and each $k \in \{1, 2, \dots, K\}$, we have $\psi(2Kx)/2 + 1 = k$, which implies

$$\phi(x) = 2M\sigma\left(\frac{w_0}{\pi+\psi(2Kx)/2+1} + 2m_0\right) - M = 2M\sigma\left(\frac{w_0}{\pi+k} + 2m_0\right) - M.$$

For any $x \in \mathcal{I}_k$ and each $k \in \{1, 2, \dots, K\}$, we have $|x_k - x| < 1/K$, which implies $|f(x_k) - f(x)| < \varepsilon/2$ by Equation (19). Therefore, by Equation (20), we have

$$\begin{aligned} |\phi(x) - f(x)| &= \left| 2M\sigma\left(\frac{w_0}{\pi+k} + 2m_0\right) - M - f(x) \right| \\ &\leq \left| 2M\sigma\left(\frac{w_0}{\pi+k} + 2m_0\right) - M - f(x_k) \right| + |f(x_k) - f(x)| < \varepsilon/2 + \varepsilon/2 = \varepsilon, \end{aligned}$$

for any $x \in \mathcal{I}_k$ and each $k \in \{1, 2, \dots, K\}$. It follows that

$$|\phi(x) - f(x)| < \varepsilon \quad \text{for any } x \in \bigcup_{j=1}^K \mathcal{I}_j = \bigcup_{j=1}^K \left[\frac{2j-2}{2K}, \frac{2j-1}{2K} \right] = \bigcup_{k=0}^{K-1} \left[\frac{2k}{2K}, \frac{2k+1}{2K} \right].$$

It remains to show that ϕ can be generated by an EUAF network with the desired size. Observe that

$$\sigma(y) + 1 = \frac{y}{|y| + 1} + 1 = \frac{y}{-y + 1} + 1 = \frac{1}{-y + 1} \quad \text{for any } y \leq 0.$$

By setting $y = -\pi - \psi(2Kx)/2 \leq 0$ for any $x \in [0, 1]$, we have

$$\begin{aligned} \frac{1}{\pi+\psi(2Kx)/2+1} &= \frac{1}{-y+1} = \sigma(y) + 1 = \sigma\left(-\pi - \psi(2Kx)/2\right) + 1 \\ &= \sigma\left(-\pi - (2Kx - \sigma(2Kx))/2\right) + 1 \\ &= \sigma\left(-\pi - Kx + \sigma(2Kx)/2\right) + 1, \end{aligned}$$

where the large equality comes from $\psi(z) = z - \sigma(z)$ for any $z \in \mathbb{R}$. Therefore, we get

$$\begin{aligned} \phi(x) &= 2M\sigma\left(\frac{w_0}{\pi+\psi(2Kx)/2+1} + 2m_0\right) - M \\ &= 2M\sigma\left(w_0\sigma\left(-\pi - Kx + \sigma(2Kx)/2\right) + w_0 + 2m_0\right) - M. \end{aligned} \tag{21}$$

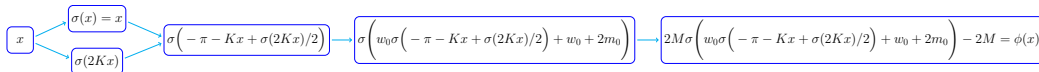


Figure 15: An illustration of the target EUAF network realizing $\phi(x)$ for $x \in [0, 1]$ based on Equation (21).

Thus, the desired EUAF network realizing ϕ is shown in Figure 15. Clearly, the network in Figure 15 has width 2 and depth 3 as desired. It is easy to verify that the network architecture corresponding ϕ is independent of the target function f and the desired error ε . That is, we can fix the architecture and only adjust parameters to achieve the desired approximation error. So we finish the proof.

6.2 Proof of Theorem 6.2

The key idea of proving Theorem 6.2 is to apply Theorem 6.1 to several horizontally shifted variants of the target function. Then a good approximation can be expected via combinations and multiplications of these variants. Thus, we need to reproduce $f(x, y) = xy$ locally via an EUAF network as shown in the following lemma.

Lemma 6.3. *For any $M > 0$, there exists a function ϕ generated by an EUAF network with width 9 and depth 2 such that*

$$\phi(x, y) = xy \quad \text{for any } x, y \in [-M, M].$$

The proof of this lemma is given in Section 6.3. Now let us first prove Theorem 6.2 by assuming this lemma is true.

Proof of Theorem 6.2. Set $\tilde{\varepsilon} = \varepsilon/4$ and extend f from $[0, 1]$ to $[-1, 1]$ by defining $f(x) = f(0)$ for $x \in [-1, 0)$. Then f is continuous on $[-1, 1]$, and, therefore, uniformly continuous. Thus, there exists $K = K(f, \varepsilon) \in \mathbb{N}^+$ with $K \geq 10$ such that

$$|f(x_1) - f(x_2)| < \tilde{\varepsilon}/2 \quad \text{for any } x_1, x_2 \in [-1, 1] \text{ with } |x_1 - x_2| < 1/K.$$

For $i = 1, 2, 3, 4$, define

$$f_i(x) := f\left(x - \frac{i}{4K}\right) \quad \text{for any } x \in [0, 1].$$

For each $i \in \{1, 2, 3, 4\}$ and any $x_1, x_2 \in [0, 1]$ with $|x_1 - x_2| < 1/K$, we have $x_1 - \frac{i}{4K}, x_2 - \frac{i}{4K} \in [-1, 1]$ and $\left|(x_1 - \frac{i}{4K}) - (x_2 - \frac{i}{4K})\right| = |x_1 - x_2| < 1/K$, which implies

$$|f_i(x_1) - f_i(x_2)| = |f(x_1 - \frac{i}{4K}) - f(x_2 - \frac{i}{4K})| < \tilde{\varepsilon}/2.$$

That is, for $i = 1, 2, 3, 4$, we have

$$|f_i(x_1) - f_i(x_2)| < \tilde{\varepsilon}/2 \quad \text{for any } x_1, x_2 \in [0, 1] \text{ with } |x_1 - x_2| < 1/K.$$

For each $i \in \{1, 2, 3, 4\}$, by Theorem 6.1, there exist a function ϕ_i generated by an EUAF network with width 2 and depth 3 such that $\|\phi_i\|_{L^\infty([0,1])} \leq \|f_i\|_{L^\infty([0,1])} + 1 \leq \|f\|_{L^\infty([-1,1])} + 1$ and

$$|\phi_i(x) - f_i(x)| < \tilde{\varepsilon} = \varepsilon/4 \quad \text{for any } x \in \bigcup_{k=0}^{K-1} \left[\frac{2k}{2K}, \frac{2k+1}{2K}\right].$$

Define

$$\psi(x) = \sigma\left(x + 1 - \sigma(x + 1)\right) \quad \text{for any } x \in \mathbb{R}.$$

See an illustration of ψ on $[0, 2K]$ for $K = 5$ in Figure 16.

Clearly, $0 \leq \psi(2Kx) \leq 1$ for any $x \in [0, 1]$, which results in

$$\left|(\phi_i(x) - f_i(x))\psi(2Kx)\right| \leq |\phi_i(x) - f_i(x)| < \varepsilon/4 \quad \text{for any } x \in \bigcup_{k=0}^{K-1} \left[\frac{2k}{2K}, \frac{2k+1}{2K}\right].$$

Observe that $\psi(y) = 0$ for $y \in \bigcup_{k=0}^{K-1} [2k+1, 2k+2]$, which implies

$$\psi(2Kx) = 0 \quad \text{for any } x \in \bigcup_{k=0}^{K-1} \left[\frac{2k+1}{2K}, \frac{2k+2}{2K}\right] \supseteq [0, 1] \setminus \bigcup_{k=0}^{K-1} \left[\frac{2k}{2K}, \frac{2k+1}{2K}\right].$$

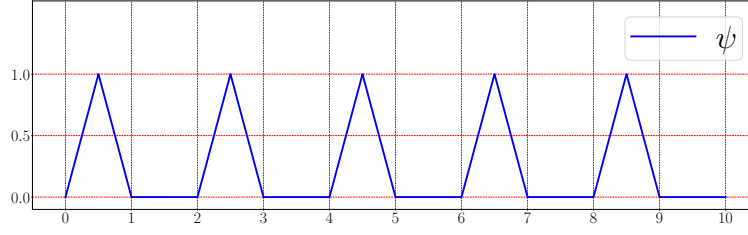


Figure 16: An illustration of ψ on $[0, 2K]$ for $K = 5$.

1156 It follows that

$$1157 \quad \left| (\phi_i(x) - f_i(x))\psi(2Kx) \right| < \varepsilon/4 \quad \text{for any } x \in [0, 1] \text{ and } i = 1, 2, 3, 4. \quad (22)$$

1158 For each $i \in \{1, 2, 3, 4\}$ and any $z \in [0, \frac{9}{10}] \subseteq [0, 1 - \frac{i}{4K}]$, we have $y_i = z + \frac{i}{4K} \in [\frac{i}{4K}, 1] \subseteq$
 1159 $[0, 1]$. Therefore, by bringing $y_i \in [0, 1]$ into Equation (22) (set $x = y_i$ therein), we have

$$\begin{aligned} 1160 \quad \varepsilon/4 &> \left| (\phi_i(y_i) - f_i(y_i))\psi(2Ky_i) \right| = \left| \phi_i(y_i)\psi(2Ky_i) - f_i(y_i)\psi(2Ky_i) \right| \\ &= \left| \phi_i(z + \frac{i}{4K})\psi(2K(z + \frac{i}{4K})) - f_i(z + \frac{i}{4K})\psi(2K(z + \frac{i}{4K})) \right| \\ &= \left| \phi_i(z + \frac{i}{4K})\psi(2Kz + \frac{i}{2}) - f(z)\psi(2Kz + \frac{i}{2}) \right|, \end{aligned} \quad (23)$$

1161 where the last equality comes from the fact that $f_i(x) = f(x - \frac{i}{4K})$ for any $x \in [0, 1] \supseteq [\frac{i}{4K}, 1]$.
 1162 The desired ϕ is defined as

$$1163 \quad \phi(x) := \sum_{i=1}^4 \phi_i(x + \frac{i}{4K})\psi(2Kx + \frac{i}{2}) \quad \text{for any } x \in [0, \frac{9}{10}].$$

1164 It is easy to verify that $\sum_{i=1}^4 \psi(x + \frac{i}{2}) = 1$ for any $x \geq 0$ based on the definition of ψ .
 1165 See Figure 17 for illustrations. It follows that $\sum_{i=1}^4 \psi(2Kz + \frac{i}{2}) = 1$ for any $z \in [0, \frac{9}{10}]$.

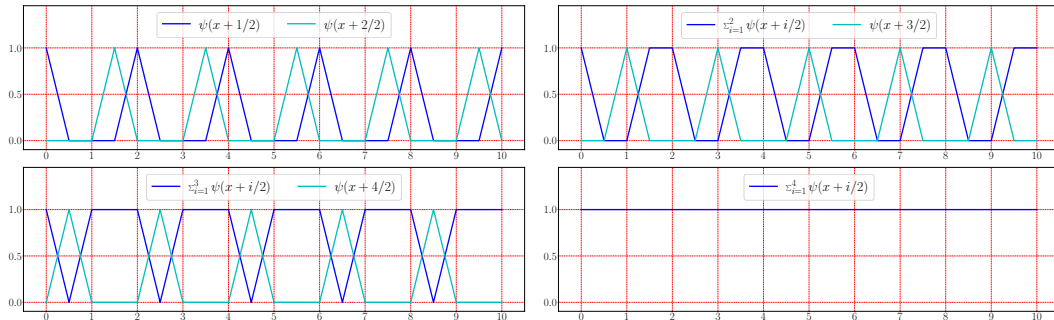


Figure 17: Illustrations of $\sum_{i=1}^4 \psi(x + i/2) = 1$ for any $x \in [0, 10]$.

Hence, by Equation (23), we have

$$\begin{aligned} |\phi(z) - f(z)| &= \left| \sum_{i=1}^4 \phi_i(z + \frac{i}{4K}) \psi(2Kz + \frac{i}{2}) - f(z) \sum_{i=1}^4 \psi(2Kz + \frac{i}{2}) \right| \\ &\leq \sum_{i=1}^4 \left| \phi_i(z + \frac{i}{4K}) \psi(2Kz + \frac{i}{2}) - f(z) \psi(2Kz + \frac{i}{2}) \right| < 4 \frac{\varepsilon}{4} = \varepsilon. \end{aligned}$$

That is, $|\phi(x) - f(x)| < \varepsilon$ for any $x \in [0, \frac{9}{10}]$ as desired. It remains to show that ϕ , limited on $[0, \frac{9}{10}]$, can be generated by an EUAF network with the desired size.

Note that $x + 1 = (2K + 1)\sigma(\frac{x+1}{2K+1})$ for any $x \in [0, 2K]$, which implies

$$\psi(x) = \sigma(x + 1 - \sigma(x + 1)) = \sigma((2K + 1)\sigma(\frac{x+1}{2K+1}) - \sigma(x + 1)).$$

This means ψ , limited on $[0, 2K]$, can be generated by an EUAF network with width 2 and depth 2. Since $0 \leq 2Kx + \frac{i}{2} \leq 2K \cdot \frac{9}{10} + 2 = 2K(\frac{9}{10} + \frac{1}{K}) \leq 2K$ for any $x \in [0, \frac{9}{10}]$, $\psi(2K \cdot + \frac{i}{2})$, limited on $[0, \frac{9}{10}]$, can also be generated by an EUAF network with width 2 and depth 2.

Note that ϕ_i , limited on $[0, 1]$, can also be generated by an EUAF network with width 2 and depth 3. Clearly, $x + \frac{i}{4K} \in [0, 1]$ for any $x \in [0, \frac{9}{10}]$, and, therefore, $\phi_i(\cdot + \frac{i}{4K})$, limited on $[0, \frac{9}{10}]$, can also be generated by an EUAF network with width 2 and depth 3.

Recall that $\|\phi_i\|_{L^\infty([0,1])} \leq \|f\|_{L^\infty([-1,1])} + 1 =: M$. Thus, $|\phi_i(x + \frac{i}{4K})| \leq M$ and $|\psi(2Kx + \frac{i}{2})| \leq 1 \leq M$ for any $x \in [0, \frac{9}{10}]$ and $i = 1, 2, 3, 4$. By Lemma 6.3, there exists a function Γ generated by an EUAF network with width 9 and depth 2 such that

$$\Gamma(x, y) = xy \quad \text{for any } x, y \in [-M, M].$$

It follows that

$$\Gamma\left(\phi_i(x + \frac{i}{4K}), \psi(2Kx + \frac{i}{2})\right) = \phi_i(x + \frac{i}{4K})\psi(2Kx + \frac{i}{2}) \quad \text{for } i = 1, 2, 3, 4.$$

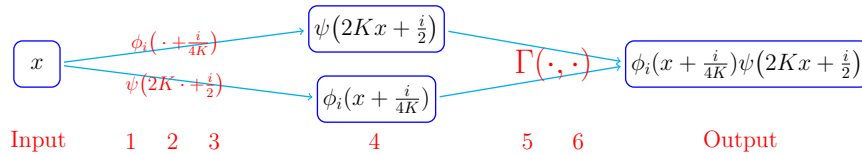


Figure 18: An illustration of the target EUAF network realizing each component of $\phi(x)$, $\phi_i(x + \frac{i}{4K})\psi(2Kx + \frac{i}{2})$, for any $x \in [0, \frac{9}{10}]$ and each $i \in \{1, 2, 3, 4\}$. The networks realizing $\phi_i(\cdot + \frac{i}{4K})$ and $\psi(2K \cdot + \frac{i}{2})$ can be placed in parallel since we can manually add a hidden layer to ψ since $\sigma \circ \psi(2Kx + \frac{i}{2}) = \psi(2Kx + \frac{i}{2})$ for any $x \in [0, \frac{9}{10}]$.

Therefore, each component of $\phi(x)$, $\phi_i(x + \frac{i}{4K})\psi(2Kx + \frac{i}{2})$ for some $i \in \{1, 2, 3, 4\}$, can be generated by the network in Figure 18 for any $x \in [0, \frac{9}{10}]$. Clearly, such a network has width 9 and depth 6. Since the 4-th hidden layer of the network in Figure 18 uses identity as activation function for each neuron in this hidden layer, we can reduce the depth by 1 via composing two adjacent affine linear maps to generate a new one. Thus, the network in Figure 18 can be interpreted as an EUAF network with width 9 and depth 5.

Note that ϕ is the sum of its four components, namely,

$$\phi(x) = \sum_{i=1}^4 \phi_i(x + \frac{i}{4K}) \psi(2Kx + \frac{i}{2}) \quad \text{for any } x \in [0, \frac{9}{10}].$$

Therefore, ϕ , limited on $[0, \frac{9}{10}]$, can be generated by an EUAF network with width $9 \times 4 = 36$ and depth 5 as desired. It is easy to verify that the designed network architecture is independent of the target function f and the desired error ε . That is, we can fix the architecture and only adjust parameters to achieve an arbitrarily desired approximation error. So we finish the proof. \square

6.3 Proof of Lemma 6.3

The key idea of proving Lemma 6.3 is the polarization identity $2xy = (x+y)^2 - x^2 - y^2$. Thus, we need to reproduce x^2 locally by an EUAF network as shown in the following lemma.

Lemma 6.4. *There exists a function ϕ generated by an EUAF network with width 3 and depth 2 such that*

$$\phi(x) = x^2 \quad \text{for any } x \in [-1, 1].$$

Proof. Observe that

$$\sigma(y) + 1 = \frac{y}{|y| + 1} + 1 = \frac{y}{-y + 1} + 1 = \frac{1}{-y + 1} \quad \text{for any } y \leq 0.$$

For any $x \in [-1, 1]$, we have $-x - 1 \leq 0$ and $-x - 2 \leq 0$, which implies

$$\begin{aligned} \sigma(-x - 1) - \sigma(-x - 2) &= \left(\sigma(-x - 1) + 1 \right) - \left(\sigma(-x - 2) + 1 \right) \\ &= \frac{1}{-(-x - 1) + 1} - \frac{1}{-(-x - 2) + 1} = \frac{1}{x + 2} - \frac{1}{x + 3} = \frac{1}{(x + 2)(x + 3)}. \end{aligned}$$

It follows from $1 - \frac{12}{(x+2)(x+3)} \leq 0$ for any $x \in [-1, 1]$ that

$$\sigma\left(1 - \frac{12}{(x + 2)(x + 3)}\right) + 1 = \frac{1}{-\left(1 - \frac{12}{(x+2)(x+3)}\right) + 1} = \frac{x^2 + 5x + 6}{12},$$

implying

$$\begin{aligned} x^2 &= 12\sigma\left(1 - \frac{12}{(x + 2)(x + 3)}\right) + 12 - (5x + 6) \\ &= 12\sigma\left(1 - 12(\sigma(-x - 1) - \sigma(-x - 2))\right) + 11\frac{6 - 5x}{11} \\ &= 12\sigma\left(1 - 12\sigma(-x - 1) + 12\sigma(-x - 2)\right) + 11\sigma\left(\frac{6 - 5x}{11}\right) := \phi(x), \end{aligned}$$

where the equality $\frac{6-5x}{11} = \sigma\left(\frac{6-5x}{11}\right)$ comes from two facts: $\frac{6-5x}{11} \in [0, 1]$ since $x \in [-1, 1]$ and $\sigma(z) = z$ for any $z \in [0, 1]$.

Then, x^2 can be generated by the network shown in Figure 19 for any $x \in [-1, 1]$. The target network has width 3 and depth 2. So we finish the proof. \square

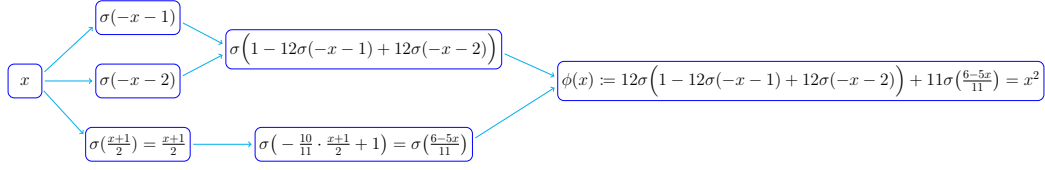


Figure 19: An illustration of the target EUAF network realizing $\phi(x) = x^2$ for $x \in [-1, 1]$.

With Lemma 6.4 at hand, we are ready to prove Lemma 6.3.

Proof of Lemma 6.3. By Lemma 6.4, there exists a function $\tilde{\phi}$ generated by an EUAF network such that $\tilde{\phi}(t) = t^2$ for any $t \in [-1, 1]$. Thus, for any $x, y \in [-M, M]$, we have

$$\begin{aligned} xy &= 2M^2 \left(\left(\frac{x+y}{2M} \right)^2 - \left(\frac{x}{2M} \right)^2 - \left(\frac{y}{2M} \right)^2 \right) \\ &= 2M^2 \left(\tilde{\phi}\left(\frac{x+y}{2M}\right) - \tilde{\phi}\left(\frac{x}{2M}\right) - \tilde{\phi}\left(\frac{y}{2M}\right) \right) =: \phi(x, y). \end{aligned}$$

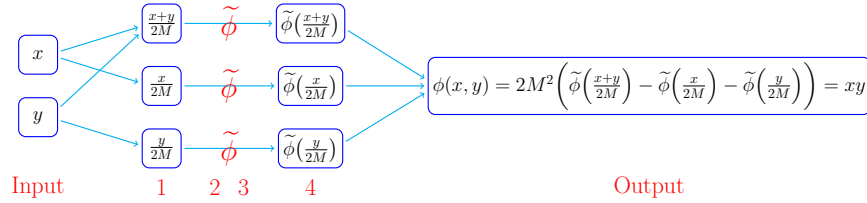


Figure 20: An illustration of the target network realizing $\phi(x, y) = xy$ for $x, y \in [-M, M]$. “ $\xrightarrow{\tilde{\phi}}$ ” means the network realizing $\tilde{\phi}$, i.e., an EUAF network with width 3 and depth 2.

The target network realizing ϕ with width 9 and depth 4 is shown in Figure 20. Note that we can reduce the depth by one if the activation function of each neuron in a hidden layer is identity. In fact, we can eliminate this hidden layer by composing two adjacent affine linear maps to generate a new one. The 1-st and 4-th hidden layers in the network in Figure 20 use identity as an activation function. Thus, the network in Figure 20 can be interpreted as an EUAF network with width 9 and depth 2. So we finish the proof. \square

7. Proof of Proposition 2.2

We will prove Proposition 2.2 in this section. The proof includes two main steps. First, we show how to simply generate a set of rationally independent numbers in Lemma 7.1 below. Next, we prove that the target point set via a winding of the generated rationally independent numbers is dense in a hypercube. Such a proof relies on the fact that an irrational winding on the torus is dense (e.g., see Lemma 2 of (Yarotsky, 2021)) as shown in Lemma 7.2 below in a hypercube.

Lemma 7.1. *Given any $K \in \mathbb{N}^+$, any transcendental number $\alpha \in \mathbb{R} \setminus \mathbb{A}$, and any pairwise distinct rational numbers $r_1, r_2, \dots, r_K \in \mathbb{Q}$, the set of numbers*

$$\left\{ \frac{1}{\alpha + r_k} : k = 1, 2, \dots, K \right\}$$

1236 are rationally independent.

1237 **Lemma 7.2.** *Given any rationally independent numbers a_1, a_2, \dots, a_K for any $K \in \mathbb{N}^+$ and*
 1238 *an arbitrary periodic function $g : \mathbb{R} \rightarrow \mathbb{R}$ with period T , i.e., $g(x + T) = g(x)$ for any $x \in \mathbb{R}$,*
 1239 *assume there exist $x_1, x_2 \in \mathbb{R}$ with $0 < x_2 - x_1 < T$ such that g is continuous on $[x_1, x_2]$.*
 1240 *Then the following set*

$$1241 \quad \left\{ [g(wa_1), g(wa_2), \dots, g(wa_K)]^T : w \in \mathbb{R} \right\}$$

1242 *is dense in $[M_1, M_2]^K$, where $M_1 = \min_{x \in [x_1, x_2]} g(x)$ and $M_2 = \max_{x \in [x_1, x_2]} g(x)$.*

1243 The proofs of these two lemmas can be found in Sections 7.1 and 7.2, respectively.
 1244 With these two lemmas at hand, the proof of Proposition 2.2 is straightforward. In fact,
 1245 we can prove a more general result in Proposition 7.3 below, which implies Proposition 2.2
 1246 immediately.

1247 **Proposition 7.3.** *Given an arbitrary periodic function $g : \mathbb{R} \rightarrow \mathbb{R}$ with period T , i.e.,*
 1248 *$g(x + T) = g(x)$ for any $x \in \mathbb{R}$, assume there exist $x_1, x_2 \in \mathbb{R}$ with $0 < x_2 - x_1 < T$ such that g*
 1249 *is continuous on $[x_1, x_2]$. Then, for any $K \in \mathbb{N}^+$, any transcendental number $\alpha \in \mathbb{R} \setminus \mathbb{A}$, and*
 1250 *any pairwise distinct rational numbers $r_1, r_2, \dots, r_K \in \mathbb{Q}$, the following set*

$$1251 \quad \left\{ \left[g\left(\frac{w}{\alpha+r_1}\right), g\left(\frac{w}{\alpha+r_2}\right), \dots, g\left(\frac{w}{\alpha+r_K}\right) \right]^T : w \in \mathbb{R} \right\}$$

1252 *is dense in $[M_1, M_2]^K$, where $M_1 = \min_{x \in [x_1, x_2]} g(x)$ and $M_2 = \max_{x \in [x_1, x_2]} g(x)$. In the case of*
 1253 *$M_1 < M_2$, the following set*

$$1254 \quad \left\{ \left[u \cdot g\left(\frac{w}{\alpha+r_1}\right) + v, u \cdot g\left(\frac{w}{\alpha+r_2}\right) + v, \dots, u \cdot g\left(\frac{w}{\alpha+r_K}\right) + v \right]^T : u, v, w \in \mathbb{R} \right\}$$

1255 *is dense in \mathbb{R}^K .*

1256 Clearly, Proposition 2.2 is a special case of Proposition 7.3 with $g = \sigma_1$, $\alpha = \pi$, $r_k = k$ for
 1257 $k = 1, 2, \dots, K$. The transcendence of π is well known (e.g., see the Lindemann–Weierstrass
 1258 Theorem). By setting $x_1 = 0$ and $x_2 = 1$, we have $[M_1, M_2] = [0, 1]$ and σ_1 is continuous on
 1259 $[0, 1]$, which means that the following set

$$1260 \quad \left\{ \left[\sigma_1\left(\frac{w}{\pi+1}\right), \sigma_1\left(\frac{w}{\pi+2}\right), \dots, \sigma_1\left(\frac{w}{\pi+K}\right) \right]^T : w \in \mathbb{R} \right\}$$

1261 *is dense in $[0, 1]^K$ as desired.*

1262 Finally, let us prove Proposition 7.3 by assuming Lemmas 7.1 and 7.2 are true.

1263 *Proof of Proposition 7.3.* By Lemma 7.1, the set of numbers

$$1264 \quad \left\{ \frac{1}{\alpha+r_k} : k = 1, 2, \dots, K \right\}$$

1265 are rationally independent. Denote $a_k = \frac{1}{\alpha+r_k}$ for $k = 1, 2, \dots, K$. Then, by Lemma 7.2,

$$1266 \quad \begin{aligned} & \left\{ [g(wa_1), g(wa_2), \dots, g(wa_K)]^T : w \in \mathbb{R} \right\} \\ &= \left\{ \left[g\left(\frac{w}{\alpha+r_1}\right), g\left(\frac{w}{\alpha+r_2}\right), \dots, g\left(\frac{w}{\alpha+r_K}\right) \right]^T : w \in \mathbb{R} \right\} \end{aligned}$$

is dense in $[M_1, M_2]^K$. Now consider the case $M_1 < M_2$ for the latter result. For any $\varepsilon > 0$ and any $\mathbf{x} \in \mathbb{R}^K$, by setting $J = \|\mathbf{x}\|_\infty + 1 > 0$, we have $\frac{\mathbf{x}+J}{2J} \in [0, 1]^K$, and hence

$$\mathbf{y} := \frac{\mathbf{x}+J}{2J}(M_2 - M_1) + M_1 \in [M_1, M_2]^K.$$

By the former result, there exists $w_0 \in \mathbb{R}$ such that

$$\left\| \mathbf{y} - \left[g\left(\frac{w_0}{\alpha+r_1}\right), g\left(\frac{w_0}{\alpha+r_2}\right), \dots, g\left(\frac{w_0}{\alpha+r_K}\right) \right]^T \right\|_\infty < \frac{M_2-M_1}{2J} \varepsilon$$

It follows from $\mathbf{y} = \frac{\mathbf{x}+J}{2J}(M_2 - M_1) + M_1$ that $\mathbf{x} = \frac{2J}{M_2-M_1} \mathbf{y} + \frac{J(M_1+M_2)}{M_1-M_2} =: u_0 \mathbf{y} + v_0$, where $u_0 = \frac{2J}{M_2-M_1}$ and $v_0 = \frac{J(M_1+M_2)}{M_1-M_2}$. Therefore,

$$\begin{aligned} & \left\| \mathbf{x} - \left[u_0 g\left(\frac{w_0}{\alpha+r_1}\right) + v_0, u_0 g\left(\frac{w_0}{\alpha+r_2}\right) + v_0, \dots, u_0 g\left(\frac{w_0}{\alpha+r_K}\right) + v_0 \right]^T \right\|_\infty \\ &= \left\| u_0 \mathbf{y} + v_0 - \left[u_0 g\left(\frac{w_0}{\alpha+r_1}\right) + v_0, u_0 g\left(\frac{w_0}{\alpha+r_2}\right) + v_0, \dots, u_0 g\left(\frac{w_0}{\alpha+r_K}\right) + v_0 \right]^T \right\|_\infty < u_0 \frac{M_2-M_1}{2J} \varepsilon = \varepsilon. \end{aligned}$$

Since $\varepsilon > 0$ and $\mathbf{x} \in \mathbb{R}^K$ are arbitrary, the following set

$$\left\{ \left[u \cdot g\left(\frac{w}{\alpha+r_1}\right) + v, u \cdot g\left(\frac{w}{\alpha+r_2}\right) + v, \dots, u \cdot g\left(\frac{w}{\alpha+r_K}\right) + v \right]^T : u, v, w \in \mathbb{R} \right\}$$

is dense in \mathbb{R}^K . So we finish the proof. \square

7.1 Proof of Lemma 7.1

Before proving Lemma 7.1, let us have a brief discussion on related concepts. Recall that a complex number α is an algebraic number if and only if there exist $\lambda_0, \lambda_1, \dots, \lambda_J \in \mathbb{Q}$ with $\sum_{j=0}^J \lambda_j \alpha^j = 0$. The set of all algebraic numbers is denoted by \mathbb{A} . A complex number is called **transcendental** if it is not in \mathbb{A} . It is well known that the set \mathbb{A} is **countable**, and, therefore, almost all numbers are transcendental. Therefore, for almost all $\alpha \in \mathbb{R}$, the set of numbers $\left\{ \frac{1}{\alpha+k} : k = 1, 2, \dots, K \right\}$ are rationally independent. The best known transcendental numbers are π (the ratio of a circle's circumference to its diameter) and e (the natural logarithmic base). Thus, both sets of numbers $\left\{ \frac{1}{\pi+k} : k = 1, 2, \dots, K \right\}$ and $\left\{ \frac{1}{e+k} : k = 1, 2, \dots, K \right\}$ are rational independent.

In order to prove Lemma 7.1, we need an auxiliary lemma below, characterizing some properties of coefficients of Lagrange basis polynomials. Recall that, for any given pairwise distinct numbers $x_1, x_2, \dots, x_K \in \mathbb{R}$, the Lagrange basis polynomials are

$$p_k(x) := \prod_{\substack{j \in \{1, 2, \dots, K\} \\ j \neq k}} \frac{x - x_j}{x_k - x_j} = \frac{x - x_1}{x_k - x_1} \dots \frac{x - x_{k-1}}{x_k - x_{k-1}} \frac{x - x_{k+1}}{x_k - x_{k+1}} \dots \frac{x - x_K}{x_k - x_K}, \quad (24)$$

for $k = 1, 2, \dots, K$. They are polynomials of degree $\leq K - 1$. Thus, the coefficients of these K Lagrange basis polynomials form a matrix

$$\mathbf{A} = (a_{i,j}) = \begin{bmatrix} a_{1,1} & a_{1,2} & \dots & a_{1,K} \\ a_{2,1} & a_{2,2} & \dots & a_{2,K} \\ \vdots & \vdots & \ddots & \vdots \\ a_{K,1} & a_{K,2} & \dots & a_{K,K} \end{bmatrix} \in \mathbb{R}^{K \times K}, \quad (25)$$

1295 which satisfies the following equality

$$1296 \quad p_k(x) = \sum_{j=1}^K a_{k,j} x^{j-1} = a_{k,1} + a_{k,2}x + \cdots + a_{k,K}x^{K-1} \quad \text{for } k = 1, 2, \dots, K \text{ and any } x \in \mathbb{R}.$$

1297 The lemma below essentially characterizes the linear independence of Lagrange basis
1298 polynomials.

1299 **Lemma 7.4.** *With the same setting just above, the matrix \mathbf{A} given in Equation (25) is*
1300 *invertible.*

1301 *Proof.* For any $\mathbf{y} = [y_1, y_2, \dots, y_K] \in \mathbb{R}^K$, by the definition of Lagrange basis polynomials
1302 $p_k(x)$ for $k = 1, 2, \dots, K$ in Equation (24), $p(x) = \sum_{k=1}^K y_k p_k(x)$ is the target interpolation
1303 polynomial for sample points $(x_1, y_1), (x_2, y_2), \dots, (x_K, y_K)$. That is, for any $\ell \in \{1, 2, \dots, K\}$,
1304 we have

$$\begin{aligned} y_\ell = p(x_\ell) &= \sum_{k=1}^K y_k p_k(x_\ell) = \sum_{k=1}^K y_k \sum_{j=1}^K a_{k,j} x_\ell^{j-1} \\ 1305 \quad &= [y_1, y_2, \dots, y_K] \cdot \begin{bmatrix} a_{1,1} & a_{1,2} & \cdots & a_{1,K} \\ a_{2,1} & a_{2,2} & \cdots & a_{2,K} \\ \vdots & \vdots & \ddots & \vdots \\ a_{K,1} & a_{K,2} & \cdots & a_{K,K} \end{bmatrix} \cdot \begin{bmatrix} x_\ell^0 \\ x_\ell^1 \\ \vdots \\ x_\ell^{K-1} \end{bmatrix} = \mathbf{y}^T \mathbf{A} \begin{bmatrix} x_\ell^0 \\ x_\ell^1 \\ \vdots \\ x_\ell^{K-1} \end{bmatrix}. \end{aligned}$$

1306 It follows that

$$1307 \quad \mathbf{y}^T = [y_1, y_2, \dots, y_K] = \mathbf{y}^T \mathbf{A} \begin{bmatrix} x_1^0 & x_2^0 & \cdots & x_K^0 \\ x_1^1 & x_2^1 & \cdots & x_K^1 \\ \vdots & \vdots & \ddots & \vdots \\ x_1^{K-1} & x_2^{K-1} & \cdots & x_K^{K-1} \end{bmatrix}.$$

1308 Since $\mathbf{y} \in \mathbb{R}^K$ is arbitrary, we have

$$1309 \quad \mathbf{A} \begin{bmatrix} x_1^0 & x_2^0 & \cdots & x_K^0 \\ x_1^1 & x_2^1 & \cdots & x_K^1 \\ \vdots & \vdots & \ddots & \vdots \\ x_1^{K-1} & x_2^{K-1} & \cdots & x_K^{K-1} \end{bmatrix} = \mathbf{I}_K,$$

1310 where $\mathbf{I}_K \in \mathbb{R}^{K \times K}$ is the identity matrix. Recall that x_1, x_2, \dots, x_K are pairwise distinct,
1311 which implies the Vandermonde matrix

$$1312 \quad \begin{bmatrix} x_1^0 & x_2^0 & \cdots & x_K^0 \\ x_1^1 & x_2^1 & \cdots & x_K^1 \\ \vdots & \vdots & \ddots & \vdots \\ x_1^{K-1} & x_2^{K-1} & \cdots & x_K^{K-1} \end{bmatrix}$$

1313 is invertible. Thus, \mathbf{A} is also invertible. So we complete the proof. □

1314 With Lemma 7.4 at hand, we are ready to prove Lemma 7.1.

1315 *Proof of Lemma 7.1.* Let $x_k = -r_k \in \mathbb{Q}$ for $k = 1, 2, \dots, K$ and define the Lagrange basis
 1316 polynomials as

$$1317 \quad p_k(x) := \prod_{\substack{j \in \{1, 2, \dots, K\} \\ j \neq k}} \frac{x - x_j}{x_k - x_j} = w_k \prod_{\substack{j \in \{1, 2, \dots, K\} \\ j \neq k}} (x - x_j), \quad \text{where } w_k = \prod_{\substack{j \in \{1, 2, \dots, K\} \\ j \neq k}} \frac{1}{x_k - x_j} \neq 0,$$

1318 for $k = 1, 2, \dots, K$. Note that w_k is rational and nonzero for any k , which is important for
 1319 later proof. The coefficients of these K Lagrange basis polynomials form a matrix

$$1320 \quad \mathbf{A} = (a_{i,j}) = \begin{bmatrix} a_{1,1} & a_{1,2} & \cdots & a_{1,K} \\ a_{2,1} & a_{2,2} & \cdots & a_{2,K} \\ \vdots & \vdots & \ddots & \vdots \\ a_{K,1} & a_{K,2} & \cdots & a_{K,K} \end{bmatrix} \in \mathbb{R}^{K \times K},$$

1321 which satisfies the following equality

$$1322 \quad p_k(x) = \sum_{j=1}^K a_{k,j} x^{j-1} = a_{k,1} + a_{k,2}x + \cdots + a_{k,K}x^{K-1} \quad \text{for } k = 1, 2, \dots, K \text{ and any } x \in \mathbb{R}.$$

1323 Now assume there exist $\lambda_1, \lambda_2, \dots, \lambda_K \in \mathbb{Q}$ such that $\sum_{k=1}^K \lambda_k \cdot \frac{1}{\alpha + r_k} = 0$. Our goal is to
 1324 prove $\lambda_1 = \lambda_2 = \cdots = \lambda_K = 0$. Clearly, we have

$$\begin{aligned} 0 &= \sum_{k=1}^K \lambda_k \cdot \frac{1}{\alpha + r_k} = \sum_{k=1}^K \underbrace{\frac{\lambda_k}{\alpha - x_k}}_{=0} = \prod_{j=1}^K (\alpha - x_j) \cdot \sum_{k=1}^K \underbrace{\frac{\lambda_k}{\alpha - x_k}}_{=0} = \sum_{k=1}^K \frac{\lambda_k}{w_k} \cdot w_k \prod_{\substack{j \in \{1, 2, \dots, K\} \\ j \neq k}} (\alpha - x_j) \\ 1325 \quad &= \sum_{k=1}^K \frac{\lambda_k}{w_k} \cdot p_k(\alpha) = \sum_{k=1}^K \frac{\lambda_k}{w_k} \sum_{j=1}^K a_{k,j} \alpha^{j-1} = \sum_{j=1}^K \left(\underbrace{\sum_{k=1}^K \frac{\lambda_k}{w_k} a_{k,j}}_{=0 \text{ since } \alpha \in \mathbb{R} \setminus \mathbb{A}} \right) \cdot \alpha^{j-1}. \end{aligned}$$

1326 Note that $\alpha \in \mathbb{R} \setminus \mathbb{A}$ is not an algebraic number and $\frac{\lambda_k}{w_k} \in \mathbb{Q}$ since $\lambda_k, w_k \in \mathbb{Q}$ for any k . Thus,
 1327 the coefficients must be 0, namely,

$$1328 \quad \sum_{k=1}^K \frac{\lambda_k}{w_k} a_{k,j} = 0 \quad \text{for } j = 1, 2, \dots, K.$$

1329 It follows that

$$1330 \quad \mathbf{0} = \left[\frac{\lambda_1}{w_1}, \frac{\lambda_2}{w_2}, \dots, \frac{\lambda_K}{w_K} \right] \begin{bmatrix} a_{1,1} & a_{1,2} & \cdots & a_{1,K} \\ a_{2,1} & a_{2,2} & \cdots & a_{2,K} \\ \vdots & \vdots & \ddots & \vdots \\ a_{K,1} & a_{K,2} & \cdots & a_{K,K} \end{bmatrix} = \left[\frac{\lambda_1}{w_1}, \frac{\lambda_2}{w_2}, \dots, \frac{\lambda_K}{w_K} \right] \mathbf{A}.$$

1331 By Lemma 7.4, \mathbf{A} is invertible. Thus, $\left[\frac{\lambda_1}{w_1}, \frac{\lambda_2}{w_2}, \dots, \frac{\lambda_K}{w_K} \right] = \mathbf{0}$, which implies $\lambda_1 = \lambda_2 = \cdots =$
 1332 $\lambda_K = 0$. Hence, the set of numbers $\left\{ \frac{1}{\alpha + r_k} : k = 1, 2, \dots, K \right\}$ are rationally independent, which
 1333 means we finish the proof. \square

7.2 Proof of Lemma 7.2

The proof of Lemma 7.2 is mainly based on the fact that an irrational winding is dense on the torus (e.g., see Lemma 2 of (Yarotsky, 2021)). For completeness, we establish a lemma below and give its detailed proof.

Lemma 7.5. *Given any $K \in \mathbb{N}^+$ and an arbitrary set of rationally independent numbers $\{a_k : k = 1, 2, \dots, K\} \subseteq \mathbb{R}$, the following set*

$$\left\{ \left[\tau(wa_1), \tau(wa_2), \dots, \tau(wa_K) \right]^T : w \in \mathbb{R} \right\} \subseteq [0, 1)^K$$

is dense in $[0, 1]^K$, where $\tau(x) := x - \lfloor x \rfloor$ for any $x \in \mathbb{R}$.

The proof of Lemma 7.5 can be found later in this section. Now let us first prove Lemma 7.2 by assuming Lemma 7.5 is true.

Proof of Lemma 7.2. Define $\tilde{g}(x) := g(Tx)$ for any $x \in \mathbb{R}$. The continuity of g on $[x_1, x_2]$ implies \tilde{g} is continuous on $[\frac{x_1}{T}, \frac{x_2}{T}]$, and, therefore, uniformly continuous on $[\frac{x_1}{T}, \frac{x_2}{T}]$. For any $\varepsilon > 0$, there exists $\delta \in (0, \frac{x_2 - x_1}{T})$ such that

$$|\tilde{g}(u) - \tilde{g}(v)| < \varepsilon \quad \text{for any } u, v \in [\frac{x_1}{T}, \frac{x_2}{T}] \text{ with } |u - v| < \delta. \quad (26)$$

Given any $\boldsymbol{\xi} = [\xi_1, \xi_2, \dots, \xi_K] \in [M_1, M_2]^K$, by the intermediate value theorem, there exists $z_1, z_2, \dots, z_K \in [x_1, x_2]$ such that $g(z_k) = \xi_k$ for any $k = 1, 2, \dots, K$.

For any $k = 1, 2, \dots, K$, set $y_k = z_k/T \in [\frac{x_1}{T}, \frac{x_2}{T}]$ and

$$\tilde{y}_k = y_k + \frac{\delta}{2} \cdot \mathbb{1}_{\{y_k \leq \frac{x_1}{T} + \frac{\delta}{2}\}} - \frac{\delta}{2} \cdot \mathbb{1}_{\{y_k \geq \frac{x_2}{T} - \frac{\delta}{2}\}}.$$

Then, for $k = 1, 2, \dots, K$, we have

$$\tilde{y}_k = y_k + \frac{\delta}{2} \cdot \mathbb{1}_{\{y_k \leq \frac{x_1}{T} + \frac{\delta}{2}\}} - \frac{\delta}{2} \cdot \mathbb{1}_{\{y_k \geq \frac{x_2}{T} - \frac{\delta}{2}\}} \in \left[\frac{x_1}{T} + \frac{\delta}{2}, \frac{x_2}{T} - \frac{\delta}{2} \right]$$

and

$$|\tilde{y}_k - y_k| \leq \left| \frac{\delta}{2} \cdot \mathbb{1}_{\{y_k \leq \frac{x_1}{T} + \frac{\delta}{2}\}} - \frac{\delta}{2} \cdot \mathbb{1}_{\{y_k \geq \frac{x_2}{T} - \frac{\delta}{2}\}} \right| \leq \delta/2.$$

Define $\tau(x) = x - \lfloor x \rfloor$ for any $x \in \mathbb{R}$. Clearly, $[\tau(\tilde{y}_1), \tau(\tilde{y}_2), \dots, \tau(\tilde{y}_K)]^T \in [0, 1]^K$. Then by Lemma 7.5, there exists $w_0 \in \mathbb{R}$ such that

$$|\tau(w_0 a_k) - \tau(\tilde{y}_k)| < \delta/2 \quad \text{for } k = 1, 2, \dots, K.$$

It follows that

$$\left| \tau(w_0 a_k) + \lfloor \tilde{y}_k \rfloor - \tilde{y}_k \right| = \left| \tau(w_0 a_k) - (\tilde{y}_k - \lfloor \tilde{y}_k \rfloor) \right| = \left| \tau(w_0 a_k) - \tau(\tilde{y}_k) \right| < \delta/2,$$

for $k = 1, 2, \dots, K$. Since $\tilde{y}_k \in [\frac{x_1}{T} + \frac{\delta}{2}, \frac{x_2}{T} - \frac{\delta}{2}]$, we have $\tau(w_0 a_k) + \lfloor \tilde{y}_k \rfloor \in [\frac{x_1}{T}, \frac{x_2}{T}]$. Besides,

$$\left| \tau(w_0 a_k) + \lfloor \tilde{y}_k \rfloor - y_k \right| \leq \left| \tau(w_0 a_k) + \lfloor \tilde{y}_k \rfloor - \tilde{y}_k \right| + |\tilde{y}_k - y_k| < \delta/2 + \delta/2 = \delta,$$

1363 for $k = 1, 2, \dots, K$. Then, by Equation (26), we have

$$1364 \quad \left| \widetilde{g}(\tau(w_0 a_k) + \lfloor \widetilde{y}_k \rfloor) - \widetilde{g}(y_k) \right| < \varepsilon \quad \text{for } k = 1, 2, \dots, K.$$

1365 By the definition of \widetilde{g} , it is periodic with period 1 since g is periodic with period T . This
1366 implies

$$1367 \quad \widetilde{g}(\tau(w_0 a_k) + \lfloor \widetilde{y}_k \rfloor) = \widetilde{g}(w_0 a_k - \lfloor w_0 a_k \rfloor + \lfloor \widetilde{y}_k \rfloor) = \widetilde{g}(w_0 a_k) = g(T \cdot w_0 a_k),$$

1368 for $k = 1, 2, \dots, K$. Also, $\widetilde{g}(y_k) = g(T y_k) = g(z_k) = \xi_k$ for $k = 1, 2, \dots, K$. It follows that

$$1369 \quad |g(T \cdot w_0 a_k) - \xi_k| = \left| \widetilde{g}(\tau(w_0 a_k) + \lfloor \widetilde{y}_k \rfloor) - \widetilde{g}(y_k) \right| < \varepsilon \quad \text{for } k = 1, 2, \dots, K.$$

1370 That is

$$1371 \quad \left\| [g(w_1 a_1), g(w_1 a_2), \dots, g(w_1 a_K)]^T - \boldsymbol{\xi} \right\|_\infty < \varepsilon,$$

1372 where $w_1 = T \cdot w_0 \in \mathbb{R}$. Since $\boldsymbol{\xi} \in [M_1, M_2]^K$ and $\varepsilon > 0$ are arbitrary, the following set

$$1373 \quad \left\{ [g(w a_1), g(w a_2), \dots, g(w a_K)]^T : w \in \mathbb{R} \right\}$$

1374 is dense in $[M_1, M_2]^K$ as desired. So we finish the proof. \square

1375 Finally, let us present the detailed proof of Lemma 7.5.

1376 *Proof of Lemma 7.5.* We prove this lemma by mathematical induction. First, we consider
1377 the case $K = 1$. Note that $a_1 \neq 0$ since it is rationally independent. Thus, we have
1378 $\{\tau(w a_1) : w \in \mathbb{R}\} = [0, 1)$, which implies $\{\tau(w a_1) : w \in \mathbb{R}\}$ is dense in $[0, 1]$.

1379 Now assume this lemma holds for $K = J - 1 \in \mathbb{N}^+$. Our goal is to prove the case $K = J$.
1380 Given any $\varepsilon \in (0, 1/100)$ and arbitrary $\boldsymbol{\xi} = [\xi_1, \xi_2, \dots, \xi_J]^T \in [0, 1]^J$, our goal is to find a
1381 proper $w \in \mathbb{R}$ such that

$$1382 \quad |\tau(w a_j) - \xi_j| < C\varepsilon \quad \text{for } j = 1, 2, \dots, J, \quad \text{where } C \text{ is an absolute constant.} \quad (27)$$

1383 As we shall see later, we need an assumption that the given point is in $[6\varepsilon, 1 - 6\varepsilon]^J$. Thus,
1384 we set

$$1385 \quad \widetilde{\xi}_j = \xi_j + 6\varepsilon \cdot \mathbf{1}_{\{\xi_j \leq 6\varepsilon\}} - 6\varepsilon \cdot \mathbf{1}_{\{\xi_j \geq 1 - 6\varepsilon\}} \quad \text{for } j = 1, 2, \dots, J.$$

1386 Then, we have

$$1387 \quad \widetilde{\xi}_j \in [6\varepsilon, 1 - 6\varepsilon] \quad \text{for } j = 1, 2, \dots, J \quad (28)$$

1388 and

$$1389 \quad |\xi_j - \widetilde{\xi}_j| = |6\varepsilon \cdot \mathbf{1}_{\{\xi_j \leq 6\varepsilon\}} - 6\varepsilon \cdot \mathbf{1}_{\{\xi_j \geq 1 - 6\varepsilon\}}| \leq 6\varepsilon \quad \text{for } j = 1, 2, \dots, J. \quad (29)$$

1390 Define

$$1391 \quad \widehat{\xi}_j := \tau(\widetilde{\xi}_j - \frac{\widetilde{\xi}_J}{a_J} a_j) \quad \text{for } j = 1, 2, \dots, J. \quad (30)$$

1392 Then $\widehat{\xi}_J = 0$ and $\widehat{\xi}_j \in [0, 1)$ for $j = 1, 2, \dots, J - 1$. To approximate $[\widehat{\xi}_1, \widehat{\xi}_2, \dots, \widehat{\xi}_{J-1}]^T \in [0, 1)^{J-1}$,
1393 we only need to consider $J - 1$ indices, and, therefore, we can use the induction hypothesis
1394 to continue our proof.

Clearly, the rational independence of a_1, a_2, \dots, a_J implies none of them is equal to zero.

Define

$$\mathbf{b}_n := \left[\tau\left(\frac{n}{a_J}a_1\right), \tau\left(\frac{n}{a_J}a_2\right), \dots, \tau\left(\frac{n}{a_J}a_{J-1}\right) \right]^T \in [0, 1)^{J-1}.$$

Then the bounded sequence $(\mathbf{b}_n)_{n=1}^\infty$ has a convergent subsequence by the Bolzano-Weierstrass Theorem. Thus, there exist $n_1, n_2 \in \mathbb{N}^+$ with $n_1 < n_2$ such that $\|\mathbf{b}_{n_2} - \mathbf{b}_{n_1}\|_\infty < \varepsilon$. That is,

$$\left| \tau\left(\frac{n_2}{a_J}a_j\right) - \tau\left(\frac{n_1}{a_J}a_j\right) \right| < \varepsilon \quad \text{for } j = 1, 2, \dots, J-1.$$

Set $\widehat{n} = n_2 - n_1 \in \mathbb{N}^+$ and $k_j = \left\lfloor \frac{n_1}{a_J}a_j \right\rfloor - \left\lfloor \frac{n_2}{a_J}a_j \right\rfloor$ for $j = 1, 2, \dots, J-1$. Then, by defining

$$\widehat{a}_j := \frac{\widehat{n}}{a_J}a_j + k_j \quad \text{for } j = 1, 2, \dots, J-1,$$

we have

$$\begin{aligned} |\widehat{a}_j| &= \left| \frac{\widehat{n}}{a_J}a_j + k_j \right| = \left| \frac{n_2}{a_J}a_j - \frac{n_1}{a_J}a_j + \left\lfloor \frac{n_1}{a_J}a_j \right\rfloor - \left\lfloor \frac{n_2}{a_J}a_j \right\rfloor \right| \\ &= \left| \left(\frac{n_2}{a_J}a_j - \left\lfloor \frac{n_2}{a_J}a_j \right\rfloor \right) - \left(\frac{n_1}{a_J}a_j - \left\lfloor \frac{n_1}{a_J}a_j \right\rfloor \right) \right| = \left| \tau\left(\frac{n_2}{a_J}a_j\right) - \tau\left(\frac{n_1}{a_J}a_j\right) \right| < \varepsilon. \end{aligned} \quad (31)$$

It is easy to verify that $\widehat{a}_1, \widehat{a}_2, \dots, \widehat{a}_{J-1}$ are rationally independent. To see this, assume there exist $\lambda_1, \lambda_2, \dots, \lambda_{J-1} \in \mathbb{Q}$ such that

$$0 = \sum_{j=1}^{J-1} \lambda_j \widehat{a}_j = \sum_{j=1}^{J-1} \lambda_j \left(\frac{\widehat{n}}{a_J}a_j + k_j \right) = \sum_{j=1}^{J-1} \lambda_j \frac{\widehat{n}}{a_J}a_j + \sum_{j=1}^{J-1} \lambda_j k_j,$$

then

$$0 = \sum_{j=1}^{J-1} \lambda_j \widehat{n} a_j + \left(\sum_{j=1}^{J-1} \lambda_j k_j \right) a_J.$$

Since a_1, a_2, \dots, a_J are rationally independent, we have $\lambda_j \widehat{n} = 0$ for $j = 1, 2, \dots, J-1$. It follows from $\widehat{n} = n_2 - n_1 > 0$ that $\lambda_1 = \lambda_2 = \dots = \lambda_{J-1} = 0$. Thus, $\widehat{a}_1, \widehat{a}_2, \dots, \widehat{a}_{J-1}$ are rationally independent as desired.

By the induction hypothesis, the following set

$$\left\{ \left[\tau(s \cdot \widehat{a}_1), \tau(s \cdot \widehat{a}_2), \dots, \tau(s \cdot \widehat{a}_{J-1}) \right]^T : s \in \mathbb{R} \right\} \subseteq [0, 1)^{J-1}$$

is dense in $[0, 1]^{J-1}$. Recall that $\widehat{\xi}_j \in [0, 1]$ for $j = 1, \dots, J-1$, which implies

$$\widehat{\xi}_j + 3\varepsilon \cdot \mathbf{1}_{\{\widehat{\xi}_j \leq 3\varepsilon\}} - 3\varepsilon \cdot \mathbf{1}_{\{\widehat{\xi}_j \geq 1-3\varepsilon\}} \in [3\varepsilon, 1-3\varepsilon] \quad \text{for } j = 1, \dots, J-1.$$

Hence, there exists $s_0 \in \mathbb{R}$ such that

$$\left| \tau(s_0 \widehat{a}_j) - \left(\widehat{\xi}_j + 3\varepsilon \cdot \mathbf{1}_{\{\widehat{\xi}_j \leq 3\varepsilon\}} - 3\varepsilon \cdot \mathbf{1}_{\{\widehat{\xi}_j \geq 1-3\varepsilon\}} \right) \right| < \varepsilon \quad \text{for } j = 1, \dots, J-1.$$

It follows that

$$\tau(s_0 \widehat{a}_j) \in [2\varepsilon, 1-2\varepsilon] \quad \text{for } j = 1, \dots, J-1$$

and

$$\left| \tau(s_0 \widehat{a}_j) - \widehat{\xi}_j \right| < \varepsilon + \left| 3\varepsilon \cdot \mathbf{1}_{\{\widehat{\xi}_j \leq 3\varepsilon\}} - 3\varepsilon \cdot \mathbf{1}_{\{\widehat{\xi}_j \geq 1-3\varepsilon\}} \right| \leq 4\varepsilon \quad \text{for } j = 1, \dots, J-1. \quad (32)$$

1423 To estimate $\tau(\lfloor s_0 \rfloor \widehat{a}_j) - \widehat{\xi}_j$, we need to bound $\tau(s_0 \widehat{a}_j) - \tau(\lfloor s_0 \rfloor \widehat{a}_j)$. To this end, we need
 1424 an observation for any $x, y \in \mathbb{R}$ as follows.

$$1425 \quad |x - y| < \varepsilon \quad \text{and} \quad \tau(x) \in [2\varepsilon, 1 - 2\varepsilon] \quad \implies \quad |\tau(x) - \tau(y)| < \varepsilon. \quad (33)$$

1426 In fact, $\tau(x) \in [2\varepsilon, 1 - 2\varepsilon]$ implies $\varepsilon \leq \tau(x) - \varepsilon \leq \tau(x) + \varepsilon \leq 1 - \varepsilon$, deducing

$$1427 \quad y \in [x - \varepsilon, x + \varepsilon] = \left[\underbrace{\lfloor x \rfloor + \tau(x) - \varepsilon}_{\geq \varepsilon}, \underbrace{\lfloor x \rfloor + \tau(x) + \varepsilon}_{\leq 1 - \varepsilon} \right] \subseteq \left[\lfloor x \rfloor + \varepsilon, \lfloor x \rfloor + 1 - \varepsilon \right] \subseteq \left[\lfloor x \rfloor, \lfloor x \rfloor + 1 \right).$$

1428 Thus, $\lfloor y \rfloor = \lfloor x \rfloor$, which implies $|\tau(x) - \tau(y)| = |\tau(x) - \tau(y) + \lfloor x \rfloor - \lfloor y \rfloor| = |x - y| < \varepsilon$ as desired.

1429 By Equation (31), we have

$$1430 \quad \left| s_0 \widehat{a}_j - \lfloor s_0 \rfloor \widehat{a}_j \right| \leq \left| s_0 - \lfloor s_0 \rfloor \right| \cdot |\widehat{a}_j| < \varepsilon \quad \text{for } j = 1, 2, \dots, J - 1.$$

1431 Recall that $\tau(s_0 \widehat{a}_j) \in [2\varepsilon, 1 - 2\varepsilon]$ for $j = 1, \dots, J - 1$. Then, for each $j \in \{1, 2, \dots, J - 1\}$,
 1432 by the observation above in Equation (33) (set $x = s_0 \widehat{a}_j$ and $y = \lfloor s_0 \rfloor \widehat{a}_j$ therein), we have
 1433 $|\tau(s_0 \widehat{a}_j) - \tau(\lfloor s_0 \rfloor \widehat{a}_j)| < \varepsilon$. Therefore, by Equations (30) and (32), we have

$$1434 \quad \begin{aligned} \left| \tau(\lfloor s_0 \rfloor \widehat{a}_j) - \tau(\widetilde{\xi}_j - \frac{\widetilde{\xi}_J}{a_J} a_j) \right| &= \left| \tau(\lfloor s_0 \rfloor \widehat{a}_j) - \widehat{\xi}_j \right| \\ &\leq \left| \tau(\lfloor s_0 \rfloor \widehat{a}_j) - \tau(s_0 \widehat{a}_j) \right| + \left| \tau(s_0 \widehat{a}_j) - \widehat{\xi}_j \right| < \varepsilon + 4\varepsilon = 5\varepsilon, \end{aligned}$$

1435 for $j = 1, 2, \dots, J - 1$. Recall the fact: For any $x, y \in \mathbb{R}$, it holds that $\tau(x) - \tau(y) = x - \lfloor x \rfloor -$
 1436 $(y - \lfloor y \rfloor) = x - y - z$, where $z = \lfloor x \rfloor - \lfloor y \rfloor \in \mathbb{Z}$.

1437 Therefore, for $j = 1, 2, \dots, J - 1$, there exists $z_j \in \mathbb{Z}$ such that

$$1438 \quad \tau(\lfloor s_0 \rfloor \widehat{a}_j) - \tau(\widetilde{\xi}_j - \frac{\widetilde{\xi}_J}{a_J} a_j) = \lfloor s_0 \rfloor \widehat{a}_j - (\widetilde{\xi}_j - \frac{\widetilde{\xi}_J}{a_J} a_j) - z_j = \lfloor s_0 \rfloor \widehat{a}_j + \frac{\widetilde{\xi}_J}{a_J} a_j - (z_j + \widetilde{\xi}_j),$$

1439 which implies

$$1440 \quad \left| \lfloor s_0 \rfloor \widehat{a}_j + \frac{\widetilde{\xi}_J}{a_J} a_j - (z_j + \widetilde{\xi}_j) \right| = \left| \tau(\lfloor s_0 \rfloor \widehat{a}_j) - \tau(\widetilde{\xi}_j - \frac{\widetilde{\xi}_J}{a_J} a_j) \right| < 5\varepsilon.$$

1441 It follows that

$$1442 \quad \lfloor s_0 \rfloor \widehat{a}_j + \frac{\widetilde{\xi}_J}{a_J} a_j \in \underbrace{[z_j + \widetilde{\xi}_j - 5\varepsilon, z_j + \widetilde{\xi}_j + 5\varepsilon]}_{\geq \varepsilon} \subseteq \underbrace{[z_j + \varepsilon, z_j + 1 - \varepsilon]}_{\leq 1 - \varepsilon} \quad \text{for } j = 1, 2, \dots, J - 1,$$

1443 where the fact $\varepsilon \leq \widetilde{\xi}_j - 5\varepsilon \leq \widetilde{\xi}_j + 5\varepsilon \leq 1 - \varepsilon$ comes from Equation (28). Therefore,

$$1444 \quad \tau(\lfloor s_0 \rfloor \widehat{a}_j + \frac{\widetilde{\xi}_J}{a_J} a_j) = (\lfloor s_0 \rfloor \widehat{a}_j + \frac{\widetilde{\xi}_J}{a_J} a_j) - z_j \in [\widetilde{\xi}_j - 5\varepsilon, \widetilde{\xi}_j + 5\varepsilon] \quad \text{for } j = 1, 2, \dots, J - 1.$$

1445 For $j = 1, 2, \dots, J - 1$, we have

$$1446 \quad \lfloor s_0 \rfloor \widehat{a}_j + \frac{\widetilde{\xi}_J}{a_J} a_j = \lfloor s_0 \rfloor \left(\frac{\widehat{n}}{a_J} a_j + k_j \right) + \frac{\widetilde{\xi}_J}{a_J} a_j = \frac{\lfloor s_0 \rfloor \widehat{n} + \widetilde{\xi}_J}{a_J} a_j + \underbrace{k_j \lfloor s_0 \rfloor}_{\in \mathbb{Z}},$$

which implies

$$\tau\left(\frac{\lfloor s_0 \rfloor \widehat{n} + \widetilde{\xi}_J}{a_J} a_J\right) = \tau(\lfloor s_0 \rfloor \widehat{a}_j + \frac{\widetilde{\xi}_J}{a_J} a_j) \in [\widetilde{\xi}_j - 5\varepsilon, \widetilde{\xi}_j + 5\varepsilon] \quad \text{for } j = 1, 2, \dots, J-1.$$

By Equation (28), we have $\widetilde{\xi}_J \in [6\varepsilon, 1 - 6\varepsilon]$, which implies

$$\tau\left(\frac{\lfloor s_0 \rfloor \widehat{n} + \widetilde{\xi}_J}{a_J} a_J\right) = \tau(\lfloor s_0 \rfloor \widehat{n} + \widetilde{\xi}_J) = \widetilde{\xi}_J.$$

Thus, for $j = 1, 2, \dots, J$, we have

$$\left| \tau\left(\frac{\lfloor s_0 \rfloor \widehat{n} + \widetilde{\xi}_J}{a_J} a_j\right) - \widetilde{\xi}_j \right| \leq 5\varepsilon.$$

By Equation (29), we have $|\widetilde{\xi}_j - \xi_j| < 6\varepsilon$ for $j = 1, 2, \dots, J$, which implies

$$\left| \tau\left(\frac{\lfloor s_0 \rfloor \widehat{n} + \widetilde{\xi}_J}{a_J} a_j\right) - \xi_j \right| \leq \left| \tau\left(\frac{\lfloor s_0 \rfloor \widehat{n} + \widetilde{\xi}_J}{a_J} a_j\right) - \widetilde{\xi}_j \right| + |\widetilde{\xi}_j - \xi_j| \leq 5\varepsilon + 6\varepsilon = 11\varepsilon.$$

Therefore, $w_0 = \frac{\lfloor s_0 \rfloor \widehat{n} + \widetilde{\xi}_J}{a_J}$ is the desired w in Equation (27). That is,

$$\left| \tau(w_0 a_j) - \xi_j \right| \leq 11\varepsilon \quad \text{for } j = 1, 2, \dots, J.$$

Since $\boldsymbol{\xi} = [\xi_1, \xi_2, \dots, \xi_J]^T \in [0, 1]^J$ is arbitrary, the following set

$$\left\{ [\tau(w a_1), \tau(w a_2), \dots, \tau(w a_J)]^T : w \in \mathbb{R} \right\} \subseteq [0, 1]^J$$

is dense in $[0, 1]^J$ as desired. We finish the process of mathematical induction, and, therefore, finish the proof by the principle of mathematical induction. \square

We remark that the target parameter $w_0 = \frac{\lfloor s_0 \rfloor \widehat{n} + \widetilde{\xi}_J}{a_J}$ designed in the above proof may not be bounded uniformly for any approximation error ε since \widehat{n} can be arbitrarily large depending on ε . Therefore, the network in Theorem 1.1 may require sufficiently large parameters to achieve a target error ε .

8. Conclusion

This paper studies the super approximation power of deep feed-forward neural networks with a fixed size. It is proved by construction that there exists an EUAF network architecture with d input neurons, a maximum width $36d(2d+1)$, 11 hidden layers, and at most $5437(d+1)(2d+1)$ nonzero parameters, achieving the universal approximation property by only adjusting its finitely many parameters. That is, without changing the network size, our EUAF network can approximate any continuous function $f : [a, b]^d \rightarrow \mathbb{R}$ within an arbitrarily small error $\varepsilon > 0$ with appropriate parameters depending on f , ε , d , a , and b . Moreover, augmenting this EUAF network using one more layer with 2 neurons can exactly realize a classification function $\sum_{j=1}^J r_j \cdot \mathbb{1}_{E_j}$ in $\cup_{j=1}^J E_j$ for any $J \in \mathbb{N}^+$, where r_1, r_2, \dots, r_J are distinct rational numbers and E_1, E_2, \dots, E_J are arbitrary pairwise disjoint bounded closed subsets of \mathbb{R}^d .

While we are interested in the analysis of the approximation error here, it would be very interesting to investigate the generalization and optimization errors of EUAF networks. Acting as a proof of concept, our experimentation shows the numerical advantages of EUAF compared to ReLU. We believe our EUAF activation function could be further developed and applied to real-world applications.

Acknowledgments

Z. Shen is supported by Distinguished Professorship of National University of Singapore. H. Yang was partially supported by the US National Science Foundation under award DMS-1945029.

References

- Andrew R. Barron. Universal approximation bounds for superpositions of a sigmoidal function. *IEEE Transactions on Information Theory*, 39(3):930–945, May 1993. ISSN 0018-9448. doi: 10.1109/18.256500.
- Andrea D. Beck, Jonas Zeifang, Anna Schwarz, and David G. Flad. A neural network based shock detection and localization approach for discontinuous Galerkin methods. *Journal of Computational Physics*, 423:109824, 2020. ISSN 0021-9991. doi: 10.1016/j.jcp.2020.109824.
- Christian Beck, Martin Hutzenthaler, Arnulf Jentzen, and Benno Kuckuck. An overview on deep learning-based approximation methods for partial differential equations. *arXiv e-prints*, art. arXiv:2012.12348, December 2020.
- David E. Bernholdt, Mark R. Cianciosa, David L. Green, Jin M. Park, Kody J. H. Law, and Clement Etienam. Cluster, classify, regress: A general method for learning discontinuous functions. *Foundations of Data Science*, 1(4):491–506, 2019.
- Helmut Bölcskei, Philipp Grohs, Gitta Kutyniok, and Philipp Petersen. Optimal approximation with sparsely connected deep neural networks. *SIAM Journal on Mathematics of Data Science*, 1(1):8–45, Jan 2019. ISSN 2577-0187. doi: 10.1137/18m118709x.
- Andrea Bonito, Ronald DeVore, Peter Jantsch Diane Guignard, and Guergana Petrova. Polynomial approximation of anisotropic analytic functions of several variables. *Constructive Approximation*, 53:319–348, 2021. doi: 10.1007/s00365-020-09511-4.
- Liang Chen and Congwei Wu. A note on the expressive power of deep rectified linear unit networks in high-dimensional spaces. *Mathematical Methods in the Applied Sciences*, 42(9):3400–3404, 2019. doi: 10.1002/mma.5575.
- Albert Cohen, Ronald DeVore, Guergana Petrova, and Przemyslaw Wojtaszczyk. Optimal stable nonlinear approximation. *arXiv e-prints*, art. arXiv:2009.09907, September 2020.
- George Cybenko. Approximation by superpositions of a sigmoidal function. *MCSS*, 2:303–314, 1989.
- Ingrid Daubechies, Ronald DeVore, Simon Foucart, Boris Hanin, and Guergana Petrova. Nonlinear approximation and (deep) ReLU networks. *Constructive Approximation*, 2021. doi: 10.1007/s00365-021-09548-z.
- Ronald A. DeVore. Nonlinear approximation. *Acta Numerica*, 7:51–150, 1998. doi: 10.1017/S0962492900002816.

- 1518 Weinan E and Qingcan Wang. Exponential convergence of the deep neural network approx-
 1519 imation for analytic functions. *CoRR*, abs/1807.00297, 2018. URL [http://arxiv.org/](http://arxiv.org/abs/1807.00297)
 1520 [abs/1807.00297](http://arxiv.org/abs/1807.00297).
- 1521 Weinan E and Stephan Wojtowytsch. A priori estimates for classification problems using
 1522 neural networks. *CoRR*, abs/2009.13500, 2020. URL [https://arxiv.org/abs/2009.](https://arxiv.org/abs/2009.13500)
 1523 [13500](https://arxiv.org/abs/2009.13500).
- 1524 Weinan E and Stephan Wojtowytsch. Representation formulas and pointwise properties for
 1525 Barron functions. *Calculus of Variations and Partial Differential Equations*, 61(2), April
 1526 2022. ISSN 0944-2669. doi: 10.1007/s00526-021-02156-6.
- 1527 Weinan E, Chao Ma, and Qingcan Wang. A priori estimates of the population risk for
 1528 residual networks. *CoRR*, abs/1903.02154, 2019a. URL [http://arxiv.org/abs/1903.](http://arxiv.org/abs/1903.02154)
 1529 [02154](http://arxiv.org/abs/1903.02154).
- 1530 Weinan E, Chao Ma, and Lei Wu. A priori estimates of the population risk for two-layer
 1531 neural networks. *Communications in Mathematical Sciences*, 17(5):1407–1425, 2019b.
- 1532 Dennis Elbrächter, Philipp Grohs, Arnulf Jentzen, and Christoph Schwab. Dnn expres-
 1533 sion rate analysis of high-dimensional pdes: Application to option pricing. *Constructive*
 1534 *Approximation*, 2021. doi: 10.1007/s00365-021-09541-6.
- 1535 Johannes Gedeon, Jonathan Schmidt, Matthew J.P. Hodgson, Jack Wetherell, Carlos L.
 1536 Benavides-Riveros, and Miguel A. L. Marques. Machine learning the derivative discon-
 1537 tinuity of density-functional theory. *Machine Learning: Science and Technology*, 2021.
 1538 URL <http://iopscience.iop.org/article/10.1088/2632-2153/ac3149>.
- 1539 Vanshika Gupta, Sharad Kumar Gupta, and Jungrack Kim. Automated discontinuity de-
 1540 tection and reconstruction in subsurface environment of mars using deep learning: A
 1541 case study of sharad observation. *Applied Sciences*, 10(7), 2020. ISSN 2076-3417. URL
 1542 <https://www.mdpi.com/2076-3417/10/7/2279>.
- 1543 Jun Han and Claudio Moraga. The influence of the sigmoid function parameters on the speed
 1544 of backpropagation learning. In José Mira and Francisco Sandoval, editors, *From Natural*
 1545 *to Artificial Neural Computation*, pages 195–201, Berlin, Heidelberg, 1995. Springer Berlin
 1546 Heidelberg. ISBN 978-3-540-49288-7.
- 1547 Juncal He, Xiaodong Jia, Jinchao Xu, Lian Zhang, and Liang Zhao. Make ℓ_1 regularization
 1548 effective in training sparse CNN. *Computational Optimization and Applications*, 77(1):
 1549 163–182, 2020. doi: 10.1007/s10589-020-00202-1.
- 1550 Geoffrey E. Hinton, Nitish Srivastava, Alex Krizhevsky, Ilya Sutskever, and Ruslan
 1551 Salakhutdinov. Improving neural networks by preventing co-adaptation of feature de-
 1552 tectors. *CoRR*, abs/1207.0580, 2012. URL <http://arxiv.org/abs/1207.0580>.
- 1553 Sean Hon and Haizhao Yang. Simultaneous neural network approximations in Sobolev
 1554 spaces. *arXiv e-prints*, art. arXiv:2109.00161, August 2021.

- 1555 Kurt Hornik. Approximation capabilities of multilayer feedforward networks. *Neural Net-*
1556 *works*, 4(2):251–257, 1991. ISSN 0893-6080. doi: 10.1016/0893-6080(91)90009-T.
- 1557 Kurt Hornik, Maxwell Stinchcombe, and Halbert White. Multilayer feedforward networks
1558 are universal approximators. *Neural Networks*, 2(5):359–366, 1989. ISSN 0893-6080. doi:
1559 10.1016/0893-6080(89)90020-8.
- 1560 Wei-Fan Hu, Te-Sheng Lin, and Ming-Chih Lai. A Discontinuity Capturing Shallow Neural
1561 Network for Elliptic Interface Problems. *arXiv e-prints*, art. arXiv:2106.05587, June 2021.
- 1562 Sergey Ioffe and Christian Szegedy. Batch normalization: Accelerating deep network train-
1563 ing by reducing internal covariate shift. In *Proceedings of the 32nd International Con-*
1564 *ference on International Conference on Machine Learning - Volume 37*, ICML’15, page
1565 448–456. JMLR.org, 2015.
- 1566 Yuling Jiao, Yanming Lai, Xiliang Lu, and Jerry Zhijian Yang. Deep neural networks with
1567 ReLU-sine-exponential activations break curse of dimensionality on Hölder class. *CoRR*,
1568 abs/2103.00542, 2021. URL <https://arxiv.org/abs/2103.00542>.
- 1569 Kenji Kawaguchi. Deep learning without poor local minima. In D. D. Lee, M. Sugiyama,
1570 U. V. Luxburg, I. Guyon, and R. Garnett, editors, *Advances in Neural Information*
1571 *Processing Systems 29*, pages 586–594. Curran Associates, Inc., 2016. URL [http://](http://papers.nips.cc/paper/6112-deep-learning-without-poor-local-minima.pdf)
1572 papers.nips.cc/paper/6112-deep-learning-without-poor-local-minima.pdf.
- 1573 Kenji Kawaguchi and Yoshua Bengio. Depth with nonlinearity creates no bad local minima
1574 in resnets. *Neural Networks*, 118:167–174, 2019. ISSN 0893-6080. doi: 10.1016/j.neunet.
1575 2019.06.009.
- 1576 Andrei Nikolaevich Kolmogorov. On the representation of continuous functions of many
1577 variables by superposition of continuous functions of one variable and addition. *Doklady*
1578 *Akademii Nauk SSSR*, 114(5):953–956, 1957. URL <http://mi.mathnet.ru/dan22050>.
- 1579 Phong Le and Willem Zuidema. Compositional distributional semantics with long short
1580 term memory. In *Proceedings of the Fourth Joint Conference on Lexical and Computa-*
1581 *tional Semantics*, pages 10–19, Denver, Colorado, June 2015. Association for Computa-
1582 tional Linguistics. doi: 10.18653/v1/S15-1002.
- 1583 Qianxiao Li, Cheng Tai, and Weinan E. Stochastic modified equations and dynamics of
1584 stochastic gradient algorithms I: Mathematical foundations. *Journal of Machine Learning*
1585 *Research*, 20(40):1–47, 2019. URL <http://jmlr.org/papers/v20/17-526.html>.
- 1586 Qianxiao Li, Ting Lin, and Zuowei Shen. Deep learning via dynamical systems: An ap-
1587 proximation perspective. *Journal of European Mathematical Society*, to appear.
- 1588 Hongzhou Lin and Stefanie Jegelka. Resnet with one-neuron hidden layers is a universal
1589 approximator. In S. Bengio, H. Wallach, H. Larochelle, K. Grauman, N. Cesa-Bianchi,
1590 and R. Garnett, editors, *Advances in Neural Information Processing Systems*, volume 31.
1591 Curran Associates, Inc., 2018. URL [https://proceedings.neurips.cc/paper/2018/](https://proceedings.neurips.cc/paper/2018/file/03bfc1d4783966c69cc6aef8247e0103-Paper.pdf)
1592 [file/03bfc1d4783966c69cc6aef8247e0103-Paper.pdf](https://proceedings.neurips.cc/paper/2018/file/03bfc1d4783966c69cc6aef8247e0103-Paper.pdf).

- 1593 Liyuan Liu, Haoming Jiang, Pengcheng He, Weizhu Chen, Xiaodong Liu, Jianfeng Gao, and
1594 Jiawei Han. On the variance of the adaptive learning rate and beyond. In *International*
1595 *Conference on Learning Representations*, 2020. URL [https://openreview.net/forum?](https://openreview.net/forum?id=rkgz2aEKDr)
1596 [id=rkgz2aEKDr](https://openreview.net/forum?id=rkgz2aEKDr).
- 1597 Jianfeng Lu, Zuowei Shen, Haizhao Yang, and Shijun Zhang. Deep network approximation
1598 for smooth functions. *SIAM Journal on Mathematical Analysis*, 53(5):5465–5506, 2021.
1599 doi: 10.1137/20M134695X.
- 1600 Vitaly Maiorov and Allan Pinkus. Lower bounds for approximation by MLP neural net-
1601 works. *Neurocomputing*, 25(1):81–91, 1999. ISSN 0925-2312. doi: 10.1016/S0925-2312(98)
1602 00111-8.
- 1603 Hadrien Montanelli, Haizhao Yang, and Qiang Du. Deep ReLU networks overcome the
1604 curse of dimensionality for generalized bandlimited functions. *Journal of Computational*
1605 *Mathematics*, 39(6):801–815, 2021. ISSN 1991-7139. doi: 10.4208/jcm.2007-m2019-0239.
- 1606 Behnam Neyshabur, Zhiyuan Li, Srinadh Bhojanapalli, Yann LeCun, and Nathan Srebro.
1607 The role of over-parametrization in generalization of neural networks. In *International*
1608 *Conference on Learning Representations*, 2019. URL [https://openreview.net/forum?](https://openreview.net/forum?id=BygfghAcYX)
1609 [id=BygfghAcYX](https://openreview.net/forum?id=BygfghAcYX).
- 1610 Quynh N. Nguyen and Matthias Hein. The loss surface of deep and wide neural networks.
1611 *CoRR*, abs/1704.08045, 2017. URL <http://arxiv.org/abs/1704.08045>.
- 1612 Philipp Petersen and Felix Voigtlaender. Optimal approximation of piecewise smooth func-
1613 tions using deep ReLU neural networks. *Neural Networks*, 108:296–330, 2018. ISSN
1614 0893-6080. doi: 10.1016/j.neunet.2018.08.019.
- 1615 Zuowei Shen, Haizhao Yang, and Shijun Zhang. Deep network approximation characterized
1616 by number of neurons. *Communications in Computational Physics*, 28(5):1768–1811,
1617 2020. ISSN 1991-7120. doi: 10.4208/cicp.OA-2020-0149.
- 1618 Zuowei Shen, Haizhao Yang, and Shijun Zhang. Deep network with approximation error
1619 being reciprocal of width to power of square root of depth. *Neural Computation*, 33(4):
1620 1005–1036, 03 2021a. ISSN 0899-7667. doi: 10.1162/neco_a_01364.
- 1621 Zuowei Shen, Haizhao Yang, and Shijun Zhang. Neural network approximation: Three
1622 hidden layers are enough. *Neural Networks*, 141:160–173, 2021b. ISSN 0893-6080. doi:
1623 10.1016/j.neunet.2021.04.011.
- 1624 Zuowei Shen, Haizhao Yang, and Shijun Zhang. Optimal approximation rate of ReLU
1625 networks in terms of width and depth. *Journal de Mathématiques Pures et Appliquées*,
1626 157:101–135, 2022. ISSN 0021-7824. doi: 10.1016/j.matpur.2021.07.009.
- 1627 Jonathan W. Siegel and Jinchao Xu. Optimal approximation rates and metric entropy of
1628 ReLU^k and cosine networks. *arXiv e-prints*, art. arXiv:2101.12365, January 2021.

- 1629 Nitish Srivastava, Geoffrey Hinton, Alex Krizhevsky, Ilya Sutskever, and Ruslan Salakhut-
 1630 dinov. Dropout: A simple way to prevent neural networks from overfitting. *Journal of*
 1631 *Machine Learning Research*, 15(56):1929–1958, 2014. URL [http://jmlr.org/papers/](http://jmlr.org/papers/v15/srivastava14a.html)
 1632 [v15/srivastava14a.html](http://jmlr.org/papers/v15/srivastava14a.html).
- 1633 Elias M. Stein and Rami Shakarchi. *Real Analysis: Measure Theory, Integration, and*
 1634 *Hilbert Spaces*. Princeton University Press, Princeton, New Jersey, USA, 2005. ISBN
 1635 9780691113869.
- 1636 Joseph Turian, James Bergstra, and Yoshua Bengio. Quadratic features and deep architec-
 1637 tures for chunking. In *Proceedings of Human Language Technologies: The 2009 Annual*
 1638 *Conference of the North American Chapter of the Association for Computational Linguis-*
 1639 *tics, Companion Volume: Short Papers*, NAACL-Short '09, pages 245–248, USA, 2009.
 1640 Association for Computational Linguistics.
- 1641 Han Xiao, Kashif Rasul, and Roland Vollgraf. Fashion-MNIST: a Novel Image Dataset
 1642 for Benchmarking Machine Learning Algorithms. *arXiv e-prints*, art. arXiv:1708.07747,
 1643 August 2017.
- 1644 Yunfei Yang, Zhen Li, and Yang Wang. Approximation in shift-invariant spaces with deep
 1645 ReLU neural networks. *Neural Networks*, 153:269–281, 2022. ISSN 0893-6080. doi:
 1646 10.1016/j.neunet.2022.06.013.
- 1647 Dmitry Yarotsky. Optimal approximation of continuous functions by very deep ReLU net-
 1648 works. In Sébastien Bubeck, Vianney Perchet, and Philippe Rigollet, editors, *Proceedings*
 1649 *of the 31st Conference On Learning Theory*, volume 75 of *Proceedings of Machine Learn-*
 1650 *ing Research*, pages 639–649. PMLR, 06–09 Jul 2018. URL [http://proceedings.mlr.](http://proceedings.mlr.press/v75/yarotsky18a.html)
 1651 [press/v75/yarotsky18a.html](http://proceedings.mlr.press/v75/yarotsky18a.html).
- 1652 Dmitry Yarotsky. Elementary superexpressive activations. In Marina Meila and Tong
 1653 Zhang, editors, *Proceedings of the 38th International Conference on Machine Learning*,
 1654 volume 139 of *Proceedings of Machine Learning Research*, pages 11932–11940. PMLR,
 1655 18–24 Jul 2021. URL <https://proceedings.mlr.press/v139/yarotsky21a.html>.
- 1656 Dmitry Yarotsky and Anton Zhevnerchuk. The phase diagram of approximation rates for
 1657 deep neural networks. In H. Larochelle, M. Ranzato, R. Hadsell, M. F. Balcan, and
 1658 H. Lin, editors, *Advances in Neural Information Processing Systems*, volume 33, pages
 1659 13005–13015. Curran Associates, Inc., 2020. URL [https://proceedings.neurips.cc/](https://proceedings.neurips.cc/paper/2020/file/979a3f14bae523dc5101c52120c535e9-Paper.pdf)
 1660 [paper/2020/file/979a3f14bae523dc5101c52120c535e9-Paper.pdf](https://proceedings.neurips.cc/paper/2020/file/979a3f14bae523dc5101c52120c535e9-Paper.pdf).
- 1661 Shijun Zhang. Deep neural network approximation via function compositions. *PhD The-*
 1662 *sis, National University of Singapore*, 2020. URL [https://scholarbank.nus.edu.sg/](https://scholarbank.nus.edu.sg/handle/10635/186064)
 1663 [handle/10635/186064](https://scholarbank.nus.edu.sg/handle/10635/186064).